Institut de Biochimie
Université de Fribourg (Suisse)

Neutrophil Chemotaxis:
Crucial Role of Phosphoinositide 3-Kinase γ and Rho
Family GTP-Binding Proteins

THESE

présentée à la Faculté des Sciences de l'Université de Fribourg
(Suisse) pour l'obtention du grade de
Doctor rerum naturalium

par

Vladimir L. Katanaev
de
Krasnoyarsk, Russie

Thèse No 1289
Mécanography de l'Université
Fribourg
2000

Acceptée par la Faculté des Sciences de l'Université de Fribourg (Suisse) sur la proposition du Dr. Matthias P. Wymann, du Prof. Michael Way et du Prof. Verena Niggli.
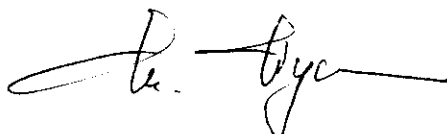
Fribourg, le 25.01.2000

Le Doyen

Prof. Beat Hirsbrunner

Le directeur de thèse

Dr. Matthias P. Wymann

CONTENTS

SUMMARY

Neutrophils represent a key component of organism's innate immunity. They are able to sense bacterial infection, migrate to its source, and destroy the invading pathogen. The vast array of neutrophil activities is controlled by an elaborated net of signal transduction cascades, linking surface receptors with the cell interior and regulating cell responses to the extracellular milieu.

Chemoattractants like fMLP or interleukin-8 activate neutrophil receptors coupled to trimeric G proteins. The latter signal to phosphoinositide 3-kinase γ (PI3Kγ), an enzyme phosphorylating D3-position of PIP_2 and also possessing a protein kinase activity. To elucidate the role of PI3Kγ in neutrophil signalling, we analyzed neutrophil functions in PI3Kγ knock-out mice. Several responses to chemoattractants were impaired in PI3Kγ -/- neutrophils. After priming with lipopolysaccharide, wild type but not knock-out neutrophils responded to fMLP with a production of oxygen radicals. Chemoattractant-induced cell adhesion and actin polymerization were reduced in PI3Kγ-null neutrophils. Finally, chemotaxis of neutrophils *in vitro* and *in vivo* was impaired, resulting in reduced protection of PI3Kγ knock-out mice from infecting bacteria. These data demonstrate a crucial role of PI3Kγ in neutrophil responses in inflammation. They also put forward the enzyme as a promising target for the development of anti-inflammatory drugs.

Regulated in time and space rearrangements of actin cytoskeleton are crucial to exert such cell activities as chemotaxis, adhesion, and phagocytosis. To characterize biochemically signalling to actin polymerization, we designed a cell-free system from the cytosol of human neutrophils. In this system addition of GTPγS, a non-hydrolyzable analogue of GTP, induced massive actin polymerization and cross-linking. This effect was due to constitutive activation of small Rho family GTP-binding proteins, proving their role in the control of neutrophil actin cytoskeleton. Rho-protein induced actin polymerization was shown to require a plasma membrane-associated guanine nucleotide exchange factor(s). It was also shown to be exerted via a kinase-independent mechanism, excluding a multitude of proposed downstream targets of Rho proteins in the induction of actin polymerization in the neutrophil cytosol. We suggested that Rac and Cdc42 could not be the proteins mediating the effect of GTPγS. In contrast, we found that Rho and a CIP4-binding protein could initiate actin polymerization. These data are an important contribution to the molecular dissecting of cell signalling to actin cytoskeleton, and the established cell-free system will provide more insights into the mechanisms of cell activation.

RESUME

Des neutrophiles représentent le composant principal de l'immunité innée des organismes. Ils sont capables détecter des infections bactériennes, de migrer vers ces dernieres afin de détruire les pathogènes envahisseurs. La vaste palette des activités des neutrophiles est contrôlée par un réseau élaboré de cascades de signalisation, qui lient des récepteurs de la surface avec l'intérieur des cellules régulant ainsi les réponses cellulaires au milieu environnant.

Des agents chimiotactiques comme le fMLP ou l'interleukin-8 agissent sur les neutrophiles par l'intermediaire de récepteurs liés aux proteins G trimériques capable d'activer la phosphoinositide 3-kinase de type γ (PI3Kγ), enzyme phosphorylant la position D3 du PIP$_2$ et possédant une activité protéine kinase. Pour élucider le rôle de PI3Kγ dans la signalisation des neutrophiles, nous avons utilisé des souris délétées du gène codant pour la PI3Kγ (PI3Kγ -/-). Nous avons pu montré une diminution des réponses des neutrophiles PI3Kγ-/- à des agents chimiotactiques. En effet, après un "*priming*" avec du lipopolysaccharide, la production de radicaux oxygénés induite par le fMLP était abolie. Après induction par des agents chimiotactiques, l'adhésion et la polymérisation d'actine des neutrophiles PI3Kγ-/- étaient réduites. Enfin, le chimiotactisme des neutrophiles *in vitro* et *in vivo* était diminué, induisant ainsi une protection réduite des souris PI3Kγ -/- contre l'infection bactérienne. Ces données montrent un rôle crucial de la PI3Kγ dans les réponses inflammatoires des neutrophiles et ouvrent des perspectives quant au développement de nouvelles drogues ayant pour cible la PI3Kγ .

Les réarrangements du cytosquelette d'actine sont des évènements indispensables pour des activités cellulaires comme le chimiotactisme, l'adhésion, et la phagocytose. Pour caractériser biochimiquement la signalisation conduisant à la polymérisation d'actine, nous avons mis au point un système *in vitro* utilisant le cytoplasme de neutrophiles humains dans lequel l'ajout de GTPγS (analogue non hydrolysable du GTP) induisait la polymérisation et la formation de réseaux d'actine. Nous avons pu montré que cet effet dépendait de l'activation des petites proteines G de la famille Rho, elles-même sous le controle de facteurs d'échanges nucléotidiques (GEF) membranaires, montrant ainsi leur rôle dans le controle du cytosquelette d'actine des neutrophiles. De façon surprenante, cette signalisation est indépendante de kinases, excluant l'implication de nombreuses cibles des protéines Rho dans l'initiation de la polymétisation d'actine. Nous avons suggéré que l'effet du GTPγS n'était pas induit par Rac et Cdc42, mais par Rho et une protéine liée à CIP4 . L'ensemble de ces données ainsi que la mise au point d'un système *in vitro,* contribuent à une meilleure compréhension des mécanismes moléculaires impliqués dans la signalisation conduisant au cytosquelette d'actine.

SIGNAL TRANSDUCTION IN NEUTROPHIL MOTILITY

I. Physiology and morphology of neutrophil motility.

Neutrophils (polymorphonuclear leukocytes) constitute more than half of circulating white blood cells in humans and provide a major defence system against microorganisms. Their crucial role in innate immunity is highlighted by severe susceptibility to bacterial infections in patients with neutrophil disorders, such as various forms of neutropenia (Sievers and Dale, 1996), leukocyte adhesion deficiency (Lipnick *et al*., 1996), or chronic granulomatous disease (Thrasher *et al*., 1994). On the other hand, hyperactivated neutrophils cause pathologies. Reperfusion injury (Williams, 1994), vasculitis (Savage and Rees, 1994), adult respiratory distress syndrome (Hasleton and Roberts, 1999), or glomerulonephritis (Lefkowith, 1997) evidence the medical importance of neutrophil overactivation.

Neutrophils possess a large armament of antibacterial activities, including phagocytosis (Kwiatkowska and Sobota, 1999), production of oxygen radicals (Segal and Shatwell, 1997), and secretion of various degrading enzymes (Gullberg *et al*., 1997). Resting nonadherent neutrophils are circular cells of about 7 μm in diameter (Worthen *et al*., 1989). Upon stimulation, they markedly change their shape, forming asymmetric protrusions called pseudopodia, which serve for cell migration when in contact with substratum. Physiologically, before migration through a tissue to the source of infection, a circulating neutrophil has to cross the blood vessel endothelium (Fig. 1). This preferentially happens in the postcapillary venules and involves several steps (Springer, 1995): attachment to and rolling on the endothelium, followed by firm adhesion and finally transendothelial migration or diapedesis. For the latter the neutrophil has to pull itself between endothelial cells through a hole which is several times narrower than the neutrophil diameter, a phenomenon demonstrating remarkable flexibility of neutrophil membranes and the cytoskeleton (Fig. 1).

Actin cytoskeleton is absolutely required for cell crawling, which is the main type of cell motility in muticellular organisms. Newly polymerized actin filaments are enriched in the leading edge of a migrating cell (Fechheimer and Zigmond, 1983; Valerius *et al*., 1981), and pseudopod formation correlates temporarily with increases in filamentous actin (Wymann *et al*., 1990). Prevention of actin polymerization abolishes chemotaxis (Carter, 1967; Becker *et al*., 1972; Zigmond and Hirsch, 1972; Norgauer *et al*., 1988). These and other data have led to a widely accepted model that actin polymerization is the driving force of the cell leading edge protrusion (Condeelis, 1993; Elson *et al*., 1999).

Neutrophil motility has been modelled *in vitro* on two-dimensional surfaces or in three-dimensional gels. These studies and investigation of neutrophils in suspension
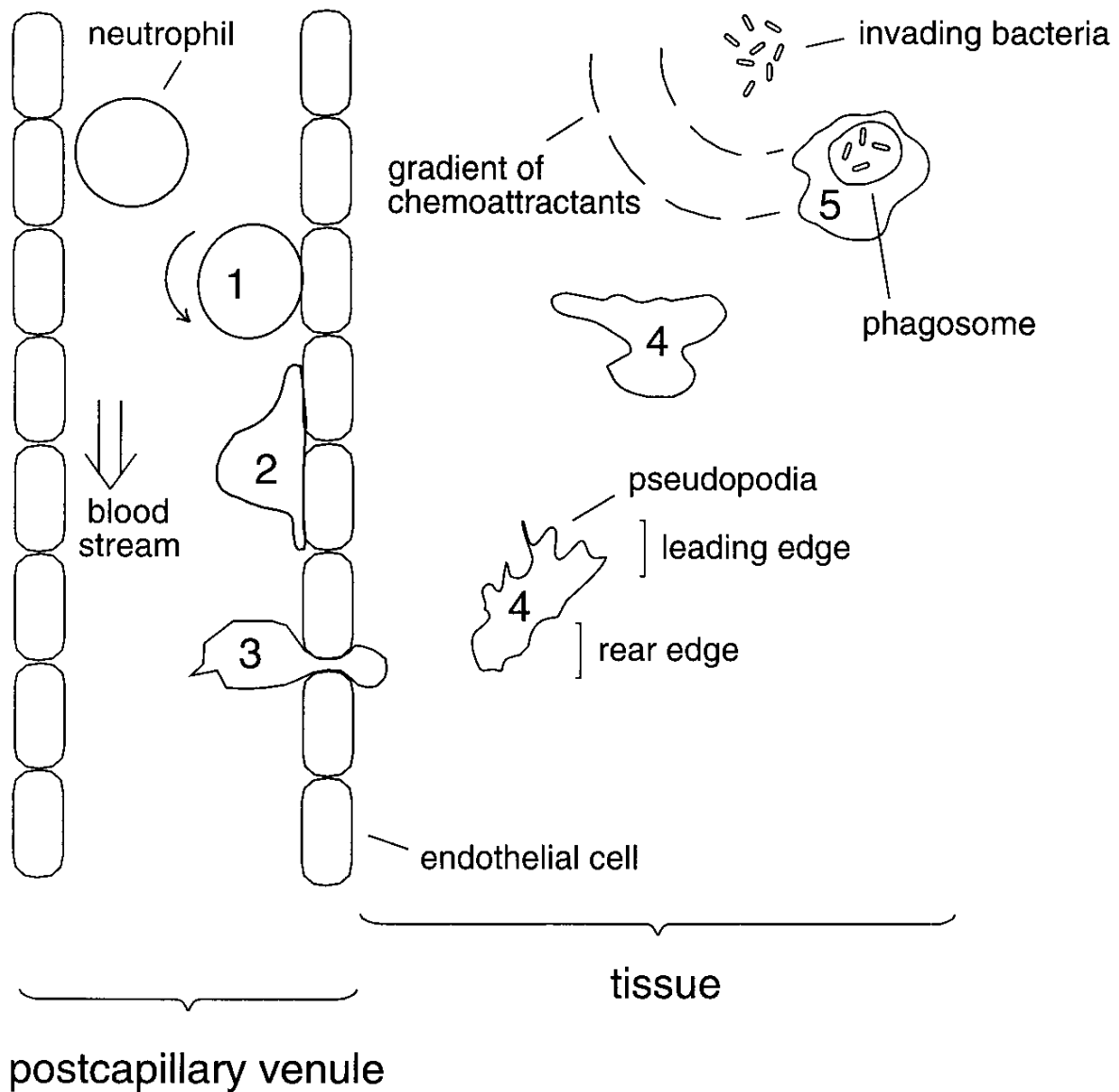
Fig. 1. A scheme of neutrophil emigration from a blood vessel to a tissue infected with bacteria. Upon receaval of a chemoattractic signal, a circulating neutrophil comes through several stages (numbered on the scheme) of interaction with neibouring cells. These include: 1) rolling of the neutrophil on the surface of endothelial cells, a process mainly mediated by selectins; 2) firm integrin- mediated adhesion of the neutrophil to the endothelial cells; 3) diapedesis or neutrophil transmigration through the endothelial layer; 4) chemotaxis through the post- endothelial tissue to the source of bacterial infection; and 5) killing of bacteria by phagocytosis, production of oxigen radicals and release of the antibacterial granule content.

have revealed striking periodicities in neutrophil behaviour upon stimulation (reviewed in Coates, 1996). When stimulated in suspension, neutrophils change their shape every 8 seconds (Wymann *et al.*, 1987). This is reflected by an eight second periodicity in neutrophil motility on a substratum (Franke and Gruler, 1994; Hartman *et al.*, 1994), and is achieved by oscillatory protrusion and retraction of pseudopodia. In addition to this small-scale oscillations, crawling neutrophils also pause and re-establish the direction of migration every 45-60 seconds, which is mediated by cell repolarization and probably necessary for the correct gradient perception (Coates *et al.*, 1996). Thus neutrophil migration seems to be timed by two superimposed molecular clocks enabling cell response to a multitude of stimuli.

II. Chemoattractants and receptors in neutrophil motility.

1. "Non-classical" chemoattractants and their receptors.

In vitro studies have identified a multitude of agents inducing neutrophil chemotaxis (directed migration) or chemokinesis (random migration) . Although "classical" chemoattractants bind to G protein- coupled receptors, there are other reported chemotactic or chemokinetic molecules which act on different receptors.

In addition to their well-known role in hematopoesis (Tarr, 1996; Anderlini *et al.*, 1996) granulocyte colony-stimulating factor (G-CSF) and granulocyte-macrophage colony-stimulating factor (GM-CSF) were reported to activate chemokinesis but not chemotaxis in neutrophils (Smith *et al.*, 1994; Yong, 1996; Harakawa *et al.*, 1997). These cytokines bind to monomeric (G-CSF) or heterodimeric (GM-CSF) non-catalytic receptors which in turn activate Ser/Thr/Tyr kinases called the Janus kinases (Jaks) (Ihle *et al.*, 1995).

TNFα induces neutrophil chemotaxis (Ming *et al.*, 1987; Lukacs *et al.*, 1995; Loike *et al.*, 1995) via activation of TNF receptor clustering and signal transduction through multiple protein-protein interactions. Neutrophils possess two TNF receptors (Menegazzi *et al.*, 1994), a p75 TNF receptor (CD120b) propagates the signal through TNF-receptor- associated proteins, while death-domain proteins are involved in signal transduction by a p55 receptor (CD120a) (Bazzoni and Beutler, 1996; Wallach *et al.*, 1999). It is not known which pathway induces neutrophil chemotaxis, although p55 receptor was recently shown to modulate chemotactic responses in macrophages (Peppelenbosch *et al.*, 1999). Conflicting reports exist on whether lymphotoxin (TNFβ), which shares the same p75 TNF receptor with TNFα, is chemotactic for neutrophils (Newman and Wilkinson, 1989; Mrowietz *et al.*, 1989). Recently, soluble Fas ligand has been shown to induce neutrophil chemotaxis (Seino *et al.*, 1998; Ottonello *et al.*, 1999). Fas (Apo1/ CD95) is another representative of TNF-like receptors and when activated induces apoptosis in many cells upon signalling through death domain proteins

(reviewed in Wallach *et al.*, 1999). The chemotactic activity of the Fas ligand has been shown to occur at concentrations incapable of inducing neutrophil apoptosis (Ottonello *et al.*, 1999), and through a death domain- independent mechanism (Seino *et al.*, 1998).

The most potent chemoattractant for neutrophils identified so far, inducing chemotaxis at femtomolar concentrations, is the transforming growth factor β (TGFβ), an agonist for a receptor tyrosine kinase (for a review see Hubbard, 1999). TGFβ is a "pure" chemoattractant since unlike classical chemoattractants it does not stimulate other neutrophil activities besides chemotaxis (Reibman *et al.*, 1991; Hannigan *et al.*, 1998). Surprisingly, TGFβ-directed chemotaxis is sensitive to pertussis toxin (Haines *et al.*, 1993), implying an involvement of trimeric G proteins, also crucial for the signalling induced by "classical" chemoattractants (see below). Among other agonists for receptors of the receptor tyrosine kinase superfamily, platelet-derived growth factor (Thelen *et al.*, 1995) and insulin (Oldenborg and Sehlin, 1998) were reported to display on neutrophils chemotactic and chemokinetic effects, respectively.

2. G protein- coupled receptor agonists as neutrophil chemoattractants.

Based on their molecular nature, one could distinguish five classes of "classical" leukocytes chemoattractants, acting through G protein- coupled (serpentine, seven-transmembrane helix) receptors (Boulay *et al.*, 1997) (Fig. 2). These would include 1) *N*-formylated peptides such as fMLP derived from bacterial proteins (Panaro and Mitolo, 1999); 2) platelet- activating factor (PAF) produced by activated platelets, neutrophils and other cells (Hanahan, 1986); 3) leukotriene B4 (LTB4) derived from arachidonic acid metabolism and produced by various myeloid cells (Crooks *et al.*, 1998); 4) C5a anaphylotoxin obtained after cleavage of the complement protein C5 (Gerard and Gerard, 1994), and 5) chemokines, a family of proteins of 68 to 103 amino acids with four conserved cysteines linked by disulphide bonds, which are produced locally in many tissues (Baggiolini, 1998). Based on whether the first two cysteines are adjacent or separated by one amino acid, CC and CXC chemokine subfamilies are defined (Moser *et al.*, 1998). At excessive concentrations, these chemoattractants induce wide range of responses on neutrophils, including phagocytosis, respiratory burst, degranulation, intracellular Ca^{2+} rises, and protein synthesis, while chemotaxis requires the lowest, typically nanomolar, concentrations of the stimulators.

Schematic structures of the representatives of the five groups of neutrophil chemoattractants are shown on Fig. 2. The receptors for many of these molecules are cloned. Besides the apparent differences of their ligands, all of them belong to the same subfamily of seven-transmembrane helix receptors based on sequence homologies
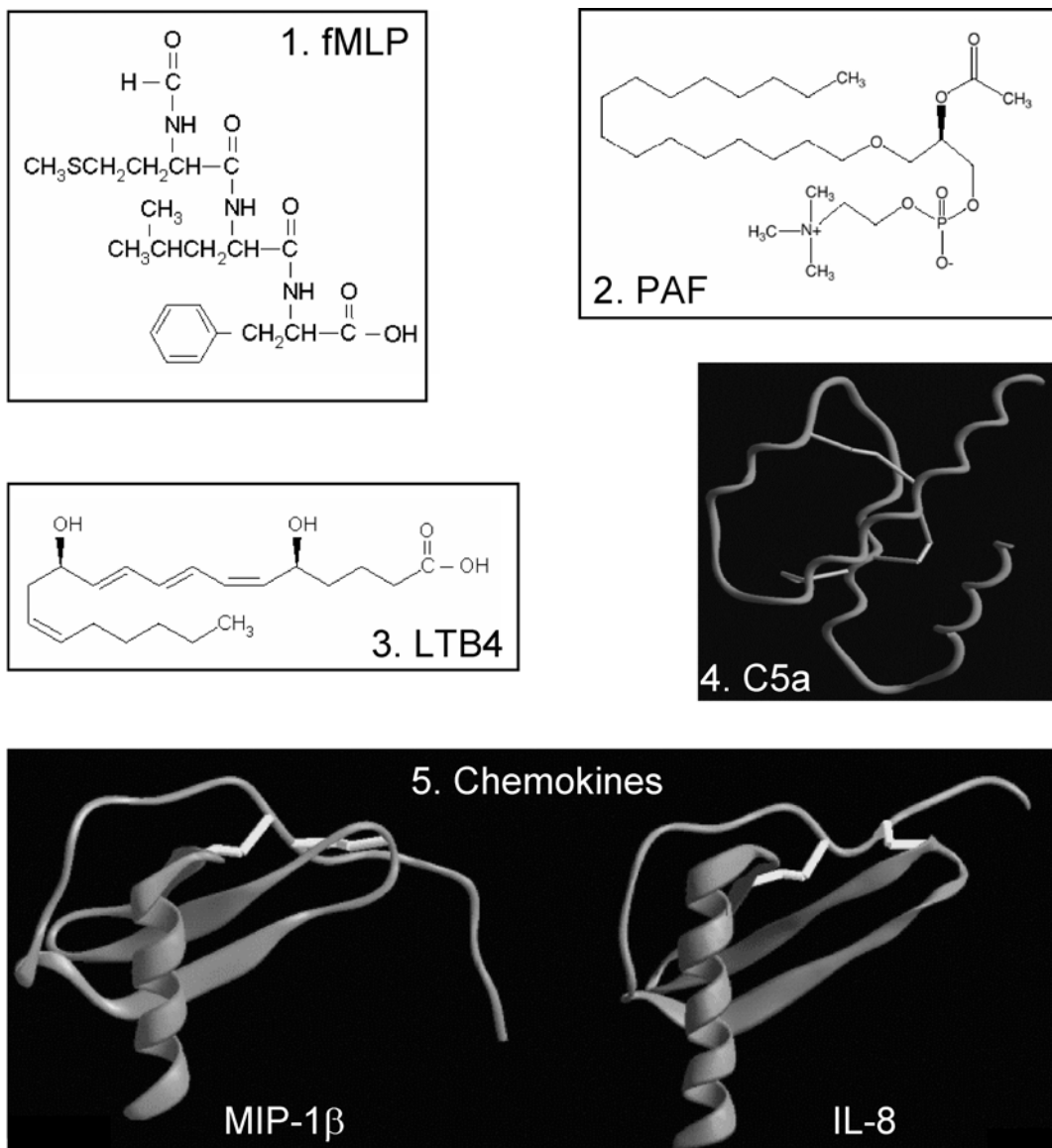
Fig. 2. Structures of representatives of five groups of chemoattractants for neutrophils acting through G protein-coupled receptors. 1. fMLP (*N*-formyl-methionyl-leucyl-phenylalanine) chemical structure. Note the *N*-formyl group capping the N-terminus of the peptide (to the top) which is a characteristic of bacterial but not eukaryotic proteins. 2. PAF (platelet activating factor) chemical structure. 3. LTB4 (leukotriene B4) chemical structure. 4. C5a anaphylotoxin solution structure. 5. A CC chemokine (MIP-1β, macrophage inflammatory protein 1β) and a CXC chemokine (IL-8, interleukin-8) solution structures are presented. The structures of fMLP, PAF and LTB4 are obtained from www.sigma.com internet address. NMR structures of C5a, MIP-1β and IL-8 are taken from the swiss-3dimage database (ftp.expasy.ch/databases/swiss-3dimage) and based on (Williamson *et al.*, 1990) (C5a), (Lodi *et al.*, 1994) (MIP-1β), and (Clore *et al.*, 1990) (IL-8).

(Bockaert and Pin, 1999). In addition to features typical to serpentine receptors as an extracellular N- and intracellular C- terminus, seven transmembrane domains (TM), and extracellular (e1-e3) and intracellular (i1-i3) loops (see Fig. 3, (Baldwin, 1993; Unger *et al.*, 1997)), the chemoattractant receptors share other structural similarities. These include an S-S bridge between e1 and e2, multiple Ser/Thr phosphorylation sites in the C-terminus, highly acidic N-terminus, basic sequences in the short i3, and the unusually small for the serpentine receptor size (ca. 350 amino acids) (Murphy, 1994; Bockaert and Pin, 1999). High affinity ligand binding is mediated by the extracellular face of the receptor, namely by the N-terminus (binding of C5a to the C5aR (Mery *et al.*, 1994), IL-8 to the CXCR1 (Gayle *et al.*, 1993; Ahuja *et al.*, 1996), or MCP-1 to the CCR2 (Monteclaro and Charo, 1996)), by the e1 (fMLP binding by FPR (Quehenberger *et al.*, 1997)), e2 (binding of GROα and NAP2 by the CXCR2 (Ahuja *et al.*, 1996), or e3 (binding of MIP-1α by the CCR1 (Monteclaro and Charo, 1996)). In addition to the high affinity ligand binding site on the N-terminus, the existence of low affinity sites on the extracellular loops has been demonstrated for some chemoattractant receptors (Ahuja *et al.*, 1996; Monteclaro and Charo, 1996). Interestingly, these low affinity sites have been shown to be sufficient for signal transduction through the receptor (Ahuja *et al.*, 1996; Monteclaro and Charo, 1996). These data might indicate that no matter where on the receptor the high affinity ligand binding site is, ligand interaction with the extracellular loops of the receptor will be crucial for the activation of the latter. This seems reasonable since G protein-coupled receptor activation is mediated by a change in relative orientation of the transmembrane domains, especially of TM3 and TM6 (Bourne, 1997; Farrens *et al.*, 1996; Baranski *et al.*, 1999). This reorientation depends on conserved Asp in TM2 and AspArgTyr tripeptide at the TM3-i2 interface (Bockaert and Pin, 1999; Scheer *et al.*, 1996; Parent *et al.*, 1996) and unmasks G protein-binding sites of the i2 (Schreiber *et al.*, 1994; Xie *et al.*, 1997), i3 (Carlson *et al.*, 1996), or the C-terminus (Schreiber *et al.*, 1994).

III. Signalling downstream of G protein-coupled chemoattractant   receptors in neutrophils.

1. Activation of trimeric G proteins.

Signalling through chemoattractant serpentine receptors in neutrophils is sensitive to pertussis toxin (Becker *et al.*, 1985; Goldman *et al.*, 1985; Lad *et al.*, 1986), indicating the involvement of G_i trimeric G proteins, including $G_{i\alpha2}$ and $G_{i\alpha3}$, downstream from the receptors (Wu *et al.*, 1993). Trimeric G proteins are membrane-bound complexes consisting of GDP-binding α-subunit and the βγ unit (Hamm and Gilchrist, 1996). Upon serpentine receptor activation, the $G_{\alpha\beta\gamma}$ heterotrimer binds to the

receptor, mainly through the α-subunit (Bourne, 1997). This induces GDP to GTP exchange on the α-subunit, resulting in dissociation of the βγ heterodimer from G_α-GTP. When GTP is hydrolyzed to GDP and phosphate due to intrinsic GTPase activity of the α-subunit, the G protein complex reassociates and is ready to receive a new signal (Hamm and Gilchrist, 1996).

Unlike believed previously, probably not the GTP-loaded α-subunit, but the βγ heterodimer of the trimeric G proteins transduces the signal from seven transmembrane helix receptors to chemotaxis in motile cells (Parent and Devreotes, 1999). Important experiments confirming that were done in cultured lymphocyte- or fibroblast-like cells transfected with serpentine receptors. Addition of respective agonists induced chemotaxis of these cells, which was completely prevented by pertussis toxin or by βγ-sequestering proteins G_α of transducin or βARK-ct (Neptune and Bourne, 1997; Arai *et al.*, 1997). In contrast, agonist-induced intracellular calcium mobilization, inhibition of adenylate cyclase, or MAPK activation were only partially decreased by the proteins (Neptune and Bourne, 1997; Arai *et al.*, 1997). As soon as $G_{\beta\gamma}$ is released, $G_{i\alpha}$ is not required for activation of chemotaxis (Neptune *et al.*, 1999). The pivotal role of βγ heterodimers has been demonstrated in signalling to chemotaxis of *D. discoideum* and directed growth in yeasts (Jin *et al.*, 1998; Nern and Arkowitz, 1998). Finally, certain mutations of the β3 subunit can enhance neutrophil chemotaxis (Virchow *et al.*, 1999).

2. Signalling downstream from trimeric G proteins.

Among different targets reported for the βγ heterodimer (Clapham and Neer, 1997), we will discuss the ones which might have relevance for neutrophil chemotaxis (see Fig. 3). These will include phospholipases Cβ, PI-3 kinase γ, and various pleckstrin homology (PH) domain proteins.

2.1. Phospholipase Cβ - protein kinase C pathway.

Phospholipases Cβ, namely PLCβ1-3, but not PLCβ4, can interact directly with and be activated by βγ heterodimers (Clapham and Neer, 1997) through the PH domain or a region in the catalytic domain (Wang *et al.*, 1999; Katan, 1998). $G_{i\alpha}$, unlike α-subunits of some pertussis toxin-insensitive G proteins, can not activate PLCβ (Katan, 1998). PLCβ catalyzes hydrolysis of phosphatidylinositol 4,5-bisphosphate (PIP_2) to inositol 3,4,5-trisphosphate (IP3) and diacylglycerol (DAG) (Katan, 1998). The latter can activate classical (α,β,γ) and novel (δ,ε,η,θ), but not atypical (τ,ζ), isoforms of protein kinase C (PKC) (Mellor and Parker, 1998). PLCβ2 is expressed in hematopoetic cells (Park *et al.*, 1992) and is responsible for 90% of the fMLP-induced IP3 production and consequently 70% of the $[Ca^{2+}]$ rise in neutrophils (Jiang *et al.*, 1997). The fMLP-induced respiratory burst is ten-fold decreased in the PLCβ2 gene-
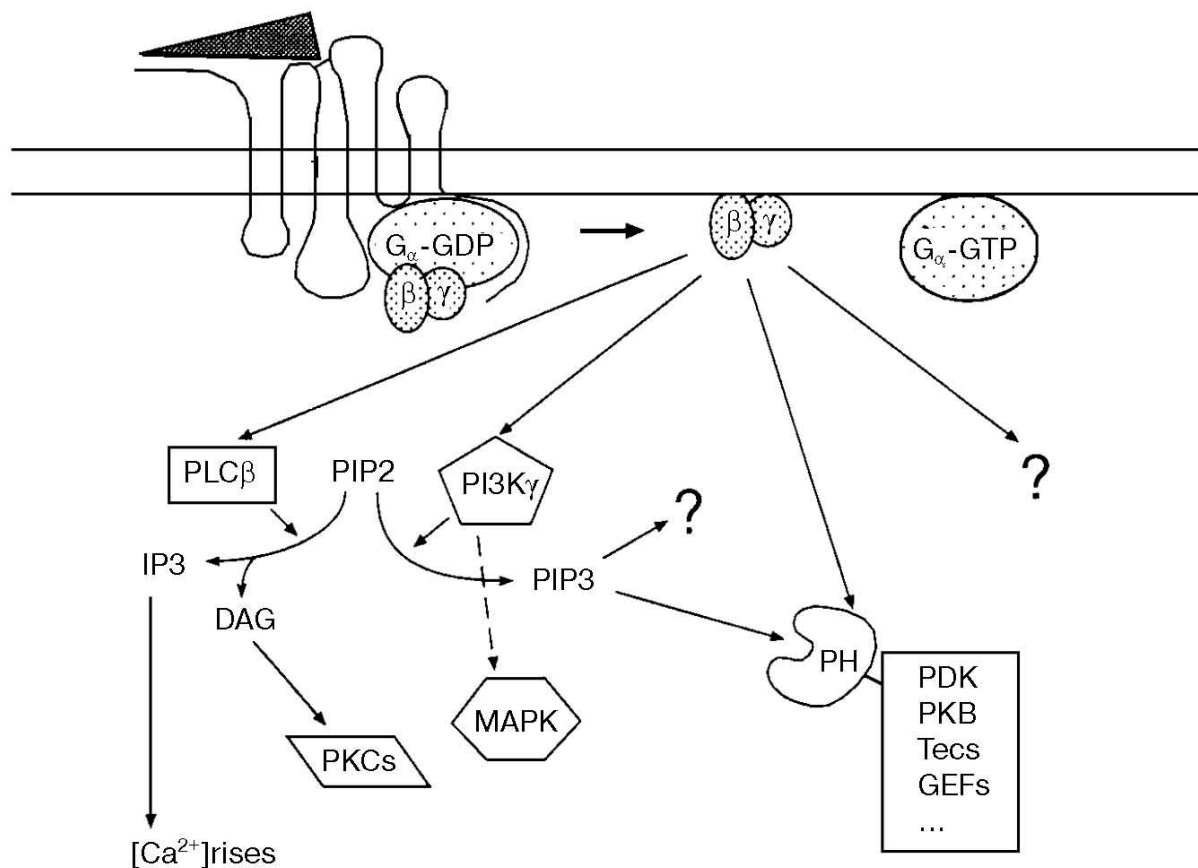
Fig. 3. A scheme of signalling events initiated by activation of a seven-transmembrane helix receptor. Only the βγ-mediated signalling is shown. See text for description. Gα-GDP and Gα-GTP: GDP or GTPbound α subunit of trimeric G proteins. βγ: βγ subunits of the trimeric G proteins. PLCβ: phospholipase Cβ. PIP2: phosphatidylinositol 4,5-bisphosphate. IP3: inositoltrisphosphate. DAG: diacylglycerol. PKCs: protein kinases C. PI3Kγ: phosphatidylinositol 3-kinase γ. PIP3: phosphatidylinositol 3,4,5-trisphosphate. PH: pleckstrin homology domain. PDK: phosphoinositide-dependent kinase. PKB: protein kinase B. GEFs: guanine nucleotide exchange factors.

less neutrophils (Jiang *et al*., 1997), supporting the key role of DAG-stimulated PKCs in the respiratory burst activation (Babior, 1995). However, despite a prevention of the $\alpha_M\beta_2$ (Mac-1, CD11b/CD18) integrin upregulation, neutrophil chemotaxis to fMLP or IL-8 was not impaired by PLCβ2 gene deletion (Jiang *et al*., 1997). This confirms previous reports that PIP$_2$ breakdown is not necessary for neutrophil chemotaxis (Bengtsson *et al*., 1988; Perez *et al*., 1989). Hence, any role of DAG-dependent PKCs in chemotaxis signalling in neutrophils downstream from PLCβ2 can be excluded. Reports of neutrophil chemotaxis sensitivity to PKC inhibitors (Niggli and Keller, 1993; Laudanna *et al*., 1998; Xiao *et al*., 1998) can thus be explained proposing an involvement of PKC isoform(s) in some signalling events located further downstream. Since neutrophils can chemotax efficiently even when intracellular [Ca^{2+}] rises are prevented (Perez *et al*., 1989), Ca^{2+}- insensitive novel or atypical PKCs might be involved in chemotaxis. Of these, expression of PKC δ and ζ has been observed in neutrophils (Kent *et al*., 1996; Stasia *et al*., 1990). Broad range inhibitors blocking PKC δ but not ζ were shown to prevent chemoattractant-induced polarization but not actin polymerization of neutrophils (Niggli and Keller, 1991; Niggli and Keller, 1993; Xiao *et al*., 1998). Neutrophils translocate PKC δ to the particulate fraction 45 seconds after fMLP stimulation (Kent *et al*., 1996), coinciding with the time of cell polarity development (see Coates, 1996). In contrast, PKC ζ was shown to control neutrophil chemotaxis at the actin polymerization level and to be translocated to the plasma membrane within 10 seconds after cell stimulation (Laudanna *et al*., 1998). These data might indicate that different PKC isoforms regulate neutrophil chemotaxis at different levels: PKC ζ involved in switching on the immediate motile response, and a novel PKC like PKC δ regulating the choice of the migrating neutrophil where to go. However, these roles of PKCs must lie quite downstream in the signalling cascades, and might be controlled by PDK-1 or small GTPases (see below).

2.2. PI-3 kinase γ pathway.

Phosphoinositide 3-kinases (PI3Ks) are lipid kinases catalyzing phosphate addition to the third position of inositol ring of phosphatidylinositol (PI), PI-4-P, and PI-4,5-P$_2$ (Wymann and Pirola, 1998). The best-studied PI-3 kinase, PI3Kα, is implicated in a variety of signalling cascades downstream from receptor tyrosine kinases (Wymann and Pirola, 1998). In contrast, PI3Kγ, which is strongly expressed in hematopoetic cells including neutrophils (Bernstein *et al*., 1998; Hirsch *et al*., in press), is proposed to be activated by G protein- coupled receptors (Stephens *et al*., 1994; Stoyanov *et al*., 1995). This is mediated by the βγ heterodimers; their binding to and activation of PI3Kγ can be achieved directly (Stoyanov *et al*., 1995; Leopoldt *et al*., 1998) or through the PI3Kγ adapter protein, p101 (Stephens *et al*., 1997; Krugmann *et al*., 1999).

The mechanism of PI3Kγ activation by the $G_{\beta\gamma}$ may be a mere translocation of PI3Kγ to the plasma membrane, where it gets access to its lipid substrates. Indeed, targeting of PI3Kγ to the membrane was sufficient for the constitutive PIP_3 production (Bondeva *et al.*, 1998). However, the ability of PI3Kγ to phosphorylate proteins has recently been shown necessary and sufficient in signalling leading to MAPK activation (Bondeva *et al.*, 1998). The detailed mechanism of activating the Ser-Thr protein kinase activity of PI3Kγ is not clear, but it rather requires a cytosolic than a membrane localization of the PI3Kγ (Bondeva *et al.*, 1998; Wymann *et al.*, 1999). It has been recently proposed that PI3Kγ may serve as a functional homologue of the Ste5 yeast scaffold protein (Lopez-Ilasaca *et al.*, submitted; Lopez-Ilasaca *et al.*, 1997; Rubio *et al.*, 1997). Ste5 is indispensible for the G protein- coupled receptor pheromone signalling in yeast. Through multiple protein-protein interactions, Ste5 organises a complex of *Saccharomyces cerevisiae* MEKK, MEK, and MAPK, which activates MAPK and leads to initiation of the mating process in yeasts (Choi *et al.*, 1994).

A highly specific for PI3Ks covalent inhibitor wortmannin (Wymann *et al.*, 1996; Stoyanova *et al.*, 1997) was used to assess PI3K involvement in neutrophil functions. Wortmannin could inhibit fMLP-induced actin polymerization (Arcaro and Wymann, 1993) and cross-linking (Niggli and Keller, 1997) by ca. 20% and 50%, respectively. Wortmannin was also shown to inhibit IL-8- induced neutrophil adhesion (Knall *et al.*, 1996). Depending on the experimental set-up, neutrophil motility can be wortmannin-insensitive (fMLP and IL-8 as stimuli, (Thelen *et al.*, 1995)), completely prevented by wortmannin (IL-8 (Knall *et al.*, 1997) or fMLP (Niggli and Keller, 1997) as stimuli), or reduced by 50% by the inhibitor (MIP-2, CINC-1, and PAF as stimuli, (Xiao *et al.*, 1998)). Among other neutrophil responses to chemoattractants, respiratory burst and exocytosis have been shown wortmannin- sensitive (Arcaro and Wymann, 1993; Baggiolini *et al.*, 1987).

Activation of PI3Ks other than PI3Kγ by trimeric G proteins has been proposed (Katada *et al.*, 1999; Vicente-Manzanares *et al.*, 1999). To clarify the role of PI3Kγ in chemoattractant-induced neutrophil responses, we have generated PI3Kγ gene-deficient mice (Hirsch *et al.*, in press). PI3Kγ $^{-/-}$ neutrophils completely lack chemoattractant-induced PIP_3 production and PKB activation, and fMLP-induced respiratory burst is also strongly affected in PI3Kγ-null cells. Upon stimulation with IL-8 and fMLP, these cells polymerize less actin and adhere worse to fibronectin than wild-type neutrophils (Hirsch *et al.*, in press; Katanaev and Wymann, unpublished). Most importantly, chemotaxis *in vitro* and *in vivo* is severely impaired in PI3Kγ-null neutrophils and macrophages, demonstrating a crucial role of PI3Kγ in cell motility (Hirsch *et al.*, in press).

2.3. PH domain- containing kinases.

Several proteins possess a ca. 100- amino acid-long domain called pleckstrin homology (PH) domain (Shaw, 1996). PH domains of different proteins have a week sequence homology, but a high degree of conservation of the 3D structure (Rebecchi and Scarlata, 1998). Some PH domains have been shown to interact with phosphorylated lipids, including the products of PI3 kinases and βγ heterodimers of trimeric G proteins (Shaw, 1996; Bottomley *et al.*, 1998). They can thus occupy upstream positions in signalling cascades to transduce signals from G proteins or phospholipid kinases to the cytoplasm.

2.3.1. PH domain- containing serine/threonine protein kinases.

Phosphoinositide-dependent kinase-1 (PDK-1) (Belham *et al.*, 1999) has been shown to possess a PH domain which is indispensable for its activation by the lipid products of PI3K (Alessi *et al.*, 1997; Currie *et al.*, 1999). PDK-1 has been proposed to phosphorylate PKCs (Chou *et al.*, 1998; Le Good *et al.*, 1998; Dutil *et al.*, 1998), including PKC δ and ζ, whose possible role in controlling neutrophil chemotaxis was discussed in section 2.1. PDK-1 contributes to the activation of p70^{S6K} (Alessi *et al.*, 1998), PKA (Cheng *et al.*, 1998), and PKB (Alessi *et al.*, 1997; Stephens *et al.*, 1998). The latter, which is activated in neutrophils upon their stimulation with chemoattractants (Hirsch *et al.*, in press), can also be directly activated via its PH domain by the lipid products of PI3K (Klippel *et al.*, 1997; Franke *et al.*, 1997). Neutrophil and macrophage PKB activation by chemoattractants is lost in PI3Kγ gene knock-out mice (Hirsch *et al.*, in press). Whether this is the reason for a decrease in chemotactic properties of PI3Kγ-null cells (see above) remains to be elucidated.

2.3.2. PH domain- containing tyrosine kinases.

The Tec family of cytoplasmic PH domain- containing tyrosine kinases includes Tec, Btk (Bruton's tyrosine kinase), Itk (Tsk), Bmx, and Txk kinases (reviewed in Neet and Hunter, 1996). These proteins are predominantly expressed in hematopoetic cells where their primary role is believed to be the control of cell differentiation downstream from cytokine or similar receptors (Satterthwaite *et al.*, 1998). PH domains of Tsk and Btk have been shown to interact with and to be responsible for kinase activation by βγ heterodimers of trimeric G proteins (Tsukada *et al.*, 1994; Langhans-Rajasekaran *et al.*, 1995). Phospholipid binding by the Btk PH domain was also shown (Fukuda *et al.*, 1996; Rameh *et al.*, 1997). Although Tec is expressed in a wide range of hematopoetic cells including neutrophils (Mano *et al.*, 1990), and Bmx is predominantly expressed in granulocytes (Kaukonen *et al.*, 1996; Weil *et al.*, 1997), their role in neutrophil signalling is not clear. Tec family protein kinases could potentially be involved in chemotaxis signalling downstream of G$_{\beta\gamma}$ or PI3Kγ, which would explain the reports of

sensitivity of neutrophil migration to tyrosine kinase inhibitors (Gaudry *et al.*, 1992; Yasui *et al.*, 1994; Xiao *et al.*, 1998).

IV. Role of small GTP-binding proteins of the Rho family in neutrophil motility.

1. Rho family G proteins, their regulators, and the actin cytoskeleton control.

Rho family of GTPases together with Ras-, Rab-, Ran-, and Arf-like proteins constitutes the superfamily of small GTP-binding proteins. The mammalian Rho family currently includes Rho (RhoA-C), Rac (Rac1-3), and Rnd (Rnd1-3) isoforms, as well as RhoG, Cdc42, TC10, RhoD, RhoG, and RhoH proteins (for a recent review, see Aspenström, 1999a). As other G proteins, Rho family members are active when bound to GTP. Hydrolyzing it to GDP, they become inactivated, while GDP to GTP exchange renders them active again. This on-off switch is controlled by several regulatory proteins (reviewed in Van Aelst and D'Souza-Schorey, 1997). GTPase activating proteins (GAPs) stimulate the GTP hydrolysis on Rho proteins and convert them to the switched-off state. The opposite role is played by guanine nucleotide exchange factors (GEFs) which facilitate the GDP to GTP substitution on Rho proteins. Finally, guanine nucleotide dissociation inhibitors (GDIs) are able to "freeze" Rho proteins in GDP- and, with a lower affinity, GTP-bound forms, counteracting the effects of other regulators. Additionally, GDIs can shuttle the Rho proteins from or to the plasma membrane, an important site of their action (Olofsson, 1999).

Several functions of Rho proteins were found in different cells. Transcription regulation by Rac and Cdc42 via the control of Jun kinase is rather ubiquitous (Symons, 1996), while some other activities, like granulocyte respiratory burst activation by Rac isozymes (Bokoch, 1994), are more restricted. However, the overwhelming role of Rho proteins, established in all eukaryotic cells tested, is the control of the actin cytoskeleton (Hall, 1998; Ridley, 1999). The classical pattern of the cytoskeleton regulation by Rho proteins has been obtained in studies with fibroblasts. In this system, cell stimulation with a seven transmembrane helix receptor agonist LPA induces formation of stress fibres, thick long bundles of actin-myosin filaments necessary for firm cell adhesion to the substratum. The action of LPA could be mimicked by microinjection of constitutively active form of RhoA protein; moreover, inhibiting RhoA could prevent stress fibre formation by LPA (Ridley and Hall 1992). Fibroblast stimulation with growth factors or a seven transmembrane helix receptor agonist bombesin induced lamellopodia and membrane ruffling, key structures in cell motility, and this action was shown to be transduced by Rac1 protein (Ridley *et al.*, 1992). Finally, another serpentine receptor ligand bradykinin induces long finger-like protrusions called

filopodia in fibroblasts, and Cdc42 was identified as a key regulator of this phenomenon (Kozma *et al*., 1995; Nobes *et al*., 1995).

The differential action of Rho, Rac, and Cdc42 on the fibroblast actin cytoskeleton was reproduced in other cell systems, such as neurones, epithelial and mast cells (Norman *et al*., 1994; Ridley *et al*., 1995; Kozma *et al*., 1997). By microinjection studies in macrophages, Ridley and coworkers have demonstrated that macrophage motility in GM-CSF gradients was inhibited by counteracting Rho and Rac proteins, while Cdc42 block could prevent the gradient perception by the motile macrophage but not the motility *per ce* (Allen *et al*., 1998). As in fibroblasts, Cdc42 was shown to control filopodia formation in macrophages, and Rho and Rac were inducing stress fibres and lamellopodia, respectively (Allen *et al*., 1997).

In neutrophils, Rac, Rho, and Cdc42 were reported activated and partially translocated to the plasma membrane upon cell stimulation with seven transmembrane helix receptor agonists (Quinn *et al*., 1993; Bokoch *et al*., 1994; Benard *et al*., 1999). Several neutrophil functions dependent on the actin network have been shown to be under regulation of Rho proteins. Inhibition of Rho by C3 toxin eliminates neutrophil chemotaxis (Stasia *et al*., 1991) by adhesion impairment (Laudanna *et al*., 1996). In addition to trimeric G proteins, a role of a small G protein in fMLP- or GTPγS- induced actin polymerization was suggested by studies in permeabilized neutrophils (Therrien and Naccache, 1989; Redmond *et al*., 1994). In a cell-free system from neutrophil cytosol this small G protein was shown to belong to the Rho family, since it was inactivated by recombinant RhoGDI and *Clostridium difficile* toxin B, both specific inhibitors of Rho family proteins (Katanaev and Wymann, 1998a). The molecular nature of this G protein was suggested to be (Zigmond *et al*., 1997) or to be not (Katanaev and Wymann, 1998a) identical to Cdc42. In intact cells, using gene inactivation by homologous recombination, a crucial role of Rac2 in transducing fMLP, LTB4, and IL-8 signalling to actin polymerization and chemotaxis was demonstrated (Roberts *et al*., 1999). Additionally, neutrophil rolling on Glycam-1 was deficient in Rac2-less neutrophils (Roberts *et al*., 1999), in agreement with previous results obtained with T lymphocytes (Brenner *et al*., 1997). Altogether these data highlight a key role of Rho family proteins in transducing signalling to chemotaxis in neutrophils, supporting the results obtained with other leukocytes (Sanchez-Madrid *et al*., 1999; Reif and Cantrell, 1998).

2. Connecting serpentine receptor activation to Rho proteins.

How is activation of G protein- coupled receptors linked to Rho family proteins? Several possibilities exist, although none of them have been proved to be involved in chemotaxis signalling in mammalian cells. An intriguing connection between the α subunit of G_{13} protein and Rho has been recently proposed (Kozasa *et al*., 1998; Hart *et*

al., 1998). There, the direct binding of p115 RhoGEF to $G_{13\alpha}$ has been shown to stimulate the p115 RhoGEF-mediated GDP-GTP exchange on Rho (Hart *et al*., 1998). The interaction is achieved via the p115 RhoGEF's RGS (Regulators of G protein Signalling) domain, which can activate GTP hydrolysis on $G_{\alpha12}$ and $G_{\alpha13}$ (Kozasa *et al*., 1998). p115 RhoGEF plays a crucial role in Rho activation downstream from $G_{\alpha13}$ during development (Barrett *et al*., 1997). However, as explained above, G_i but not G_{12} or G_{13} trimeric G proteins signal to chemotaxis in neutrophils; moreover, their $\beta\gamma$ subunits are crucial for chemotaxis.

Most GEFs for Rho family proteins identified so far contain a PH domain (Cerione and Zheng, 1996), which is necessary for the cellular functioning of GEFs Dbl (Zheng *et al*., 1996), Lbc (Olson *et al*., 1997), and Tiam-1 (Michiels *et al*., 1997). The Dbl PH domain was shown to bind $G_{\beta\gamma}$ *in vitro* (Mahadevan *et al*., 1995), and *in vivo*, but this binding was not sufficient for Dbl activation (Nishida *et al*., 1999). In transfected COS-7 fibroblasts, chemoattractant receptor signalling to actin polymerization was proposed to be mediated by a $G_{\beta\gamma}$-PI3Kγ-Vav-Rac pathway, implicating the PH domain of the GEF Vav in its coupling to PI3Kγ (Ma *et al*., 1998). Although PH domains of the Rho GEFs Tiam-1 (Rameth *et al*., 1997) and Vav (Han *et al*., 1998) were shown to bind lipid products of PI3 kinases, this binding occurs with relatively low affinity and specificity (Bottomley *et al*., 1998; Lemmon, 1999) and is not confirmed in physiologic assays (Isakoff *et al*., 1998; Lemmon, 1999).

In yeasts, a connection of $G_{\beta\gamma}$ with Cdc24, the GEF for the small G protein Cdc42, regulates the directed growth (Nern and Arkowitz, 1998). This connection is achieved by a multiprotein assembly where the pivotal role is played by a scaffold protein Far1 (Butty *et al*., 1998). This essential protein binds Cdc24 recognizing a stretch of amino acids which is also present in mammalian Dbl and lies outside of the PH and Dbl homology domains (Nern and Arkowitz, 1998; Butty *et al*., 1998). No functional homologues of Far1 are identified up to now in higher eukaryotes. However, recent data on the ability of certain proteins (Nef, EPS8-E3B1) to activate Rac and Cdc42 by PH domain-independent interactions with their exchange factors Vav (Fackler *et al*., 1999) and Sos-1 (Scita *et al*., 1999) indicates that a link between trimeric and small G proteins mediated by protein-protein interactions might be involved in chemotaxis signalling in mammalian cells.

3. Connecting Rho proteins with the actin cytoskeleton in chemotaxis.

Several dozens of putative Rho protein targets has been identified (Van Aelst and D'Souza-Schorey, 1997; Aspenström, 1999b), and more appear every month. Some were proposed based on physical interactions in two hybrid systems, others established in functional assays. Despite of the abundance of the announced Rho protein effectors,

few links to the actin rearrangements were clearly described. We will concentrate on some Rho protein-actin cytoskeleton connections discovered recently, which could have implications in signal transduction to chemotaxis in motile cells.

3.1. Rac and Rho can control actin binding proteins by regulation of PIP$_2$ synthesis (Fig. 4).

Rho and Rac were shown to regulate PI(4,5)P$_2$ synthesis in fibroblasts and platelets, respectively (Chong *et al*., 1994; Hartwig *et al*., 1995). This is achieved by a physical interaction of a type I phosphatidylinositol-4-phosphate (PIP) 5-kinase with the small GTPases, which occurs *in vitro* in a GTP-independent manner (Tolias *et al*., 1995; Ren *et al*., 1996). *In vivo*, Rac and PIP5-kinase form a multiprotein complex including also a diacylglycerol kinase and RhoGDI (Tolias *et al*., 1998). These findings are important since a multitude of actin binding proteins are regulatable by phosphoinositides in general and PIP$_2$ specifically (reviewed in Janmey, 1994). For example, capping proteins gelsolin and CapZ are dissociated from actin filaments under certain conditions *in vitro* by addition of PIP$_2$ micelles, allowing fast barbed end actin polymerization (Janmey *et al*., 1987; Heiss and Cooper, 1991). Moreover,
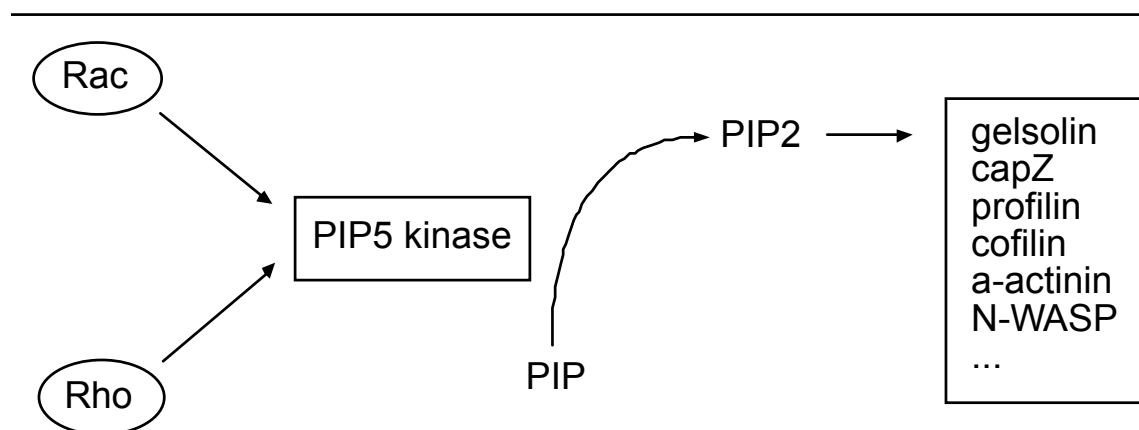
Fig. 4. Rac and Rho GTPases regulate activity of PIP (phosphatidylinositol-4-phosphate) 5-kinase, inducing production of PIP$_2$, which in turn controls the activity of many actin-binding proteins via their phospholipid-binding domains.

phosphoinositide delivery to permeabilized platelets induced cellular F-actin decapping (Hartwig *et al*., 1995), while overexpression of PIP5-kinase in fibroblasts led to massive actin polymerization (Shibasaki *et al*., 1997). A link between Rac and gelsolin was reported based on an inability of fibroblasts from gelsolin knock-out mice to exert Rac-transduced cytoskeletal changes (Azuma *et al*., 1998). These data have led to a model,

where Rho GTPase constitutive interaction with the PIP5-kinase results upon cell activation in increased production of PIP$_2$ which in turn may decap actin filaments allowing their elongation at the plasma membrane (Carpenter *et al*., 1999; Janmey, 1998). However, in contrast to platelets, most of the cells including neutrophils respond with a rapid decrease and not increase of PIP$_2$ when stimulated (Korchak *et al*., 1985). While local increases in PIP$_2$ upon neutrophil stimulation are not excluded, this model remains neither proved nor disproved for neutrophils.

3.2. Rac and Rho can stabilize actin filaments inducing phosphorylation of cofilin (Fig. 5).

      Cofilin is an essential protein ubiquitously expressed in eukaryotes (see (Bamburg *et al*., 1999) for a review). In *Dictiostelium* amoebae, cofilin overexpression stimulated cell migration (Aizawa *et al*., 1996). Cofilin and other members of its family are unique in its ability to increase the treadmilling of actin filaments (Carlier and Pantaloni, 1997). Additionally, cofilin was shown to severe actin filaments, creating
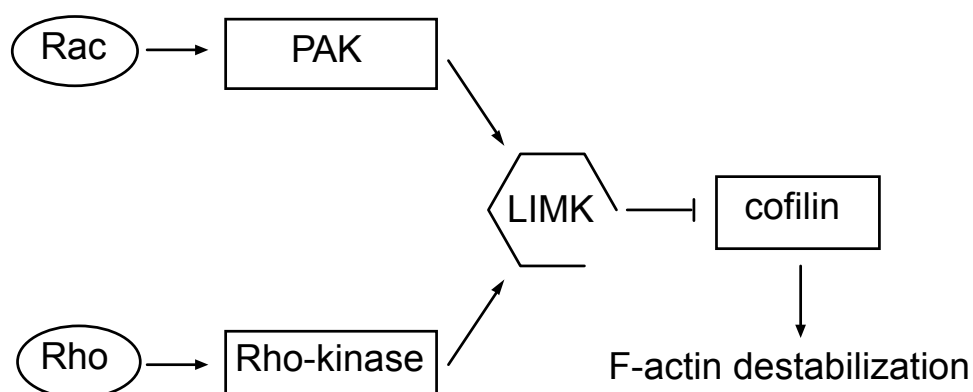
Fig. 5. Rac via PAK (p21-activated kinase) and Rho via Rho-kinase phosphorylate LIM kinase (LIMK), which in turn phosphorylates cofilin on Ser3. This leads to cofilin inactivation and prevention of depolymerization of actin filaments.

free barbed ends (Maciver *et al*., 1991). Cofilin activities are controlled by phosphorylation on Ser3 (Moriyama *et al*., 1996). The kinase phosphorylating and inactivating cofilin was demonstrated to be the LIM-kinase 1, (Arber *et al*., 1998; Yang *et al*., 1998), a protein defective in Wiliams syndrome patients (Frangiskakis *et al*., 1996). Overexpression of LIMK-1 in transfected cells led to accumulation of actin

cytoskeleton and reversed cofilin-induced actin depolymerization, moreover, LIMK-1 mediated actin rearrangements downstream from Rac and insulin (Arber *et al*., 1998; Yang *et al*., 1998). Rac-induced activation of LIMK-1 is indirect and may be mediated by PAK1, a long-known target of Rac and Cdc42 (see (Daniels and Bokoch, 1999) for a review). Chemoattractants induce rapid activation of several PAK isoforms and their translocation to lamellopodia in neutrophils (Huang *et al.*, 1988; Dharmawardhane *et al.*, 1999). PAK1 was shown to phosphorylate LIMK-1 and thus increase its ability to phosphorylate cofilin; Rac and Cdc42 were able to stimulate the PAK1 association with LIMK-1 (Edwards *et al.*, 1999). Moreover, dominant negative LIMK-1 interfered with the Cdc42-, Rac-, and PAK1- induced cytoskeletal changes in BHT cells (Edwards *et al.*, 1999). In addition to Rac and Cdc42, Rho was also shown to induce cofilin phosphorylation in cultured cells via LIMK-1; this effect is mediated by Rho-induced activation of Rho-kinase (also called ROCK, or ROCK I, or ROKα) which in turn phosphorylates LIMK-1 (Maekawa *et al.*, 1999). Thus, in cell cultures different Rho proteins seem to converge their signalling pathways to stimulate LIMK-1 and deactivate cofilin, which may lead to prevention of F-actin depolymerization and result in F-actin increase. To produce different phenotypes, this pathway must be accompanied with other pathways which are used differently by different Rho proteins. In highly motile cells like neutrophils half of cofilin is phosphorylated under resting conditions and cell stimulation leads to its rapid dephosphorylation (Okada *et al.*, 1996). This is accompanied by cofilin redistribution from the cytoplasm to F-actin rich membrane ruffles (Heyworth *et al.*, 1997; Djafarzadeh *et al.*, 1997), where its activity might be required for rapid reorganization of actin cytoskeleton.

3.3. Regulation of myosin phosphorylation by Rho proteins (Fig. 6).

 Myosins are motor proteins indispensable for muscle contraction, cellular trafficking, and cell motility (Harrington and Rodgers, 1984; Warrick and Spudich, 1987). Disruption of myosin II in *D. discoideum* leads to defects in cytokinesis and fruit body development (Knecht and Loomis, 1987; De Lozanne and Spudich, 1987), while yeast myosins are crucial for cytokinesis and actin cytoskeleton organization (Goodson *et al.*, 1996; Kitayama *et al.*, 1997). In a chemotacting neutrophil, myosin is localized in the lamellopodue (Valerius *et al.*, 1981), but is excluded from the filopodia (Takubo and Tatsumi, 1997). Myosin inhibitors prevent neutrophil transmigration across colonic epithelial cells (Hofman *et al.*, 1999) and oscillatory shape changes in neutrophils stimulated with LTB4 and PAF (Rengan and Omann, 1999). Phosphorylation has been shown to control the activities of all myosins studied so far. In case of the myosin II light chain (MLC), its phosphorylation on Ser19 results in an increase of the actin-activated ATPase activity of the myosin and thus in stimulated contraction (Tan *et al.*, 1992). In motile cells (Adelstein 1973; Kuczmarski and Spudich, 1980) including

neutrophils (Fechheimer and Zigmond, 1983), MLC is phosphorylated upon stimulation, implying a role of myosin phosphorylation in cell migration. The phosphorylation state of MLC has been shown to be controlled by several enzymes, Rho-kinase, an effector of Rho, being one of them (Amano *et al*., 1996; Kureishi *et al*., 1997). Rho-kinase has also another way of stimulating MLC phosphorylation: it can phosphorylate MLC phosphatase, rendering it inactive (Kimura *et al*., 1996). Importantly, Rho-kinase is present in neutrophils and mediates
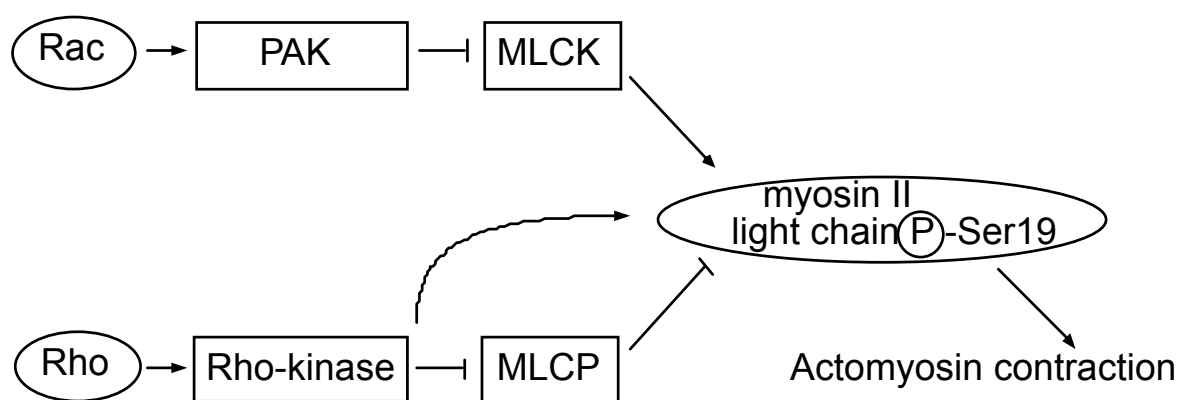
Fig. 6. Regulation of the myosin phosphorylation status by Rho GTPases. Rho-activated Rho-kinase can induce phosphorylation of Ser19 of the myosin II light chain either directly or phosphorylating and thus inhibiting the myosin light chain phosphatase (MLCP). Increase in the myosin II light chain phosphorylation leads to an increase in myosin-dependent contractility. An opposite action is played by Rac, which through PAK (p21-activated kinase) can inhibit the myosin light chain kinase (MLCK).

chemoattractant-induced MLC phosphorylation in these cells (Niggli, 1999). Moreover, pharmacological approaches have suggested that Rho-kinase activation is necessary for neutrophil polarization and chemokinesis (Niggli, 1999). The differential regulation of MLC phosphorylation may also explain the long-observed fact that Rho on one hand and Rac or Cdc42 on the other have antagonistic effects on cytoskeleton in many systems. Indeed, a recent work has shown that PAK, an effector of Rac and Cdc42, inactivates MLC kinase (Sanders *et al*., 1999), the major regulator of MLC phosphorylation identified in a multitude of cell types (Tan *et al*., 1992). Thus the myosin II- based contractility can be counterregulated by the Rac/Cdc42-PAK and Rho-

Rho-kinase pathways, which might operate such a complex phenomenon as cell motility.

3.4. Kinase-independent regulation of actin cytoskeleton.

In the examples listed above, lipid or protein kinases were proposed to be downstream targets of Rho proteins. In addition to the above-mentioned, a tyrosine kinase (Ridley and Hall, 1994), PKCζ (Laudanna *et al.*, 1998), and others (Aspenstrom, 1999b) were proposed to act downstream of Rho proteins in different systems. However, in permeabilyzed neutrophils GTPγS induces actin polymerization in a manner apparently independent from ATP (Redmond *et al.*, 1994). Similarly, in a cell-free system from neutrophil cytosol, lipid and protein kinases are not involved in propagation of the signal from Rho proteins to actin polymerization (Katanaev and Wymann, 1998a). Several non-kinase targets of Rho proteins have been proposed (reviewed in (Aspenström, 1999b)), like the Wiskott-Aldrich syndrome protein (WASP) (Snapper and Rosen, 1999) and its relatives N-WASP and Scar/WAVE.

3.5. Cdc42 can induce actin polymerization activating Arp2/3 via N-WASP (Fig. 7).

In a cell-free system from *Xenopus* oocytes, Cdc42 was shown to induce *de novo* actin polymerization (Ma *et al.*, 1998a; Moreau and Way, 1998). Using biochemical approach Kirschner and coworkers have demonstrated that N-WASP and Arp2/3 complex are necessary and sufficient to transduce the signal from GTP-loaded Cdc42 to actin (Ma *et al.*, 1998b; Rohatgi *et al.*, 1999), for the first time reconstituting a molecular link between a Rho protein and induction of actin polymerization. A role of the Arp2/3 complex in Rho-protein induced actin polymerization was also demonstrated in extracts of *Acanthamoeba* (Mullins and Pollard, 1999). Arp2/3 is a complex of seven proteins of the molecular weight ranging from 16 to 47 kDa, two of which are actin-related proteins 2 and 3, hence the name. The complex is ubiquitously expressed in eukaryotic cells and has been purified from amoebae (Machesky *et al.*, 1994), yeasts (Winter *et al.*, 1997), *Xenopus* (Ma *et al.*, 1998a), human platelets (Welsch *et al.*, 1997) and neutrophils (Machesky *et al.*, 1997). Arp2/3 is able to bind to the sides of actin filaments bundling them (Mullins *et al.*, 1997; Mullins *et al.*, 1998a). Moreover, Arp2/3 can establish branching points, so called Y-junctions, on the filaments (Mullins *et al.*, 1998b) resulting in extremely branched filament organization in the leading edge of some cells (Svitkina and Borisy, 1999). But the key function of Arp2/3 is its ability to nucleate actin filaments (Mullins *et al.*, 1998b; Welch *et al.*, 1998), bypassing the rate-limitig step in *de novo* actin polymerization (see Pollard and Cooper, 1986). Bound with high affinity to the pointed end of the filament, Arp2/3 allows rapid elongation at the barbed end. The ability of Arp2/3 to nucleate barbed-end actin polymerization is dramatically increased by WASP (Yarar *et al.*, 1999) and its relatives Scar/WAVE

(Machesky *et al.*, 1999) and N-WASP (Rohatgi *et al.*, 1999), which bind the p21 subunit of Arp2/3 (Machesky and Insall, 1998). WASPs are targets of GTP-loaded Cdc42 and Rac and induce actin polymerization when overexpressed in cultured cells (Aspenström *et al.*, 1996; Symons *et al.*, 1996; Kolluri *et al.*, 1996; Miki *et al.*, 1996; Miki *et al.*, 1998a; Miki *et al.*, 1998b). Their multidomain structure allows a complex regulation pattern (Featherstone, 1997). The fact that the C-terminal half of Scar/WAVE
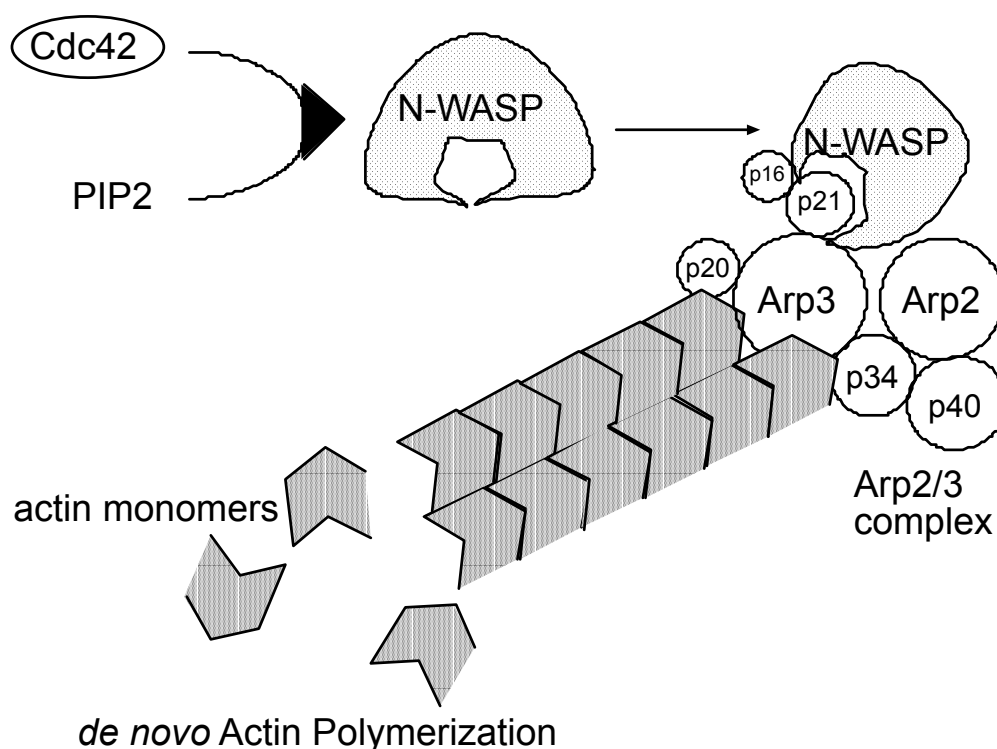
Fig. 7. Cdc42 can stimulate *de novo* actin polymerization via a kinase-independent mechanism. Cdc42 (together with PIP2) induces a conformational change in N-WASP, unmasking the binding site for p21 of Arp2/3. Activated Arp2/3 then forms nuclei for new actin filaments, which are rapidly elongated at their barbed ends. Topology of the subunits of Arp2/3 is based on the published model (Mullins *et al.*, 1997).

and N-WASP is more potent in Arp2/3 activation may indicate that the Arp2/3-binding domain of these proteins is normally hidden (Machesky *et al.*, 1999; Rohatgi *et al.*, 1999). Binding of GTP-Cdc42 and phosphoinositides was shown to unmask the Arp2/3-activating capacity of the full-length N-WASP, which leads to rapid actin polymerization, constructing a new paradigm of Rho-protein- induced actin polymerization at the plasma membrane (Rohatgi *et al.*, 1999; Miki *et al.*, 1998a). The

relevance of this paradigm in regulation of neutrophil chemotaxis is not clarified yet. N-WASP expression is limited to brain, heart and lung (Miki *et al*., 1996), while Scar/WAVE expression is strictly limited to brain (Nagase *et al*. *et al*., 1996). Although WASP is expressed in hematopoetic cells (Snapper and Rosen *et al*., 1999), neutrophils from Wiskott-Aldrich syndrome patients chemotax normally in contrast to macrophages (Zicha *et al*., 1998). Recently, two new WASP family members, WAVE2-3, have been identified, of which WAVE2 is expressed ubiquitously including peripheral blood leukocytes (Suetsugu *et al*., 1999).

V. Concluding remarks.

Chemotaxis is a multicomponent process, built up of a combination of many individual cell responses which are orchestrated in a virtually obscure way by a moving cell. Signalling to their activation is initiated by chemoattractant receptors, most of which in neutrophils belong to the superfamily of seven-transmembrane helix receptors. To induce chemotaxis, these receptors activate trimeric G_i proteins, dissociating them to $G_{\alpha i}$ and $G_{\beta \gamma}$ subunits. The latter hands downstream the chemotaxis signalling courier. PI3Kγ is one of the proteins taking it up, but other proteins doing the same awaits identification. Through some more yet unrevealed partners, the signal achieves the members of Rho family G proteins. Through effectors like Rho-kinase, PAK, and WASP, Rho GTPases regulate a multitude of actin binding proteins. Myosin, gelsolin, cofilin, and Arp2/3 are among them, whose activities culminate at highly controlled in time and space actin rearrangements, staying behind cell motility.

RESULTS

1. GTPγS-induced actin polymerisation in vitro: ATP- and phosphoinositide-independent signalling via Rho-family proteins and a plasma membrane-associated guanine nucleotide exchange factor.
Katanaev VL, Wymann MP. J. Cell Sci. 1998: 111: 1583-1594.

GTPγS-induced actin polymerisation in vitro: ATP- and phosphoinositide-independent signalling via Rho-family proteins and a plasma membrane-associated guanine nucleotide exchange factor

Vladimir L. Katanaev and Matthias P. Wymann*

Institute of Biochemistry, Rue du Musée 5, CH-1700 Fribourg, Switzerland
*Author for correspondence (e-mail: matthiaspaul.wymann@unifr.ch)

SUMMARY

In a cell-free system from neutrophil cytosol GTPγS can induce an increase in the number of free filament barbed ends and massive actin polymerisation and cross-linking. GTPγS stimulation was susceptible to an excess of GDP, but not *Bordetella pertussis* toxin and could not be mimicked by aluminium fluoride, myristoylated GTPγS·$G_{i\alpha2}$ or $G_{\beta1\gamma2}$ subunits of trimeric G proteins. In contrast, RhoGDI and *Clostridium difficile* toxin B (inactivating Rho family proteins) completely abrogated the effect of GTPγS. When recombinant, constitutively activated and GTPγS-loaded Rac1, RhoA, or Cdc42 proteins alone or in combination were probed at concentrations >100 times the endogenous, however, they were ineffective. Purified Cdc42/Rac-interactive binding (CRIB) domain of WASP or C3 transferase did not prevent actin polymerisation by GTPγS. The action of GTPγS was blocked by mM [Mg^{2+}], unless a heat- and trypsin-sensitive component present in neutrophil plasma membrane was added. Liberation of barbed ends seems therefore to be mediated by a toxin B-sensitive cytosolic Rho-family protein, requiring a membrane-associated guanine nucleotide exchange factor (GEF) for its activation by GTPγS under physiologic conditions.

The inefficiency of various protein kinase and phosphatase inhibitors (staurosporine, genistein, wortmannin, okadaic acid and vanadate) and removal of ATP by apyrase, suggests that phosphate transfer reactions are not required for the downstream propagation of the GTPγS signal. Moreover, exogenously added phosphoinositides failed to induce actin polymerisation and a PtdIns(4,5)P_2-binding peptide did not interfere with the response to GTPγS. The speed and simplicity of the presented assay applicable to protein purification techniques will facilitate the further elucidation of the molecular partners involved in actin polymerisation.

Key words: Actin, Polymerisation, Cytoskeleton, Small G protein, Guanine nucleotide exchange factor, Signal transduction

INTRODUCTION

When stimulated with chemotactic agonists, neutrophils double their F actin content within seconds (Howard and Oresajo, 1985). This process was suggested to directly mediate lamellipod formation during locomotion and shape changes (Cooper, 1991; Theriot and Mitchison, 1991; Wymann et al., 1990; Mitchison and Cramer, 1996). Actin polymerisation is thought to be triggered by the removal of capping proteins from the filament's barbed (+, fast growing) ends, allowing the addition of further monomeric G actin (Schafer and Cooper, 1995).

In neutrophils, more than half of the total actin is in its monomeric form and bound to thymosin β4 (Safer et al., 1991; Cassimeris et al., 1992) or profilin (Carlsson et al., 1977) in 1:1 complexes. While thymosin β4 serves solely as a buffer for G actin, profilin forms a productive complex that can directly add actin to barbed, but not pointed ends (see Pantaloni and

Carlier, 1993, for references). It has been reported that the interactions between actin and various binding proteins like profilin (Lassing and Lindberg, 1985), CapZ (Heiss and Cooper, 1991) and gelsolin (Janmey and Stossel, 1989; Hartwig et al., 1996) can be disrupted by polyphosphoinositides (e.g. PtdIns 4-*P* and PtdIns(4,5)P_2). How capping proteins are removed from the barbed ends to allow the growth of actin filaments due to surface receptor stimulation, however, is not clear. A major advancement in the understanding of these processes was the observation of Hall and coworkers, that constitutively activated small GTP-binding proteins of the Rho family could trigger cytoskeletal rearrangements (Ridley, 1994). While Rac induced membrane ruffles (Ridley et al., 1992), Rho mediated the formation of stress fibres (Ridley and Hall, 1992) and Cdc42Hs generated filopodia (Nobes and Hall, 1995). That these proteins indeed transduce signals from growth factor and seven transmembrane helix receptors was demonstrated by dominant negative forms

inhibiting agonist-induced actin rearrangements (Nobes and Hall, 1995; Kozma et al., 1995; Ridley, 1994). The state of Rho family proteins themselves is controlled by GTPase activating proteins (GAP) (Lamarche and Hall, 1994), guanine nucleotide dissociation inhibitors (GDI) and guanine nucleotide exchange factors (GEF) (Boguski and McCormick, 1993). GEFs of the Dbl family contain as minimal elements a Dbl homology (DH) and a pleckstrin homology (PH) domain (see Cerione and Zheng, 1996, for a recent review) of which the latter has been suggested to interact with polyphosphoinositides (Harlan et al., 1994). Some of the known GEFs act on several targets, e.g. Dbl on Rho and Cdc42Hs (Hart et al., 1994; Cerione and Zheng, 1996), Tiam-1 on Rac1 and Cdc42Hs (Michiels et al., 1995), which might lead to a bifurcation of the incoming upstream signals. Downstream of Rho family proteins, various protein kinases are at work: Rho activates e.g. p164 Rho-associated kinase (p164$^{Rho-K/ROK\alpha}$), p160 Rho-associated coiled-coil-containing protein kinase (p160^{ROCK}) and protein kinase N (p128$^{PKN/PRK1/2}$) (see Tapon and Hall, 1997, for a comprehensive list); Rac and Cdc42 interact with e.g. the protein Ser/Thr p65^{PAK} and Tyr kinase p120^{ACK} (Manser et al., 1994). While the latter two contain a CRIB (Cdc42/Rac-interactive binding; Burbelo et al., 1995) domain as is also present in WASP (Wiskott-Aldrich syndrome protein; Aspenström et al., 1996; Symons et al., 1996), other Rac targets like p67^{phox} (Prigmore et al., 1995) or POR-1 (partner of Rac-1; Van Aelst et al., 1996) interact differently. Of these molecules, Rho-K has been shown to mediate lysophosphatidic acid (LPA)/Rho-induced formation of stress fibers (Amano et al., 1997) and WASP was reported to colocalize with Cdc42 in F-actin rich patches (Symons et al., 1996). Moreover, white blood cells of Wiskott-Aldrich syndrome patients show distorted shapes and a reduced number of microvilli compared to normal cells (Kirchhausen and Rosen, 1996).

In spite of the advancements in Rho family protein signalling, is it not clear how these events finally lead to the elongation of actin filaments. From experiments carried out in permeabilized, thrombin-stimulated platelets, Hartwig and coworkers (1995) have recently proposed a model where thrombin receptor-mediated Rac activation is coupled to increased activity of phosphatidylinositol 4- and 5-kinases (PI4K and PI5K) and the resynthesis of PtdIns(4,5)P_2. Elevated levels of PtdIns(4,5)P_2 would then dissociate PI-sensitive capping proteins from actin filament barbed ends and thus trigger actin polymerisation.

In contrast to platelets, neutrophils respond to G protein-coupled receptor stimulation with a drop in PtdIns(4,5)P_2 which correlates with the increase in F-actin. Moreover, actions interfering with changes in PtdIns(4,5)P_2, like the inhibition of PLCβ by cytosolic Ca^{2+} depletion (Bengtsson et al., 1988) or the inhibition of PI3K by wortmannin (Arcaro and Wymann, 1993), do not influence actin polymerisation and repetitive polymerisation/depolymerisation cycles observed at low agonist concentrations (Wymann et al., 1989, 1990; Omann et al., 1989; Arcaro and Wymann, 1993).

To provide a tool to close the gaps in understanding of the signalling leading from surface receptor stimulation to the increase in cellular F actin, we have devised a simple and fast in vitro assay that allows the detection of GTPγS-induced actin polymerisation in the absence of lipids. The present results demonstrate that GTPγS mediates filament elongation by the liberation of barbed ends, and requires the presence of a cytosolic, Rho family G protein and, in the presence of free Mg^{2+}, a membrane-associated guanine nucleotide exchange factor (GEF) activity.

MATERIALS AND METHODS

Materials

ATPγS, ADP, GTP, GDP, apyrase grade V, cytochalasin B, heparin, sodium orthovanadate, pertussis toxin, and trypsin were from Sigma; Lymphoprep from Nycomed; Benzonase from Merck; diisopropyl fluorophosphate (DFP) was purchased from Aldrich; leupeptin from Alexis Co.; pepstatin A, ATP, NAD$^+$ from Fluka. Several batches of GTPγS (tetralithium salt) were purchased from Sigma and Fluka. Phalloidin, rhodamine phalloidin, and N-(1-pyrene)iodoacetamide were from Molecular Probes; GDPβS, DNase I and UDP-glucose from Boehringer Mannheim; genistein from ICN; G150 Sepharose (medium grade) from Pharmacia; okadaic acid from Calbiochem; and UDP-[^{14}C]glucose was from Hartmann Analytic. PtdIns, PtdIns 4-P, and PtdIns(4,5)P_2 were from Fluka, dissolved in chloroform/methanol, dried, and sonicated in water before use.

Staurosporine was a kind gift from D. Fabbro, Ciba Geigy Ltd, Basel; wortmannin was kindly provided by T. G. Payne, Sandoz Pharma Ltd, Basel; rhodamine-labelled phosphoinositide-specific peptide (corresponding to gelsolin amino acids 160-169; Janmey et al., 1992) generously donated by P. Janmey, Brigham & Women's Hospital, Boston; and buffy coats were kindly prepared by the Swiss Red Cross Transfusion Center, Fribourg.

G$\beta_1\gamma_2$ complexes were purified from baculovirus infected Sf9 cells as described (Kozasa and Gilman, 1995), myristoylated G$_{i\alpha2}$ was purified from *Escherichia coli* cotransfected with a G$_{i\alpha2}$ expression plasmid and N-myristoyl transferase (Lee et al., 1994; Mumby and Lider, 1994). Plasmids and baculovirus for the latter procedures were kindly obtained from A. G. Gilman, University of Texas, Dallas. RhoGDI, V12Rac1 and V14RhoA (Ridley et al., 1992; Ridley and Hall, 1992) and C3 transferase (kindly given by L. A. Feig, Tufts University, Boston; Dillon and Feig, 1995) were purified from *E. coli* as GST-fusion proteins. After thrombin digestion, the proteins were purified as described. *E. coli* expressed reference proteins (V12Rac1, V14RhoA, V12Cdc42 and N17Cdc42) successfully used in microinjections were also obtained from A. Ridley, LICR, London. WASP expression plasmids to produce GST-fusions of WASP (amino acids 48-321), WASPΔCRIB (48-321 without the CRIB domain at 237-257) and WASP–CRIB (235-268, with a deleted WIP-binding domain) were generously donated by U. Francke, Stanford University, Stanford (Symons et al., 1996). *Clostridium difficile* toxin B (Just et al., 1995) and *Clostridium sordellii* (strain 6018) lethal toxin (Just et al., 1996; Genth et al., 1996) were a generous gift from I. Just, University of Freiburg, Germany.

Neutrophil isolation and subcellular fractionation

Human neutrophils were isolated as described by Böyum (1968) and remaining erythrocytes were lysed by ammonium chloride treatment. Neutrophils were washed twice in 0.9% NaCl, 50 μM CaCl$_2$ and resuspended in Hepes-potassium buffer (HKB, 135 mM KCl, 10 mM NaCl, 10 mM Hepes, 2 mM EDTA, pH 7.0, 10^8 cells/ ml) or Hepes-sodium buffer (HNaB, 138 mM NaCl, 4.6 mM KCl, 20 mM Hepes, 2 mM EDTA, pH 7.4). Membrane fractions were prepared from cells suspended in HKB without EDTA but supplemented with 3 mM MgCl$_2$/2 mM EGTA.

Cells were disrupted in the above buffers supplemented with 1 mM PMSF, 0.5 mM diisopropyl fluorophosphate (DFP), 20 μM leupeptin, 18 μM pepstatin, 12.5 units/ml benzone nuclease, and 5% glycerol by nitrogen cavitation (40 minutes, 35 bar) on ice. After centrifugation for 10 minutes at 1,300 *g* the supernatant was cleared for 45 minutes at 121,000 *g*.

To prepare plasma membranes and granules, the low speed supernatant from above was fractionated by a discontinuous sucrose gradient as described earlier (Abo and Segal, 1995). Plasma membranes and cytosol performed successfully in a cell-free NADPH oxidase assay (Abo and Segal, 1995). Samples were stored at −80°C without loss of activity.

Protein concentrations were determined with the Bradford (Bio-Rad) assay using BSA as a standard. ATP concentrations were determined using an ATP luciferase bioluminescence assay kit (CLSII, Boehringer Mannheim). Total ATP was measured by the release of bound nucleotides from proteins with 400 mM perchloric acid. Free ATP was determined by the direct addition of cytosolic samples to the luminescence assay.

In protease sensitivity experiments, plasma membranes (1.3 mg/ml of total protein) were incubated without or with 150 µg/ml trypsin for 2 hours at 37°C. DFP was added to 1 mM before membranes were applied to the actin polymerisation assay.

Analysis of actin aggregates

If not indicated otherwise, cytosol was diluted with HKB to 1.8 mg total protein/ml, and incubated at 37°C in the absence or presence of 50 µM GTPγS for 20 minutes. These samples were either: (i) fixed for microscopy with 10% *p*-formaldehyde for 10 minutes on ice, and supplied with 0.6 µM rhodamine phalloidin at least one hour before they were examined on a confocal microscope (Bio-Rad MRC 1024/ Nikon E800 optics), or (ii) centrifuged at 9,000 *g*, 5 minutes. The sediments were washed twice with HKB, denatured and applied to a 10% SDS-PAGE gel. Major actin-binding proteins were subjected to MALDI-TOF-MS on a PerSeptive Biosystem Voyager Elite mass spectrometer after in-gel trypsin digestion (for references see Cottrell and Sutton, 1996).

Actin polymerisation assay in a cell-free system

The property of rhodamine phalloidin enhancing its fluorescence by approximately a factor of ten after binding to F actin (Huang et al., 1992) was exploited to measure increases in the amount of F actin in a cell-free system. The assay was set up to display a maximal sensitivity in cytosolic fractions (data not shown). If not indicated otherwise, reactions were carried out in a total volume of 35 µl HKB (with free Mg^{2+} at less than 10 µM, as calculated according to (Martell and Smith, 1974) with 1.8 mg cytosolic protein/ml. After the indicated additions and preincubations (see below) either vehicle or GTPγS was added for 20 minutes at 37°C. Aliquots of 10 µl were then removed and added to 600 µl HKB with 16.5 nM rhodamine phalloidin. Fluorescence was measured 20 minutes later in a Perkin Elmer fluorescence spectrometer LS50B (Ex. 552 nm, slit 5 nm; Em. 580 nm, slit 20 nm). After subtraction of the background rhodamine phalloidin fluorescence, the fluorescence intensity is linearly related to the amount of F actin present (data not shown).

Free barbed ends assay

ATP·actin from rabbit skeletal muscles was isolated as described previously (Pardee and Spudich, 1982), labelled with *N*-(1-pyrene)iodoacetamide according to the method of DiNubile and Southwick (1988), and pyrenyl G actin was purified as in the method of MacLean-Fletcher and Pollard (1980), its concentration being determined according to the method of Carson et al. (1986). Cytosolic reaction mixtures were treated for 15 minutes as described above. Aliquots of 20 µl were subsequently mixed with 600 µl prewarmed HKB containing 0.5 µM pyrenyl G actin, and the kinetics of pyrenyl actin fluorescence was immediately followed at 27°C (Ex. 365 nm, slit 3 nm; Em. 387 nm, slit 10 nm). Under these conditions the initial rate of fluorescence increase is the measure of amount of free barbed ends added (Carson et al., 1986).

Bacterial toxins

Cytosolic fractions were preincubated with various toxins at 37°C

before addition of GTPγS. *B. pertussis* toxin (pre-activated with 1 mM ATP and DTT for 15 minutes at 37°C) and C3 transferase were used in the presence of 20 µM NAD^+ for ADP-ribosylations. *C. difficile* toxin B (Just et al., 1995) and *C. sordellii* (strain 6018) lethal toxin (Just et al., 1996; Popoff et al., 1996; Genth et al., 1996) glucosylated small G proteins with 50 µM UDP-glucose as a co-substrate. The activities of toxin B and lethal toxin were tested at nM concentrations on NIH 3T3 fibroblasts and were found to induce the expected morphological changes (Just et al., 1996).

Toxin B-mediated glucosylation was assessed using 50 nCi UDP-[^{14}C]glucose (50 µM final). After a 30 minute incubation at 37°C, samples were analysed for 10% trichloroacetic acid (TCA)-insoluble radioactivity or by SDS-PAGE followed by autoradiography.

### Preloading of recombinant G proteins with guanine nucleotides

$G_{i\alpha2}$ (0.19 mg/ml) was preloaded with 0.1-1 mM GTPγS in the presence of 20 mM $MgCl_2$ for 1 hour at 37°C (Carty and Iyengar, 1994). Rac1, RhoA and Cdc42 were preloaded with a 5-10 molar excess of GTP or GTPγS in the presence of 10 mM EDTA for 20 minutes at RT, terminating the reaction by addition of 20 mM $MgCl_2$ (Self and Hall, 1995).

RESULTS

GTPγS triggers F actin assembly and cross-linking in vitro

When high speed cytosolic fractions from human neutrophils were incubated with GTPγS, the formation of actin filaments and aggregates was observed microscopically: F actin could be detected by rhodamine phalloidin staining both before (data not shown) and after fixation of GTPγS treated cytosol with *p*-formaldehyde, which was added to prevent further actin rearrangements (Fig. 1). While filament bundles and aggregates were numerous and of considerable size due to GTPγS addition (≤30 µm), untreated cytosols displayed only occasionally aggregates of much smaller size (<<10 µm). To determine changes in cross-linked F actin, GTPγS treated cytosolic fractions and controls were centrifuged at low speed and actin was quantified by Coomassie staining. Compared to controls, GTPγS caused typically a 6.8 (±2.5, s.d., *n*=4)-fold increase in sedimentable actin, resulting in the sedimentation of about 16% of the total actin present in the cytosol. Two major proteins co-sedimenting were identified as ABP-280 and α-actinin.

Taking advantage of the observation of Huang et al. (1992) that rhodamine phalloidin fluorescence increases about 10-fold upon its binding to F actin we have developed a functional reconstitution assay for actin polymerisation. Using the assay we found that ≥1 mg of total cytosolic protein/ml in the presence of ≥5 µM GTPγS was necessary to induce significant actin polymerisation. Higher concentrations of GTPγS up to 50 µM further increased the total amount of F actin detected after 20 minutes of incubation and reached a plateau thereafter (Fig. 2A). When the time course of actin polymerisation in response to different amounts of GTPγS was examined, we observed a strong effect of increasing GTPγS concentrations on the rate of actin polymerisation during the first 10 minutes of the reaction (Fig. 2B). The polymerisation process reached its maximum at about 10-20 minutes and F actin levels remained constant up to 40 minutes to decrease slightly to 80 minutes. The de novo polymerised actin seems therefore to remain stable, indicating
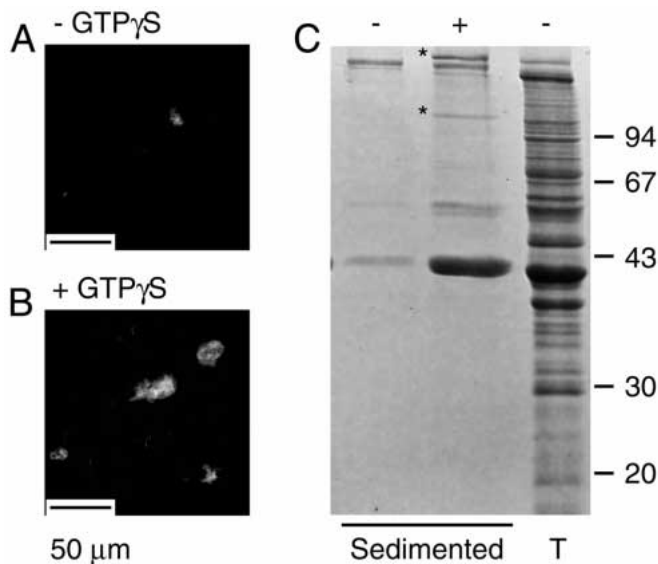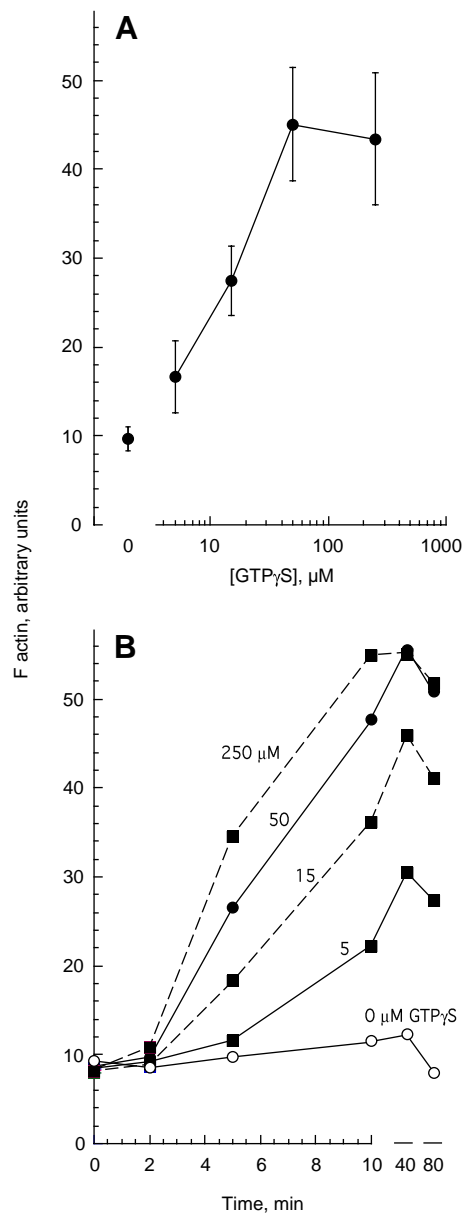
Fig. 1. GTPγS-mediated actin polymerisation and cross-linking. Cytosols from human neutrophils at a concentration of 1.8 mg/ml of total protein in HKB were incubated for 20 minutes in the absence (−, −GTPγS) or presence of 50 μM GTPγS (+, +GTPγS). (A,B) Samples for confocal microscopy were subsequently fixed with *p*-formaldehyde and stained with rhodamine phalloidin for F actin. (A) Largest aggregate found in sample; (B) representative field of view. Bar, 50 μm. (C) Alternatively, the treated samples were centrifuged at low speed, and washed sediments were subjected to SDS-PAGE and Coomassie blue staining. Total protein applied before sedimentation (T) corresponds to $^{1}/_{10}$ of the material yielding the sediments in first two lanes (Sedimented). Positions of molecular mass standards are indicated to the right (in kDa). Data are representative for ≥3 experiments. Asterisks indicate the positions of ABP-280 and α-actinin (apparent molecular mass 105 kDa), as identified by peptide mass fingerprinting analysis.

Fig. 2. Effect of increasing concentrations of GTPγS on end point and kinetics of actin polymerisation. (A) Reaction mixtures with 1.8 mg cytosolic protein/ml were incubated with the indicated concentrations of GTPγS for 20 minutes before F actin was quantified (mean ± s.e.m., *n*≥3). (B) Samples were incubated with the indicated concentrations of GTPγS for the indicated times before aliquots were removed for F actin determination (data representative for 6 experiments).

that the system reaches a new equilibrium at higher F actin levels due to GTPγS stimulation. This can be explained by the observation that free barbed ends could not be detected beyond 30 minutes after GTPγS addition (data not shown), indicating that the liberation of barbed ends is a transient process.

GTPγS is the only nucleotide to stimulate actin polymerisation

Addition of 50 μM GTPγS to cytosolic reaction mixtures increased the amount of filamentous actin by a factor of 5.17±0.59 (mean ± s.e.m., *n*>30). All tested batches of GTPγS exhibited the same effect, which was not mediated by lithium ions associated with GTPγS: LiCl up to 2 mM did not affect F actin levels (data not shown). Other nucleotides tested (ATP, ATPγS, ADP, GDP, GDPβS, all at 100 μM) failed to display any stimulatory action on actin polymerisation (*n*≥3). GTP at 100 μM induced a slight increase in F actin, and was at 1 mM about 50% as effective as GTPγS (data not shown). The absence of a stimulatory action of 100 μM ATP or ATPγS on the polymerisation process demonstrates that the effect of GTPγS does not involve the transfer of its γ-thiophosphate group to ADP by a nucleoside diphosphokinase (Parks and Agarwal, 1973).

When an excess of GDP (1 mM) was added together with

GTPγS, the effect of the latter was completely inhibited, which is a further indication of the specific action of GTPγS on a signalling molecule (Fig. 3). ADP or UDP (1 mM) added shortly before GTPγS had no effect, but prolonged preincubations increasingly lowered basal and GTPγS-controlled F actin levels (data not shown).
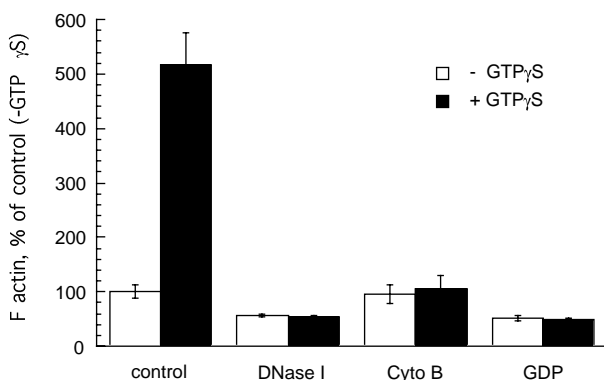
GTPγS increases the number of free barbed ends

An excess (30 μM) of DNase I, sequestrating monomeric actin

(Mannherz et al., 1975), decreased basal F actin levels as compared to untreated cytosolic reaction mixtures and completely abolished the GTPγS-mediated actin polymerisation (Fig. 3). Cytochalasin B, on the other hand, did not affect the basal signal, but potently blocked the GTPγS-induced increase in F actin. This suggests that the barbed ends (fast growing, + ends) of actin filaments have to be accessible for GTPγS to be able to trigger polymerisation. To test if the number of barbed ends indeed increased, cytosolic reaction mixtures were stimulated with 50 μM GTPγS for 15 minutes at 37°C and aliquots were subsequently tested for barbed end nucleation activity (Carson et al., 1986). While cytosol incubated in the absence of GTPγS did not trigger an increase in pyrenyl actin fluorescence, GTPγS treated samples led to a rapid incorporation of pyrenyl actin into filaments, and thus to an increase in fluorescence (Fig. 4). Cytochalasin B (5 μM) in the measurement cuvette blocked this increase, while variations of the actin concentration did not influence the initial rate of the process. Altogether, this illustrates that GTPγS promoted an increase of available barbed ends. Interestingly, no free barbed ends could be detected 30 minutes after addition of GTPγS at 37°C (data not shown). However, when samples were collected 15 minutes after GTPγS addition and then kept on ice, cytosol retained its nucleating activity for prolonged times. This might indicate that at 37°C, but not 0°C, GTPγS triggers some feedback reactions leading to recapping of barbed ends.

### The role of protein-, lipid kinases and phosphatases

The effect of two broad band protein kinase inhibitors, genistein targeting protein tyrosine kinases (Akiyama and Ogawara, 1991) and staurosporine affecting Ser/Thr kinases (Tamaoki, 1991), was examined. Both inhibitors (genistein at 50 μM and staurosporine at 500 nM) did not interfere with GTPγS-mediated in vitro actin polymerisation. Wortmannin, at nM concentrations a specific inhibitor of PI 3-kinases (Arcaro and Wymann, 1993; Yano et al., 1993), affects at μM concentrations some other lipid and protein kinases (see Wymann et al., 1996, for references). Even at 1 μM, however, the substance remained without effect (Table 1).

When cytosol was exposed to 0.5 units/ml of apyrase (converting ATP and ADP to AMP and P_i; Kettlun et al., 1982) for 70 minutes on ice, >99% of the free ATP remaining after cell fractionation (initially 2.5 μM) was hydrolysed resulting in an [ATP] of about 22 nM. The amount of protein-bound ATP, however, was only reduced from 2.1 μM to approx. 220 nM. At the same time, GTPγS was still able to produce a >2-fold increase in F actin, the partial inhibitory effect of apyrase being best explained by the loss of actin-bound ATP. Similarly, prolonged incubations with 1 mM ADP before GTPγS addition decreased subsequent actin polymerisation, most likely also interfering by the elimination of ATP·actin from the system. The above, the inhibitor data and the fact that addition of 1 mM ATP to cytosolic reaction mixtures did not enhance the GTPγS-mediated increase in F actin (data not shown), suggest that lipid- and protein kinase activities are not involved in the GTPγS-mediated process.

Two protein phosphatase inhibitors, okadaic acid (Hardie et al., 1991) and vanadate (Gordon, 1991), were tested on GTPγS-stimulated actin polymerisation (Table 1). Okadaic acid at 0.5 μM did not display a significant effect, while vanadate at 3 mM slightly reduced both, the basal and GTPγS-induced F actin levels. The fold increase in polymerised actin triggered by GTPγS, however, remained unchanged. Vanadate seems therefore to mediate its weak action not via inhibition of protein phosphatases, but rather by its direct interaction with
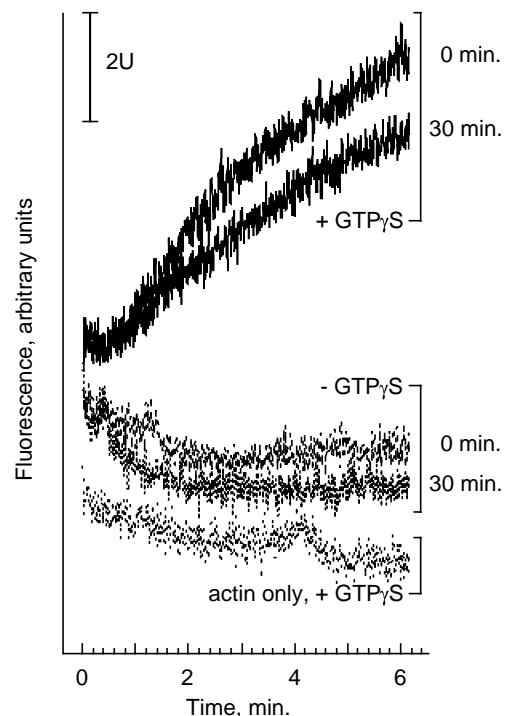
Fig. 4. Barbed end nucleation assay. Cytosolic reaction mixtures were incubated with 50 μM GTPγS (solid lines) or vehicle only (broken lines) for 15 minutes, before aliquots were transferred directly (0 minutes) to the measurement cuvette containing 0.5 μM pyrenyl G actin or kept on ice before the assay (for 30 minutes). The fluorescence of pyrenylated rabbit skeletal muscle G actin after the addition of 50 μM GTPγS is represented by the dotted curve. The curves were set off from each other for clarity (representative for 5 experiments).

Fig. 3. Inhibition of GTPγS-mediated actin polymerisation by DNase I, cytochalasin B, and GDP. Directly after the addition of vehicle (control), or 30 μM DNase I, 5 μM cytochalasin B, or 1 mM GDP, cytosolic reaction mixtures were incubated in the absence (open bars) or presence of 50 μM GTPγS (closed bar) for 30 minutes at 37°C, before F actin contents were measured. Data is presented as percentage of the control without additions (mean ± s.e.m., $n \geq 3$).

Table 1. Treatments not affecting GTPγS-mediated actin polymerisation

Additions	Max. concentrations used	Action of treatment
Genistein	50 μM	Broad protein tyrosine kinase inhibitor
Staurosporine	500 nM	Broad protein Ser/Thr kinase inhibitor
Wortmannin	1 μM	PI 3-kinase inhibitor
PPI-binding peptide	10 μM	Binds PtdIns(4,5)P_2
Na-orthovanadate	3 mM	Broad protein phosphatase inhibitor
Okadaic acid	250 nM	Broad protein phosphatase inhibitor
Aluminium fluoride*	20 mM NaF	Activator of trimeric G proteins
	10 μM AlCl$_3$	
B. pertussis toxin**	2 μg/ml	ADP-ribosylation of $G_{i\alpha}$ subunits
$G_{i\alpha}2$·GTPγS*	15 μg/ml	Activated $G_{i\alpha}2$ subunits
$G_{\beta 1\gamma 2}$*	20 μg/ml	βγ subunit of trimeric G proteins
C. sordellii lethal toxin		
strain 6018***	10 μg/ml	Glucosylation of Rac1, Ras, Rap, Ral
C3 transferase**,‡	100 μg/ml	ADP-ribosylation of RhoA, B, C
V12Rac1·GTPγS*	10 μM	Constitutively activated Rac1
V14RhoA·GTPγS*	10 μM	Constitutively activated RhoA
V12Cdc42·GTPγS*	10 μM	Constitutively activated Cdc42
Permutations of Rho proteins§	tot. 12 μM	See V12Rac1, V14RhoA, V12Cdc42
N17Cdc42¶	5 μM	Dominant negative form of Cdc42
GST-WASP-CRIB domain	30 μM	Binds Cdc42·GTP and some Rac·GTP

Protein and lipid kinase and phosphatase inhibitors were preincubated with cytosol for 10 minutes at 37°C before GTPγS addition.

*Actin polymerisation was studied in the absence of further added GTPγS.

**Used with 20 μM NAD$^+$.

***Used with 50 μM UDP-glucose and 0.1-0.4 mM free Mn^{2+} for up to 1 h, before complexation of divalent cations with EDTA and addition of GTPγS.

‡At the highest concentrations used, the C3 transferase preparations reduced polymerised actin by ca. 40%. This reduction, however, also occurred with heat inactivated preparations.

§Added to a total concentration of 12 μM. Combinations of 12, 6+6, 4+4+4 μM V12Rac1·GTPγS, V14RhoA·GTPγS and V12Cdc42·GTPγS were tested.

¶Was tested in the system containing plasma membrane and Mg^{2+} (see Fig. 7B for conditions). Identical results were obtained in the cytosolic system without membranes and Mg^{2+}.

actin filaments, as it has been reported before (Combeau and Carlier, 1988).

## Involvement of Rho-family but not trimeric GTP-binding proteins

The results presented above point to GTP-binding proteins being the mediators of the observed rise in F actin. Candidates might thus be either trimeric or small G proteins. To test the importance of trimeric G proteins, cytosols were pretreated with *B. pertussis* toxin, or aluminium fluoride, recombinant $G_{\beta 1\gamma 2}$ or GTPγS-loaded $G_{i\alpha}2$ were added. None of these treatments, however, showed any inhibitory or stimulatory effect (see Table 1).

C. difficile toxin B (inactivating Rho proteins by glucosylation using UDP-glucose as a co-substrate; Just et al., 1995), on the other hand, completely inhibited GTPγS-mediated actin polymerisation in a concentration dependent way. This inhibition correlated with the incorporation of [^{14}C]glucose into total TCA-precipitatable protein and into a 20 kDa family of proteins (Fig. 5). Additionally, we found that increasing amounts of recombinant RhoGDI eliminated the action of GTPγS, but did not affect basal F actin levels (Fig. 6). Pretreatment of the cytosol with 10 μg/ml *C. sordellii* lethal toxin, known to inactivate several ras-subfamily proteins and Rac1 (Just et al., 1996), could not prevent the action of GTPγS (Table 1). The stimulatory effect of GTPγS was also dependent on the free Mg^{2+} concentration and was completely blocked at 1 mM (Fig. 7A), which is typical for small, but not for trimeric G proteins (Self and Hall, 1995; Gilman, 1987). Altogether, the above results show that the target of GTPγS is not a trimeric, but a Rho family-related G protein. To elucidate the nature of the small G protein, we supplied the cytosolic reaction

mixtures with Rho proteins purified from *E. coli*. At 10 μM none of the constitutively activated and GTPγS-loaded V12Rac, V14RhoA and V12Cdc42 proteins could trigger actin polymerisation. Permutations of mixtures of these proteins (total combined concentration was 12 μM added as 12, 6/6 or 4/4/4 μM sets) were equally ineffective. GST-WASP fusion proteins were added to the cytosol to bind GTP-loaded Cdc42: GST-WASP (amino acids 48-321) and WASPΔCRIB (48-321, a.a. 237-257 deleted, used as a negative control) at 3 μM, and the GST fusion of the WASP CRIB domain (235-268) up to 30 μM all failed to interfere with GTPγS signalling. C3 transferase, ADP ribosylating RhoA-C (Dillon and Feig, 1995), did not produce any effect on the system at 5 μg. When concentrations where elevated to 100 μg/ml, an approx. 40% drop in GTPγS-mediated actin polymerisation could be achieved. This reduction, however, was independent of the presence of NAD$^+$ and heat inactivation of C3 (Table 1). In the presence of 25 μM PtdIns, reported to stimulate the access of bacterial toxins to Rho proteins due to their dissociation from RhoGDI (see Dillon and Feig, 1995, for references), virtually no effect of C3 transferase was observed (data not shown).

Membrane-associated protein(s) reverse the inhibitory action of Mg^{2+}

As shown in Fig. 7A, free Mg^{2+} inhibits GTPγS-induced actin polymerisation in a concentration dependent way. While the basal level of F actin was not affected significantly, GTPγS-mediated increases were totally abolished at 1 mM free Mg^{2+}. This behaviour of the cytosolic system suggests, that it does not contain a guanine nucleotide exchange factor (GEF) activity that would allow the nucleotide exchange on the aftersought G protein at physiological Mg^{2+} concentrations.
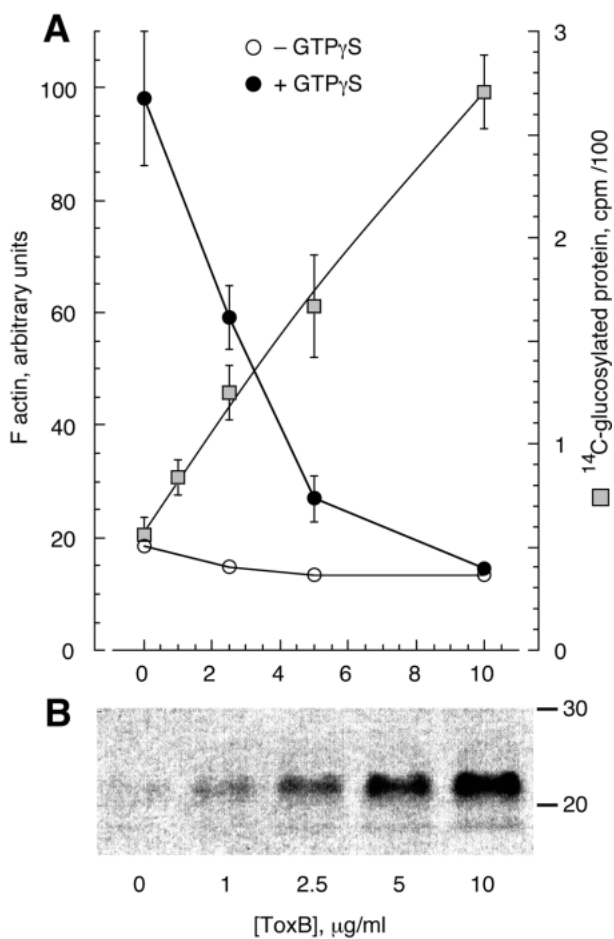
Fig. 5. Inhibition of GTPγS-mediated actin polymerisation by *C. difficile* toxin B. The indicated amounts of toxin B (ToxB) with 50 μM UDP-glucose as co-substrate were incubated with cytosol for 30 minutes at 37°C. (A) Aliquots were thereafter incubated with vehicle (open circles) or 50 μM GTPγS (closed circles) before the F actin content was determined. Covalent [^{14}C]glucosylation of proteins was assessed by the measurement of radioactivity present in the trichloroacetic acid-insoluble material (grey squares; mean ± s.e.m., *n*=3; s.e.m. bars omitted where smaller than the symbols).
(B) Alternatively, samples were denatured and subjected to SDS-PAGE before to the detection of [^{14}C]glucosylated protein. The location of molecular mass markers is indicated to the right (representative for 3 experiments).

Fig. 6. Recombinant RhoGDI inhibits the effect of GTPγS. The indicated amounts of rhoGDI purified from *E. coli* were preincubated with cytosolic reaction mixtures. Vehicle (open circles) or 50 μM GTPγS (closed circles) were added subsequently. After 25 minutes at 37°C F actin was quantified (mean ± s.e.m., *n*=3). Values obtained in the presence of GTPγS for RhoGDI dilution buffer only or RhoGDI denatured by boiling are denoted by a closed triangle and square, respectively.

As many GEFs are membrane associated, we reconstituted our system by the addition of neutrophil plasma membrane. As demonstrated in Fig. 7B, addition of plasma membrane protein to 100 to 300 μg/ml, but not neutrophil granule membranes (data not shown), rescued the stimulatory effect of GTPγS in the presence of 1 mM free Mg^{2+}. While the response to GTPγS reached a plateau at about 180 μg membrane protein/ml, the basal levels of F actin slightly increased in a linear fashion. In the absence of free Mg^{2+} we could not detect any influence of plasma membrane preparations on actin polymerisation (data not shown). Dominant negative N17Cdc42 (5 μM) added to the system (+membranes and Mg^{2+}) in order to test whether the putative GEF would interact with Cdc42, could not prevent actin polymerisation.

As it has been reported before that PtdIns(4,5)P_2 exhibits GDP-dissociation activity on Cdc42 (Zheng et al., 1996), we tested the effects of pure polyphosphoinositides in cytosolic reaction mixtures. Unexpectedly, PtdIns, PtdIns4P and PtdIns(4,5)P_2 all inhibited GTPγS-mediated actin polymerisation completely in the absence of free Mg^{2+} at 25, 80 and 25 μM, respectively, and none of the tested lipids induced actin polymerisation by itself. Moreover, 10 μM of a rhodamine-labelled PtdIns(4,5)P_2-binding peptide derived from gelsolin (Janmey et al., 1992) did not block the action of GTPγS (higher concentrations of the peptide interfered with the assay and caused actin polymerisation). If free Mg^{2+} was set to 1 mM in cytosolic reaction mixtures, on the other hand, lipids compensated the inhibitory action of free Mg^{2+} on GTPγS-mediated action polymerisation (EC$_{50}$s for PtdIns, PtdIns4P and PtdIns(4,5)P_2 were 10, 100, and 120 μM, respectively), but did not induce an increase in F actin by themselves (≤240 μM). The decrease in potency of PtdIns >> PtdIns4P > PtdIns(4,5)P_2 is unlikely to be related to a previously observed GDP dissociation activity on Cdc42 and fits better with the lipid-induced dissociation of Rho proteins from RhoGDI (Chuang et al., 1993).

When plasma membrane preparations were exposed to trypsin or heat and then added to cytosol containing 1 mM free Mg^{2+}, the membrane-mediated rescue of the GTPγS-triggered response was eliminated (Fig. 7B,C). Most of the membrane associated activity could be preserved, if the serine protease inhibitor DFP was added before trypsin. These results further demonstrate that the active plasma membrane constituent which permits the action of GTPγS in the presence of high free Mg^{2+} is a protein and not a lipid.

In summary, our results reveal that GTPγS triggers actin polymerisation by the action of a toxin B-sensitive, RhoGDI-binding Rho family-related protein, which requires under physiologic conditions the presence of a membrane associated, putative GEF activity.
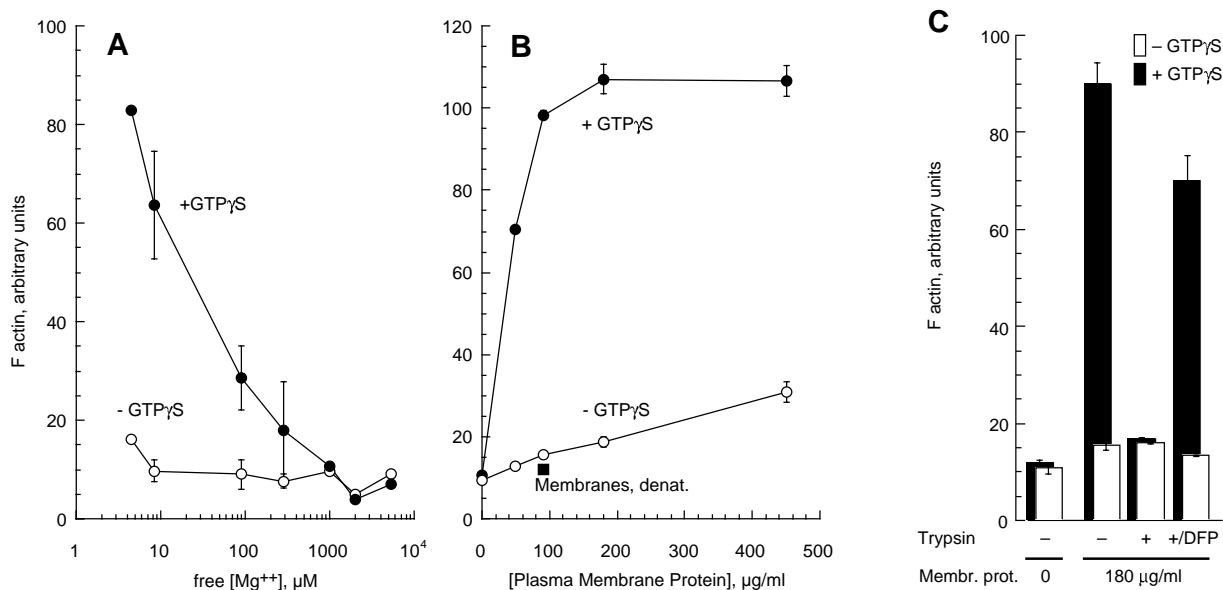
Fig. 7. Inhibition of GTPγS-triggered actin polymerisation by free Mg^{2+} and reversal by membrane proteins. (A) Increasing amounts of $MgCl_2$ were added to cytosolic reaction mixtures yielding the indicated free $[Mg^{2+}]$. Subsequently, samples were supplemented with 50 µM GTPγS (closed circles) or vehicle only (open circles) and incubated as above. (B) Cytosolic samples containing 1 mM free Mg^{2+} were combined with plasma membranes with the indicated quantity of membrane protein, before GTPγS or vehicle was added. Alternatively, membranes denatured by boiling were used in the presence of GTPγS (filled square). (C) Cytosolic samples as in B were supplemented with plasma membranes pretreated in the absence (-) or presence of trypsin (+) or trypsin and diisopropyl fluorophosphate (+/DFP). In all membrane samples DFP was brought to 1 mM before being added to cytosolic reaction mixtures. After all described incubations, F actin was quantified as above (mean ± s.e.m., $n{\geq}3$; deviations omitted where smaller than symbols).

DISCUSSION

GTPγS-mediated actin polymerisation: an in vitro approach

Although numerous actin-interacting proteins have been isolated, it is presently not clear how signals emerging from cell surface receptors trigger actin polymerisation. It has been recognised, however, that Rho family proteins relay these signals and that constitutively activated Rac, Rho and Cdc42 cause cytoskeletal rearrangements by themselves (Ridley, 1994; Ridley and Hall, 1992; Nobes and Hall, 1995; Nobes et al., 1995). Nevertheless, it is not understood how these small G proteins might cause e.g. the liberation of barbed ends to allow the elongation of actin filaments. This motivated us to develop in vitro assays to elucidate the mechanisms of signal-induced actin polymerisation.

We observed that GTPγS addition to neutrophil cytosolic fractions caused the appearance of F actin bundles and networks that grew so large that they could be easily viewed by light microscopy and sedimented by low speed centrifugation. Size, stability and appearance of the networks can be explained by the presence of ABP-280 (branching F actin at high angles; Gorlin et al., 1990), α-actinin (an actin bundling and network-forming crosslinker; Otto, 1994) and further unidentified actin-binding proteins. As cytosol after high speed centrifugation contains only filaments of less than 20 actin monomers (DiNubile and Southwick, 1988), these observations illustrate the dramatic effect of GTPγS on the elongation of actin filaments.

Based on the previously described increase in rhodamine phalloidin fluorescence upon binding to F actin (Huang et al.,

1992) we have composed an optimized assay to determine F actin changes in cytosolic samples. In comparison to other methods, we have drastically reduced both the amount of rhodamine phalloidin used and lowered the amount of total cytosolic protein required to about 40 µg/sample. The major advantage of the assay is, however, that the F actin content can be determined directly after sample treatment and that no centrifugation, washing steps or release of labelled phalloidin are required. The in vitro assay presented here is therefore the first fast and simple enough to be used along with protein purification schemes designed to identify molecules involved in the actin polymerisation process.

GTPγS liberates barbed ends

GTPγS-mediated actin polymerisation could be demonstrated before in permeabilized neutrophils (Therrien and Naccache, 1989; Bengtsson et al., 1990; Downey et al., 1990; Redmond et al., 1994) and was shown to be driven by the availability of free barbed ends (Tardif et al., 1995). In our cell-free system, both the end point levels and the rate of GTPγS-induced actin polymerisation increased with the amount of stimulator added to cytosol. Together with the observations that GTPγS increases the availability of free barbed ends and that cytochalasin B blocks GTPγS-mediated actin polymerisation, this suggests that GTPγS transiently removes capping proteins from free barbed ends or forms them de novo, similarly to what probably happens in vivo upon stimulation.

The role of protein-, lipid kinases and phosphatases, and ATP

To elucidate the role of protein and lipid kinases, we attempted

to block the GTPγS-mediated actin polymerisation with broad band inhibitors for protein tyrosine kinases (genistein; Akiyama and Ogawara, 1991), Ser/Thr protein kinases (staurosporine; Tamaoki, 1991) and PI 3-kinases (wortmannin; see Wymann et al., 1996). Even the use of elevated inhibitor concentrations did not interfere with the polymerisation response. This finding clearly excludes a variety of src- and EGF receptor-like tyrosine kinases, members of the protein kinase C family, and PI 3-kinase and related proteins from being downstream elements for the primary target of GTPγS in cytosolic fractions. This contrasts with the proposed involvement of a protein tyrosine kinase downstream of Rho in bombesin and lysophosphatidic acid-induced stress fibre formation in fibroblasts (Ridley and Hall, 1994).

As a variety of kinases might still escape the treatments above, apyrase was used to remove ATP from cytosol to eliminate phosphorylation reactions completely. Free ATP in cytosol was already lowered to about 2.5 μM after cell fractionation and decreased by a factor of >100 due the addition of apyrase. The GTPγS-induced actin polymerisation response was lowered in parallel to about $^1/_3$. As protein-bound ATP decreased to approximately $^1/_{10}$ of the initial concentration within the same time, it must be assumed that ATP was also lost from actin. It is most likely that this loss of the nucleotide interfered with the ability of actin to polymerise, but that ATP was not required for downstream kinase reactions. This is in agreement with the observations that addition of mM ATP did not enhance GTPγS-induced actin polymerisation and that mM ADP only showed inhibitory activity when incubated for prolonged periods allowing ATP/ADP exchange on actin. Redmond et al. (1994) have shown previously in streptolysin-O permeabilized neutrophils that degradation of extracellular ATP does not abrogate GTPγS-stimulated increases in F actin. A further argument against the involvement of phosphorylation reactions is that the process takes place in an excess of EDTA, leaving most kinases inactive due to their dependence on divalent cations. These findings exclude the participation of a number of protein and lipid kinases that were proposed to act downstream of Rho family proteins (see Introduction). Additionally, these results exclude an involvement of Rac-induced PtdIns(4,5)P_2 synthesis as described by Hartwig and coworkers (1995) in permeabilized platelets.

In neutrophils and platelets, okadaic acid was reported to alter cell shape and to inhibit agonist-mediated changes in F actin (Kreienbuhl et al., 1992; Downey et al., 1993; Yano et al., 1995). While it was suggested that this occurs without the involvement of myosin light chain phosphorylations, it was shown in fibroblasts that RhoA regulates myosin phosphatase through Rho-kinase (Kimura et al., 1996). In vitro actin polymerisation by GTPγS as shown here, on the other hand, was not affected by okadaic acid, nor o-vanadate, suggesting that the effects of protein phosphatases observed in neutrophils would be localised up-, but not downstream of the target of GTPγS.

The cytosolic target of GTPγS

As GTPγS can act as an activator for trimeric and small G proteins, we modulated in vitro actin polymerisation by stimulators and inhibitors for both protein families. B. pertussis toxin, which inhibits $G_{iα}$ subunits by ADP-ribosylation, was shown previously to inhibit agonist mediated F actin increases,

but did not interrupt the stimulation conferred by GTPγS in permeabilized neutrophils (Redmond et al., 1994). Likewise B. pertussis toxin left the GTPγS-mediated actin polymerisation in the cell free system intact. Activators of trimeric G protein controlled pathways, aluminium fluoride, GTPγS-loaded myristoylated $G_{iα2}$ subunits, and $G_{β1γ2}$ complexes also failed to stimulate actin polymerisation in cytosolic reaction mixtures. Although trimeric G proteins certainly mediate agonist-induced actin polymerisation in intact cells (Shefcyk et al., 1985), they are not necessary to carry on the GTPγS signal in the cytosol. All this is in agreement with the fact that trimeric G proteins require an excess of free magnesium for their activation both in vivo and in vitro (Gilman, 1987), and could thus not exchange GDP for GTPγS under the standard conditions of the assay.

It has been reported that C. difficile toxin B glucosylates a broad range of Rho family proteins (Rho, Rac, Cdc42, but not Ras) at the residue corresponding to threonine 37 in RhoA (Just et al., 1995). Moreover, it was demonstrated that microinjected glucosylated RhoA produced a dominant negative effect and disassembled actin filaments in fibroblasts (Just et al., 1995). When toxin B was tested in the cell free actin polymerisation assay for its potential to interfere with GTPγS stimulation, it was found that the dose dependent inhibition correlated with the incorporation of [^{14}C]glucose into protein and in particular with the labelling of a 20 kDa protein family. C. sordellii lethal toxin with Rac1, Ras, Rap and Ral as targets (Just et al., 1996; Genth et al., 1996), on the other hand, was not effective.

As a further strategy to block Rho family protein signalling we used recombinant RhoGDI to complex the putative small G protein, and RhoGDI was indeed capable to block the action of GTPγS at 50 μM. The effect of RhoGDI on exocytosis in mast cells (Mariot et al., 1996) or on receptor-mediated endocytosis in HeLa cells (Lamaze et al., 1996) was previously taken as proof for the involvement of Rho-related proteins in these cell responses. Together with the inhibitory action of toxin B, our data clearly demonstrate the involvement of a Rho family member in the GTPγS-mediated actin polymerisation response.

The membrane associated GEF activity

We found that the actin polymerising action of GTPγS was very sensitive to free magnesium ions. This fits well with the fact that small G proteins can exchange their loaded guanine nucleotide in vitro as long as Mg^{2+} is complexed, but that the GDP/GTP exchange is hindered if this requirement is not met (Self and Hall, 1995). In vivo, at mM free Mg^{2+} concentrations, the nucleotide exchange is accelerated by guanine nucleotide exchange factors (GEFs; Boguski and McCormick, 1993). Our data illustrate that the cytosolic fractions are devoid of a GEF activity that could mediate nucleotide exchange on the target G protein mediating actin polymerisation.

GEFs are often localised to membrane fractions (Bokoch et al., 1994; Whitehead et al., 1995; Chardin et al., 1996; Paris et al., 1997) and re-addition of plasma membranes to the system at 1 mM Mg^{2+} indeed rescued the effect of GTPγS, while neutrophil granule membranes remained ineffective. On the other hand, it has been shown that PtdIns(4,5)P_2 can accelerate the dissociation of GDP from human Cdc42 (Zheng et al., 1996) and stimulate GEFs by binding to pleckstrin homology domains (Paris et al., 1997). Working with Xenopus egg

extracts, Ma and coworkers (1998) have proposed that 4,5-phosphorylated phosphoinositides trigger actin polymerisation either by direct action on small G proteins or serving as docking site for GEFs.

The sensitivity of the plama membrane activity to heat and trypsin demonstrated here, however, illustrates clearly that either the GEF itself or an essential proteinous GEF activator is associated with the plasma membrane and that carried over lipids do not act by themselves.

In the absence of free Mg^{2+} phosphoinositides inhibited GTPγS-induced actin polymerisation. The reason for this is not clear, but it supports the notion that eventually present, but undetectable traces of cytosolic phosphoinositides are not essential to promote actin polymerisation. This is agreement with the negative results obtained with a gelsolin-derived PtdIns(4,5)P_2-binding peptide and excludes the involvement of processes like PtdIns(4,5)P_2 synthesis as they were proposed to be of importance in permeabilized platelets downstream of Rac (Hartwig et al., 1995).

When free Mg^{2+} was present, the above situation was reversed, and phosphoinositides now restored the ability of GTPγS to polymerise actin even in the absence of plasma membrane. The order of potency for PtdIns, PtdIns 4-P and PtdIns(4,5)P_2 best correlated with the previously reported capacity of the lipids to dissociate Rac/RhoGDI complexes (Chuang et al., 1993). That dissociation indeed occurred was confirmed by the increased availability of targets for toxin B-mediated [^{14}C]-glucosylation (data not shown). Although hypothetical, it is tempting to speculate that PtdIns releases a further small G protein from RhoGDI, which would, in contrast to the primary GTPγS target, possess a suitable GEF activity in the cytosol. As the cytosol reflects a very disorganised neutrophil which was once capable of performing specialised tasks like chemotaxis and phagocytosis, it is likely that the randomised system represents the multitude of signalling pathways necessary to concert the cell's actions.

While this work was being prepared for submission, Zigmond and coworkers (1977) published data supporting a role for a small G protein in a cell free actin polymerisation system. Using cytosol from *D. discoideum* mutants lacking trimeric G protein subunits they showed in an elegant way that these are not the targets for GTPγS. Furthermore, they successfully induced actin polymerisation in vitro with 100 nM Cdc42 purified from Sf9 insect cells, but not from *E. coli*. In our study, 10 μM concentrations, exceeding 100 times the ones in cytosolic fractions for Rac and Rho and 1,000 times for Cdc42 were still found to be unsuccessful in inducing actin polymerisation.

While isoprenylation seems to be important for membrane translocation and GEF-mediated GDP/GTP exchange (Bockoch et al., 1994), non-isoprenylated Rho family proteins usually interact with and activate their downstream partners normally. When produced in *E. coli*, Rho bound to and stimulated the activity of protein kinase N (Watanabe et al., 1996); Rac reconstituted cell-free NADPH oxidase (Abo and Segal, 1995); and Cdc42 induced N-WASP-mediated F actin depolymerisation (Miki et al., 1998) and IQGAP1-mediated F actin crosslinking (Fukata et al., 1997). The failure of massive amounts of recombinant Rac, Rho and Cdc42 to induce actin polymerisation in a pure cytosolic system, the fact that C3 transferase, N17Cdc42, the WASP-CRIB domain (this work)

and a Cdc42-binding PAK-derived peptide did not block GTPγS action (Zigmond et al., 1997), indicate that the endogenous small G protein might be different from the ones above.

The availability of a simple assay system for signal-induced F actin using fully fractionated material will certainly help to further elucidate the molecular mechanisms leading to actin polymerisation and allow a better definition of the cell compartements involved in the process.

REFERENCES

Abo, A. and Segal, A. W. (1995). Reconstitution of cell-free NADPH oxidase activity by purified components. *Meth. Enzymol.* **256**, 268-278.

Akiyama, T. and Ogawara, H. (1991). Use and specificity of genistein as inhibitor of protein-tyrosine kinases. *Meth. Enzymol.* **201**, 362-370.

Amano, M., Chihara, K., Kimura, K., Fukata, Y., Nakamura, N., Matsuura, Y. and Kaibuchi, K. (1997). Formation of actin stress fibers and focal adhesion enhanced by Rho-kinase. *Nature* **275**, 1308-1311.

Arcaro, A. and Wymann, M. P. (1993). Wortmannin is a potent phosphatidylinositol 3-kinase inhibitor; the role of phosphatidylinositol 3,4,5-trisphosphate in neutrophil responses. *Biochem. J.* **296**, 297-301.

Aspenström, P., Lindberg, U. and Hall, A. (1996). Two GTPases, Cdc42 and Rac, bind directly to a protein implicated in the immunodeficiency disorder Wiskott-Aldrich syndrome. *Curr. Biol.* **6**, 70-75.

Bengtsson, T., Rundquist, I., Stendahl, O., Wymann, M. P. and Andersson, T. (1988). Increased breakdown of phosphatidylinositol 4,5-bisphosphate is not an initiating factor for actin assembly in human neutrophils. *J. Biol. Chem.* **263**, 17385-17389.

Bengtsson, T., Särndahl, E., Stendahl, O. and Andersson, T. (1990). Involvement of GTP-binding proteins in actin polymerization in human neutrophils. *Proc. Nat. Acad. Sci. USA* **87**, 2921-2925.

Boguski, M. S. and McCormick, F. (1993). Proteins regulating Ras and its relatives. *Nature* **366**, 643-654.

Bokoch, G. M., Bohl, B. P. and Chuang, T. H. (1994). Guanine nucleotide exchange regulates membrane translocation of Rac/Rho GTP-binding proteins. *J. Biol. Chem.* **269**, 31674-31679.

Böyum, A. (1968). Isolation of mononuclear cells and granulocytes from blood. *Scand. J. Clin. Lab. Invest.* **97**, 77-89.

Burbelo, P. D., Drechsel, D. and Hall, A. (1995). A conserved binding motif defines numerous candidate target proteins for both Cdc42 and Rac GTPases. *J. Biol. Chem.* **270**, 29071-29074.

Carlsson, L., Nystrom, L. E., Sundkvist, I., Markey, F. and Lindberg, U. (1977). Actin polymerizability is influenced by profilin, a low molecular weight protein in non-muscle cells. *J. Mol. Biol.* **115**, 465-483.

Carson, M., Weber, A. and Zigmond, S. H. (1986). An actin-nucleating activity in polymorphonuclear leukocytes is modulated by chemotactic peptides. *J. Cell Biol.* **103**, 2707-2714.

Carty, D. J. and Iyengar, R. (1994). Guanosine 5′-(gamma-thio)triphosphate binding assay for solubilized G proteins. *Meth. Enzymol.* **237**, 38-44.

Cassimeris, L., Safer, D., Nachmias, V. T. and Zigmond, S. H. (1992). Thymosin β$_4$ sequesters the majority of G-actin in resting human polymorphonuclear leukocytes. *J. Cell Biol.* **119**, 1261-1270.

Cerione, R. A. and Zheng, Y. (1996). The Dbl family of oncogenes. *Curr. Opin. Cell Biol.* **8**, 216-222.

Chardin, P., Paris, S., Antonny, B., Robineau, S., Beraud-Dufour, S.,

Jackson, C. L. and Chabre, M. (1996). A human exchange factor for ARF contains Sec7- and pleckstrin-homology domains. *Nature* **384**, 481-484.

Chuang, T.-H., Bohl, B. P. and Bokoch, G. M. (1993). Biologically Active Lipids Are Regulators of Rac·GDI Complexation. *J. Biol. Chem.* **268**, 26206-26211.

Combeau, C. and Carlier, M. F. (1988). Probing the mechanism of ATP hydrolysis on F-actin using vanadate and the structural analogs of phosphate BeF-3 and A1F-4. *J. Biol. Chem.* **263**, 17429-17436.

Cooper, J. A. (1991). The role of actin polymerization in cell motility. *Annu. Rev. Physiol.* **53**, 585-605.

Cottrell, J. S. and Sutton, C. W. (1996). The identification of electrophoretically separated proteins by peptide mass fingerprinting. *Meth. Mol. Biol.* **61**, 67-82.

Dillon, S. T. and Feig, L. A. (1995). Purification and assay of recombinant C3 transferase. *Meth. Enzymol.* **256**, 174-184.

DiNubile, M. J. and Southwick, F. S. (1988). Contractile Proteins in Leukocytes. *Meth. Enzymol.* **162**, 246-271.

Downey, G. P., Chan, C. K., Trudel, S. and Grinstein, S. (1990). Actin assembly in electropermeabilized neutrophils: role of intracellular calcium. *J. Cell Biol.* **110**, 1975-1982.

Downey, G. P., Takai, A., Zamel, R., Grinstein, S. and Chan, C. K. (1993). Okadaic acid-induced actin assembly in neutrophils: role of protein phosphatases. *J. Cell. Physiol.* **155**, 505-519.

Fukata, M., Kuroda, S., Fujii, K., Nakamura, T., Shoji, I., Matsuura, Y., Okawa, K., Iwamatsu, A., Kikuchi, A. and Kaibuchi, K. (1997). Regulation of cross-linking of actin filament by IQGAP1, a target for Cdc42. *J. Biol. Chem.* **272**, 29579-29583.

Genth, H., Hofmann, F., Selzer, J., Rex, G., Aktories, K. and Just, I. (1996). Difference in protein substrate specificity between hemorrhagic toxin and lethal toxin from *Clostridium sordellii. Biochem. Biophys. Res. Commun.* **229**, 370-374.

Gilman, A. G. (1987). G proteins: transducers of receptor-generated signals. *Annu. Rev. Biochem.* **56**, 615-649.

Gordon, J. A. (1991). Use of vanadate as protein-phosphotyrosine phosphatase inhibitor. *Meth. Enzymol.* **201**, 477-482.

Gorlin, J. B., Yamin, R., Egan, S., Stewart, M., Stossel, T. P., Kwiatkowski, D. J. and Hartwig, J. H. (1990). Human endothelial actin-binding protein (ABP-280, nonmuscle filamin): a molecular leaf spring. *J. Cell Biol.* **111**, 1089-1105.

Hardie, D. G., Haystead, T. A. and Sim, A. T. (1991). Use of okadaic acid to inhibit protein phosphatases in intact cells. *Meth. Enzymol.* **201**, 469-476.

Harlan, J. E., Hajduk, P. J., Sup, Y. H. and Fesik, S. W. (1994). Pleckstrin homology domains bind to phosphatidylinositol-4,5-bisphosphate. *Nature* **371**, 168-170.

Hart, M. J., Eva, A., Zangrilli, D., Aaronson, S. A., Evans, T., Cerione, R. A. and Zheng, Y. (1994). Cellular transformation and guanine nucleotide exchange are catalyzed by a common domain on the Dbl oncogene product. *J. Biol. Chem.* **269**, 62-65.

Hartwig, J. H., Bokoch, G. M., Carpenter, C. L., Janmey, P. A., Taylor, L. A., Toker, A. and Stossel, T. P. (1995). Thrombin receptor ligation and activated Rac uncap actin filament barbed ends through phosphoinositide synthesis in permeabilized human platelets. *Cell* **82**, 643-653.

Hartwig, J. H., Kung, S., Kovacsovics, T., Janmey, P. A., Cantley, L. C., Stossel, T. P. and Toker, A. (1996). D3 phosphoinositides and outside-in integrin signaling by glycoprotein IIb-IIIa mediate platelet actin assembly and filopodial extension induced by phorbol 12-myristate 13-acetate. *J. Biol. Chem.* **271**, 32986-32993.

Heiss, S. G. and Cooper, J. A. (1991). Regulation of CapZ, an actin capping protein of chicken muscle, by anionic phospholipids. *Biochemistry* **30**, 8753-8758.

Howard, T. H. and Oresajo, C. O. (1985). A method for quantifying F-actin in chemotactic peptide activated neutrophils: study of the effect of tBOC peptide. *Cell Motil.* **5**, 545-557.

Huang, Z. J., Haugland, R. P., You, W. M. and Haugland, R. P. (1992). Phallotoxin and actin binding assay by fluorescence enhancement. *Anal. Biochem.* **200**, 199-204.

Janmey, P. A. and Stossel, T. P. (1989). Gelsolin-polyphosphoinositide interaction. Full expression of gelsolin-inhibiting function by polyphosphoinositides in vesicular form and inactivation by dilution, aggregation, or masking of the inositol head group. *J. Biol. Chem.* **264**, 4825-4831.

Janmey, P. A., Lamb, J., Allen, P. G. and Matsudaira, P. T. (1992). Phosphoinositide-binding peptides derived from the sequences of gelsolin and villin. *J. Biol. Chem.* **267**, 11818-11823.

Just, I., Selzer, J., Wilm, M., von, E.-S. C., Mann, M. and Aktories, K. (1995). Glucosylation of Rho proteins by *Clostridium difficile* toxin B. *Nature* **375**, 500-503.

Just, I., Selzer, J., Hofmann, F., Green, G. A. and Aktories, K. (1996). Inactivation of Ras by *Clostridium sordellii* lethal toxin-catalysed glycosylation. *J. Biol. Chem.* **271**, 10149-10153.

Kettlun, A. M., Uribe, L., Calvo, V., Silva, S., Rivera, J., Mancilla, M., Valenzuela, M. A. and Traverso-Cori, A. (1982). Properties of two apyrases from *Solanum tuberosum. Phytochemistry* **21**, 551-558.

Kimura, K., Ito, M., Amano, M., Chihara, K., Fukata, Y., Nakafuku, M., Yamamori, B., Feng, J., Nakano, T., Okawa, K., Iwamatsu, A. and Kaibuchi, K. (1996). Regulation of myosin phosphatase by Rho and Rho-associated kinase (Rho-kinase) [see comments]. *Science* **273**, 245-248.

Kirchhausen, T. and Rosen, F. S. (1996). Disease mechanism: unravelling Wiskott-Aldrich syndrome. *Curr. Biol.* **6**, 676-678.

Kozasa, T. and Gilman, A. G. (1995). Purification of recombinant G proteins from SF9 cells by hexahistidine tagging of associated subunits. Characterization of α12 and inhibition of adenylyl cyclase by αz. *J. Biol. Chem.* **270**, 1734-1741.

Kozma, R., Ahmed, S., Best, A. and Lim, L. (1995). The ras-related protein Cdc42Hs and bradikinin promote formation of periferal actin microspikes and filopodia in Swiss 3T3 fibroblasts. *Mol. Cell. Biol.* **15**, 1942-1952.

Kreienbuhl, P., Keller, H. and Niggli, V. (1992). Protein phosphatase inhibitors okadaic acid and calyculin A alter cell shape and F-actin distribution and inhibit stimulus-dependent increases in cytoskeletal actin of human neutrophils. *Blood* **80**, 2911-2919.

Lamarche, N. and Hall, A. (1994). GAPs for rho-related GTPases. *Trends Genet.* **10**, 436-440.

Lamaze, C., Chuang, T.-H., Terlecky, L. J., Bockoch, G. M. and Schmid, S. L. (1996). Regulation of receptor-mediated endocytosis by Rho and Rac. *Nature* **382**, 177-179.

Lassing, I. and Lindberg, U. (1985). Specific interaction between phosphatidylinositol 4,5-bisphosphate and profilactin. *Nature* **314**, 472-474.

Lee, E., Linder, M. E. and Gilman, A. G. (1994). Expression of G-protein a subunits in Escherichia coli. *Meth. Enzymol.* **237**, 140-160.

Ma, L., Cantley, L. C., Janmey, P. A. and Kirschner, M. W. (1998). Corequirement of specific phosphoinositides and small GTP-binding protein Cdc42 in inducing actin assembly in Xenopus egg extracts. *J. Cell Biol.* **140**, 1125-1136.

MacLean-Fletcher, S. and Pollard, T. D. (1980). Identification of a factor in conventional muscle actin preparations which inhibits actin filament self-association. *Biochem. Biophys. Res. Commun.* **96**, 18-27.

Mannherz, H. G., Leigh, J. B., Leberman, R. and Pfrang, H. (1975). A specific 1:1 G-actin:DNAase i complex formed by the action of DNAase I on F-actin. *FEBS Lett.* **60**, 34-38.

Manser, E., Leung, T., Salihuddin, H., Zhao, Z. and Lim, L. (1994). A brain serine/threonine protein kinase activated by Cdc42 and Rac1. *Nature* **367**, 40-46.

Mariot, P., O'Sullivan, J., Brown, A. M. and Tatham, P. E. R. (1996). Rho guanine nucleotide dissociation inhibitor protein (RhoGDI) inhibits exocytosis in mast cells. *EMBO J.* **15**, 6476-6482.

Martell, A. E. and Smith, R. M. (1974). *Critical Stability Constants*, vol.1. Plenum Press, New York.

Michiels, F., Habets, G. G., Stam, J. C., van der Kammen, R. A. and Collard, J. G. (1995). A role for Rac in Tiam1-induced membrane ruffling and invasion. *Nature* **375**, 338-340.

Miki, H., Sasaki, T., Takai, Y. and Takenawa, T. (1998). Induction of filopodium formation by a WASP-related actin-depolymerizing protein N-WASP. *Nature* **391**, 93-96.

Mitchison, T. J. and Cramer, L. P. (1996). Actin-based cell motility and cell locomotion. *Cell* **84**, 371-379.

Mumby, S. M. and Lider, M. E. (1994). Myristoylation of G-protein α subunits. *Meth. Enzymol.* **237**, 254-269.

Nobes, C. D. and Hall, A. (1995). Rho, rac and cdc42 GTPases regulate the assembly of multimolecular focal complexes associated with actin stress fibers, lamellipodia and filopodia. *Cell* **81**, 53-62.

Nobes, C. D., Hawkins, P., Stephens, L. and Hall, A. (1995). Activation of the small GTP-binding proteins rho and rac by growth factor receptors. *J. Cell Sci.* **108**, 225-233.

Omann, G. M., Porasik, M. M. and Sklar, L. A. (1989). Oscillating actin polymerisation/depolymerisation responses in human polymorphonuclear leukocytes. *J. Biol. Chem.* **264**, 16355-16358.

Otto, J. J. (1994). Actin-bundling proteins. *Curr. Opin. Cell Biol.* **6**, 105-109.

Pantaloni, D. and Carlier, M.-F. (1993). how profilin promotes actin filament assembly in the presence of thymosin β₄. *Cell* **75**, 1007-1014.

Pardee, J. D. and Spudich, J. A. (1982). Purification of muscle actin. *Meth. Enzymol.* **85**, 164-181.

Paris, S., Beraud-Dufour, S., Robineau, S., Bigay, J., Antonny, B., Chabre, M. and Chardin, P. (1997). Role of protein-phospholipid interactions in the activation of ARF1 by the guanine nucleotide exchange factor Arno. *J. Biol. Chem.* **272**, 22221-22226.

Parks, R. E. and Agarwal, R. P. (1973). Nucleoside diphosphokinases. In *The Enzymes*, vol. 8 (ed. P. D. Boyer), pp. 307-333. Academic Press, New York.

Popoff, M. R., Chaves-Olarte, E., Lemichez, E., von Eichel-Streiber, C., Thelestam, M., Chardin, P., Cussac, D., Antonny, B., Chavrier, P., Flatau, G., Giry, M., de Gunzburg, J. and Boquet, P. (1996). Ras, Rap, and Rac small GTP-binding proteins are targets for Clostridium sordellii lethal toxin glucosylation. *J. Biol. Chem.* **271**, 10217-10224.

Prigmore, E., Ahmed, S., Best, A., Kozma, R., Manser, E., Segal, A. W. and Lim, L. (1995). A 68-kDa kinase and NADPH oxidase component p67phox are targets for Cdc42Hs and Rac1 in neutrophils. *J. Biol. Chem.* **270**, 10717-10722.

Redmond, T., Tardiff, M. and Zigmond, S. H. (1994). Induction of actin polymerization in permeabilized neutrophils. Role of ATP. *J. Biol. Chem.* **269**, 21657-21663.

Ridley, A. J. and Hall, A. (1992). The small GTP-binding protein rho regulates the assembly of focal adhesions and actin stress fibers in response to growth factors. *Cell* **70**, 389-399.

Ridley, A. J., Paterson, H. F., Johnston, C. L., Diekmann, D. and Hall, A. (1992). The small GTP-binding protein rac regulates growth factor-induced membrane ruffling. *Cell* **70**, 401-410.

Ridley, A. J. (1994). Membrane ruffling and signal transduction. *BioEssays* **16**, 321-327.

Ridley, A. J. and Hall, A. (1994). Signal transduction pathways regulating Rho-mediated stress fibre formation: requirement for a tyrosine kinase. *EMBO J.* **13**, 2600-2610.

Safer, D., Elzinga, M. and Nachmias, V. T. (1991). Thymosin beta 4 and Fx, an actin-sequestering peptide, are indistinguishable. *J. Biol. Chem.* **266**, 4029-4032.

Schafer, D. A. and Cooper, J. A. (1995). Control of actin assembly at filament ends. *Annu. Rev. Cell Dev. Biol.* **11**, 497-518.

Self, A. J. and Hall, A. (1995). Measurement of intrinsic nucleotide exchange and GTP hydrolysis rates. *Meth. Enzymol.* **256**, 67-76.

Shefcyk, J., Yassin, R., Volpi, M., Molski, T. F. P., Naccache, P. H., Munoz, J. J., Becker, E. L., Feinstein, M. B. and Sha'afi, R. I. (1985). Pertussis but not cholera toxin inhibits the stimulated increase in actin association with the cytoskeleton in rabbit neutrophils: role of the "G proteins" in stimulus response coupling. *Biochem. Biophys. Res. Commun.* **126**, 1174-1181.

Symons, M., Derry, J. M., Karlak, B., Jiang, S., Lemahieu, V., Mccormick, F., Francke, U. and Abo, A. (1996). Wiskott-Aldrich syndrome protein, a novel effector for the GTPase CDC42Hs, is implicated in actin polymerization. *Cell* **84**, 723-734.

Tamaoki, T. (1991). Use and specificity of staurosporine, UCN-01, and calphostin C as protein kinase inhibitors. *Meth. Enzymol.* **201**, 340-347.

Tapon, N. and Hall, A. (1997). Rho, Rac and Cdc42 GTPases regulate the organization of the actin cytoskeleton. *Curr. Opin. Cell Biol.* **9**, 86-92.

Tardif, M., Huang, S., Redmond, T., Safer, D., Pring, M. and Zigmond, S. H. (1995). Actin polymerization induced by GTP gamma S in permeabilized neutrophils is induced and maintained by free barbed ends. *J. Biol. Chem.* **270**, 28075-28083.

Theriot, J. A. and Mitchison, T. J. (1991). Actin microfilament dynamics in locomoting cells. *Nature* **352**, 126-131.

Therrien, S. and Naccache, P. H. (1989). Guanine nucleotide-induced polymerization of actin in electropermeabilized human neutrophils. *J. Cell Biol.* **109**, 1125-1132.

Van Aelst, L., Joneson, T. and Bar-Sagi, D. (1996). Identification of a novel Rac1-interacting protein involved in membrane ruffling. *EMBO J.* **15**, 3778-3786.

Watanabe, G., Saito, Y., Madaule, P., Ishizaki, T., Fujisawa, K., Morii, N., Mukai, H., Ono, Y., Kakizuka, A. and Narumina, S. (1996). Protein kinase N (PKN) and PKN-related protein rhophillin as targets of small GTPase Rho. *Science* **271**, 645-648.

Whitehead, I., Kirk, H., Tognon, C., Trigo-Gonzalez, G. and Kay, R. (1995). Expression cloning of lfc, a novel oncogene with structural similarities to guanine nucleotide exchange factors and to the regulatory region of protein kinase C. *J. Biol. Chem.* **270**, 18388-18395.

Wymann, M. P., Kernen, P., Deranleau, D. A. and Baggiolini, M. (1989). Respiratory burst oscillations in human neutrophils and their correlation with fluctuations in apparent cell shape. *J. Biol. Chem.* **264**, 15829-15834.

Wymann, M. P., Kernen, P., Bengtsson, T., Andersson, T., Baggiolini, M. and Deranleau, D. A. (1990). Corresponding oscillations in neutrophil shape and filamentous actin content. *J. Biol. Chem.* **265**, 619-622.

Wymann, M. P., Bulgarelli-Leva, G., Zvelebil, M. J., Pirola, L., Vanhaesebroeck, B., Waterfield, M. D. and Panayotou, G. (1996). Wortmannin inactivates phosphoinositide 3-kinase by covalent modification of Lys-802, a residue involved in the phosphate transfer reaction. *Mol. Cell. Biol.* **16**, 1722-1733.

Yano, H., Nakanishi, S., Kimura, K., Hanai, N., Saitoh, Y., Fukui, Y., Nonomura, Y. and Matsuda, Y. (1993). Inhibition of histamine secretion by Wortmannin through the blockade of phosphatidylinositol 3-kinase in RBL-2H3 cells. *J. Biol. Chem.* **268**, 25846-25856.

Yano, Y., Sakon, M., Kambayashi, J., Kawasaki, T., Senda, T., Tanaka, K., Yamada, F. and Shibata, N. (1995). Cytoskeletal reorganization of human platelets induced by the protein phosphatase 1/2 A inhibitors okadaic acid and calyculin A. *Biochem. J.* **307**, 439-449.

Zheng, Y., Glaven, J. A., Wu, W. J. and Cerione, R. A. (1996). Phosphatidylinositol 4,5-bisphosphate provides an alternative to guanine nucleotide exchange factors by stimulating the dissociation of GDP from Cdc42Hs. *J. Biol. Chem.* **271**, 23815-23819.

Zigmond, S. H., Joyce, M., Borleis, J., Bokoch, G. M. and Devreotes, P. N. (1997). Regulation of actin polymerisation in cell-free systems by GTPγS and Cdc42. *J. Cell Biol.* **138**, 363-374.

2. Microquantification of cellular and *in vitro* F-actin by rhodamine phalloidin fluorescence enhancement.

Katanaev VL, Wymann MP. Anal. Biochem. 1998: 264: 185.

Microquantification of Cellular and *in Vitro* F-Actin by Rhodamine Phalloidin Fluorescence Enhancement

Vladimir L. Katanaev and Matthias P. Wymann[1]

Institute of Biochemistry, Rue du Musée 5, CH-1700 Fribourg, Switzerland

Based on the enhancement of rhodamine phalloidin fluorescence after its binding to actin filaments we have developed a technique to quantify F-actin, drastically ($\geqslant$100 times) reducing consumption of the expensive fluorescent dye and sample material in comparison to previous methods. Depolymerization of F-actin is prevented by utilizing short incubation times and stabilization of the filaments by actin-binding proteins or formaldehyde. Equilibrium and kinetic mathematical models relating rhodamine fluorescence with F-actin concentrations were used to predict the optimal assay conditions. The method has been applied to measure relative and absolute F-actin concentrations in cytosolic fractions and stimulus-induced actin polymerization in neutrophils. The cells were lysed with octyl-β-D-glucopyranoside, which is compatible with the assay due to its high critical micelle concentration. As the assay takes less than 1 h and eliminates all previously required washing or extraction steps, it is faster and much simpler than any other presented up to now for quantification of filamentous actin. Moreover, the method is unique for reliable and easy F-actin measurements in cell-free systems. © 1998 Academic Press

The transition of actin between monomeric and filamentous states serves as a basis for locomotion and shape changes of various nonmuscle cells (2). Actin polymerization has been extensively investigated *in vitro* with purified proteins (3). Studies of F-actin changes *in vivo* or in cell lysates were initiated by the observation that monomeric actin inhibits DNaseI (4). Quantification of so-called Triton-insoluble cytoskeleton-associated actin via SDS–PAGE analysis was set up in the 1980s as the first means to estimate cellular F-actin levels (5, 6).

The development of various fluorescence techniques opened new perspectives to study actin dynamics. On-line monitoring of actin rearrangements *in vitro* and *in vivo* by fluorescent spectrophotometry and microscopy was achieved using actin molecules covalently modified with fluorescent groups such as pyrenyl (7) and rhodamine (8) or fused to green fluorescence protein (9). A much broader application was met by fluorescent derivatives of phallotoxins (phalloidin and phallacidin) (10). These peptides bind specifically and with a high affinity to filamentous, but not to G-actin (11). A variety of fluorescent groups can be attached to the phallotoxins without significantly changing their actin-binding properties (10). Such derivatives have been widely used to quantify F-actin. This involves incubation of fixed permeabilized cells with the probe, followed by relative F-actin determination by fluorescence-activated cell sorter analysis (12) or fluorescence measurement after extraction of the bound dye (13). Since the initial description, variations of the method have been developed, such as the measurement of F-actin in cell lysates (14, 15). The disadvantage of all present protocols is their need for tedious washing and extraction steps that impaire precision.

It has been observed that certain fluorescent phallotoxins increase their fluorescence upon binding to actin filaments, the strongest fluorescence enhancement, 10- to 20-fold, displayed by rhodamine phalloidin (1, 16). This effect was exploited by Huang and co-workers (1) to measure micromolar F-actin concentrations. They showed that at 5 μM rhodamine phalloidin its fluorescence was linearly related to F-actin concentrations up to 2 μM (ca. 0.08 mg/ml). The authors emphasized that the assay is only feasible when rhodamine phalloidin concentrations are much above the dissociation constant (estimated to be in the order of 1×10^{-8} M) and exceed F-actin concentrations (1).

Here, we describe the conditions for the use of nanomolar concentrations of rhodamine phalloidin to rapidly quantify minute F-actin amounts, an advantage, which is especially critical for *in vitro* systems. We have successfully applied this principle recently to investigate guanosine 5'-O-(3-thiotriphosphate) (GTPγS)[2]-induced actin polymerization in a cell-free system from neutrophil cytosols (17). In this paper we present a mathematical treatment relating F-actin concentrations to fluorescence enhancement of rhodamine phalloidin under equilibrium and nonequilibrium conditions and demonstrating the validity of the method to quantify relative and absolute concentrations of F-actin using very low amounts of rhodamine phalloidin. We also describe the application of the rhodamine phalloidin fluorescence enhancement assay to measure chemoattractant-induced actin polymerization in whole cells.

MATERIALS AND METHODS

Materials

DNaseI was from Boehringer-Mannheim; 37% formaldehyde solution, dimethyl sulfoxide (DMSO), GTPγS, octyl-β-D-glucopyranoside, rhodamine B, and Triton X-100 from Fluka; p-formaldehyde was from Merck; N-(1-pyrene)iodoacetamide, phalloidin, fluorescein phalloidin, and rhodamine phalloidin were from Molecular Probes; and N-formylmethionylleucylphenylalanine (fMLP) and L-α-lysophosphatidylcholine were from Sigma. Rabbit muscle actin was purified and labelled with N-(1-pyrene)iodoacetamide as described in (18).

Neutrophil Isolation, Subcellular Fractionation, and in Vitro Actin Polymerization Assay

Human neutrophils and neutrophil cytosol were purified as described before (19, 17). Actin polymerization assays in a cell-free system have been performed according to Katanaev and Wymann (17). Briefly, reactions were carried out with 1.6 mg cytosolic protein/ml in the presence of 2 mM free EDTA. Actin polymerisation was induced by 50 μM GTPγS or 315 mM KCl. After a 25-min incubation at 37°C, the indicated volumes of the cytosol were mixed to the final volume of 600 μl with Hepes/KCl buffer (HKB, 135 mM KCl, 10 mM NaCl, 10 mM Hepes, pH 7.4) supplemented with rhodamine phalloidin to final concentration of 15 nM. After incubation at room temperature (RT) for 20 min, fluorescence was read in 1-ml quartz cuvettes on a Perkin–Elmer fluorescence spectrophotometer LS50B (ex 552 nm, slit 5 nm; em 580 nm, slit 20 nm).

F-Actin Quantification in Neutrophils by Rhodamine Phalloidin Fluorescence Enhancement

After stimulation of neutrophils (1×10^6–2×10^7 cells/ml) with 0.1% DMSO (control) or 100 nM fMLP for 15 s at 37°C, the cells were fixed and relative F-actin was determined in parallel by three different methods: (i) lysis of the cells with 1% Triton X-100 followed by SDS–PAGE analysis of sedimentable actin (5, 6); (ii) loading lysophosphatidylcholine-permeabilized cells with fluorescein phalloidin followed by methanol extraction of the bound dye and fluorescence measurement (13, 18) and (iii) measurement of rhodamine phalloidin fluorescence enhancement. For the latter method, cells were fixed for 15 min at RT in 4% p-formaldehyde and 1% octyl-β-D-glucopyranoside, followed by addition of phosphate-buffered saline (PBS) to 600 μl and rhodamine phalloidin to 15 nM (from a 6.6 μM stock in methanol), further incubation for 30 min, and fluorescence measurement as above.

Equilibrium and Kinetic Models for F-Actin Interaction with Rhodamine Phalloidin Measured by Fluorescence Enhancement

As first reported by Huang *et al.* (1), rhodamine phalloidin increases its fluorescence upon binding to F-actin by a factor δ:

$$\frac{\phi_b}{\phi_f} = \delta, \qquad [1]$$

where ϕ_f and ϕ_b represent quantum yields of fluorescence of free and F-actin-bound rhodamine phalloidin, respectively. If F_0 is the fluorescence of a certain concentration of rhodamine phalloidin in the absence of actin filaments, and F in their presence, the fluorescence enhancement upon interaction with actin can be described as (20)

$$\Delta F = F - F_0 = r_b \cdot (\phi_b - \phi_f) = F_0 \cdot (\delta - 1) \cdot r_b/r_t, \quad [2]$$

where r_b and r_t designate concentrations of bound and total rhodamine phalloidin, respectively. Under equilibrium conditions, assuming 1:1 stochiometry of the rhodamine phalloidin–F-actin binding, the dissociation constant for the interaction is given by

$$K_d = \frac{a_f \cdot r_f}{r_b} = \frac{(a_t - r_b) \cdot (r_t - r_b)}{r_b} \quad \text{or}$$

$$r_b^2 - r_b \cdot (a_t + K_d + r_t) + a_t \cdot r_t = 0, \quad [3]$$

where a_f and r_f are the concentrations of free F-actin and rhodamine phalloidin, respectively, and a_t is total concentration of F-actin. From this, it follows that

$$r_b = \frac{a_t + K_d + r_t - \sqrt{(a_t + K_d + r_t)^2 - 4a_t r_t}}{2}$$

$$= \frac{a_t + K_d + r_t - \sqrt{(a_t + K_d - r_t)^2 + 4K_d r_t}}{2} , \quad [4]$$

where the second solution of the quadratic Eq. [3] is omitted because it yields $r_b > r_t$. Thus, under equilibrium conditions,

$$\Delta F = F_0 \cdot (\delta - 1)$$

$$\times \frac{a_t + K_d + r_t - \sqrt{(a_t + K_d - r_t)^2 + 4K_d \cdot r_t}}{2r_t} . \quad [5]$$

To determine the total F-actin concentration, a_t, combination of Eqs. [2] and [3] yields

$$a_t = \frac{\Delta F \cdot r_t}{F_0(\delta - 1)} + \frac{\Delta F \cdot K_d}{F_0(\delta - 1) - \Delta F} . \quad [6]$$

Before equilibrium is reached, the concentration of bound rhodamine phalloidin is time-dependent (21):

$$\frac{dr_b}{dt} = k_{on} \cdot r_f a_t - k_{off} \cdot r_b . \quad [7]$$

Applying the solution of Eq. [7] given in (22) to Eq. [2] yields the fluorescence enhancement as a function of the total F-actin concentration, K_d, δ, and time (t):

$$\Delta F = F_0 \cdot (\delta - 1)$$

$$\times \left\{ 1 - \left[(d - c)/2 + \frac{d}{-1 + \dfrac{2r_t + c + d}{2r_t + c - d} \cdot \exp(k_{on} \cdot t \cdot d)} \right] \middle/ r_t \right\} ,$$

$$[8]$$

where $c = a_t - r_t + K_d$, and $d = \pm\sqrt{c^2 + 4r_t K_d}$.

To build the curves based on Eqs. [5] and [8], the following parameters were used: $r_t = 15$ nM, $K_d = 10$ nM, $k_{on} = 2.9 \times 10^4 \text{ M}^{-1}\text{s}^{-1}$ (23), $t = 1200$ s, $F_0 = 12$, and $\delta = 20$, which were determined as described below. Absolute F-actin concentrations were obtained using a Graphing Calculator program from nonequilibrium fluorescence data of the curve based on Eq. [8].

The limits of fluorescence enhancement (ΔF) which are suggested to be used for quantification of relative F-actin concentrations allow us to approximate linearly the ΔF dependence on [F-actin]. The error of the linear approximation between any two ΔF values is determined comparing the ratio of these values with

the ratio of the corresponding [F-actin] values and is $\leq 10\%$ for the range of F-actin concentrations given in Table 1.

RESULTS AND DISCUSSION

Interaction of F-actin with rhodamine phalloidin leads to a 10- to 20-fold enhancement of the fluorescence of the latter (1, 16). Huang and co-workers (1) have applied this substantial increase in fluorescence to quantify purified F-actin using micromolar concentrations of rhodamine phalloidin. While these dye and F-actin concentrations are too high for advanced experiments, we have developed conditions to reduce the sample and probe concentrations by three orders of magnitude. To support this, we have applied mathematical models describing dependence of rhodamine phalloidin fluorescence enhancement on the F-actin concentrations under equilibrium (Eq. [5]) and nonequilibrium (Eq. [8]) conditions (see Materials and Methods). These equations relate fluorescence enhancement, ΔF, with total F-actin concentration, a_t, via constants describing binding of rhodamine phalloi-
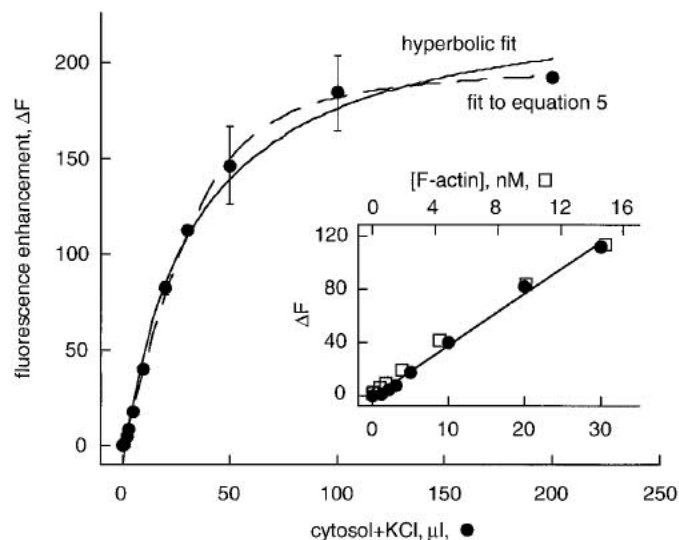
FIG. 1.   Indicated volumes of the neutrophil cytosol were pretreated with 315 mM KCl to polymerize actin and mixed with buffer (HKB) to give 600 μl containing 15 nM rhodamine phalloidin, and the fluorescence was read after 20 min of incubation. The signal from rhodamine phalloidin alone (F_0) was substracted, yielding the fluorescence enhancement (arbitrary units). The data (means $\pm$ SD, $n = 2$) were fitted with the equilibrium Eq. [5] (broken line) or a hyperbolic equation $y = a + bx/(c + x)$ (continuous line); for the former, microliters of the cytosol applied for the assay were converted into F-actin concentrations as $a_t = q \cdot \mu$l, where q was constant. The results of the fitting show $q = 0.37$ nM, $K_d = 3$ nM, and $\delta = 18$ (Eq. [5] fit) or 20 (hyperbolic fit). The inset presents the initial part of the curve. Concentrations of F-actin were calculated from the ΔF data using Eq. [8] and are shown in squares; very close values are obtained if parameter q is applied. Error bars are omitted where smaller than the symbols.
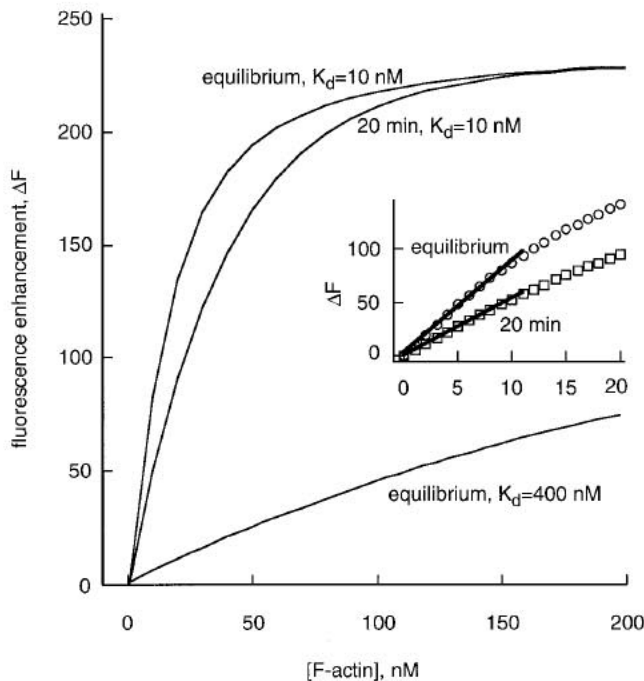
FIG. 2. Fluorescence enhancement (ΔF) values were calculated for equilibrium conditions using Eq. [5] and nonequilibrum conditions with Eq. [8] for K_d = 10 or 400 nM (time = 20 min) and plotted as a function of F-actin. The inset shows the initial parts of the curves based on K_d = 10 nM. Circles and squares reflect calculated data for the indicated conditions. Lines are introduced to illustrate the linearity from 1 to 11 nM [F-actin].

presence of various F-actin-binding proteins (16, 23, 24). To the contrary, the other constants used in the equations (δ and F_0) have to be measured for each kind of experimental setup, since they are determined by the efficiency of phalloidin labelling with rhodamine, chromophore concentration, composition of the measurement buffer, and the instrument settings.

To determine the fluorescence enhancement factor, δ, 15 nM rhodamine phalloidin in HKB was titrated with increasing amounts of F-actin, as shown in Fig. 1. The fluorescence enhancement data were then fitted by a least square algorithm to the equilibrium Eq. [5]. Alternatively, a simple hyperbolic equation $y = a + bx/(c + x)$ was used for the fitting, where $a + b$ represented the maxima the curves could reach, or ΔF_{max}, and δ was determined as $(\Delta F_{max} + F_0)/F_0$. Results from five independent experiments, in which rhodamine phalloidin was titrated with neutrophil cytosol where actin polymerisation had been induced by high salt or GTPγS, or with purified rabbit muscle F-actin stabilized or not with p-formaldehyde, yielded $\delta = 19 \pm 2$ (mean $\pm$ SD) for the fitting based on Eq. [5], and for the hyperbolic fits $\delta = 21 \pm 1$, very close to the value of (16). The dissociation constant defined by the fitting to Eq. [5] of the experimental data presented in Fig. 1 was 3 nM, also in a good agreement with recent determinations of De La Cruz and Pollard (23). F_0 value is determined directly from fluorescence measurement and for 15 nM rhodamine phalloidin used in this study is equal to 12 ± 2 ($n = 8$) under our conditions.

The curves derived from Eqs. [5] and [8] for 15 nM rhodamine phalloidin and the 20-min incubation time using the fluorescence constants determined from Fig.

din to actin filaments (K_d and k_{on}). These constants have been carefully determined recently and shown to be independent of the exact buffer composition and the

TABLE 1
Conditions for [F-Actin] Quantification

[F-Actin] range,[a] nM	[Rhodamine phalloidin],[b] nM	ΔF of upper limit[c] of range	[F-actin][d] at $\Delta F = F_0$, nM
K_d = 10 nM			
1.1–11	15	$4.5 \times F_0$	2.5
4–100	150	$10 \times F_0$	8
40–1550	1500	$17 \times F_0$	80
Apparent K_d = 400 nM[e]			
40–300	15	$4 \times F_0$	75
60–750	1500	$5.5 \times F_0$	125

[a] A nearly linear relationship between the fluorescence enhancement (ΔF) and total F-actin in a given sample is maintained when F-actin matches the given range, and when the rhodamine concentration to the right is applied ([b]). In case F-actin is unknown, the determined ΔF may not exceed the indicated value of the upper limit ([c]). Otherwise, the sample has to be diluted or a higher rhodamine phalloidin concentration has to be chosen. A rough estimation of [F-actin] can be obtained when the sample concentration at a given rhodamine phalloidin concentration is adjusted so that the fluorescence increases twice over background when the sample is added to the measurement cuvette ($\Delta F = F_0$) ([d]).

[e] When F-actin is stabilized by crosslinkers (e.g., formaldehyde), the apparent K_d is lowered by the interference of covalent modifications of actin molecules with rhodamine phalloidin binding. The K_d varies with fixation conditions and is estimated for the procedure given under Materials and Methods. For the whole table δ was 20 and time of incubation 20 min.
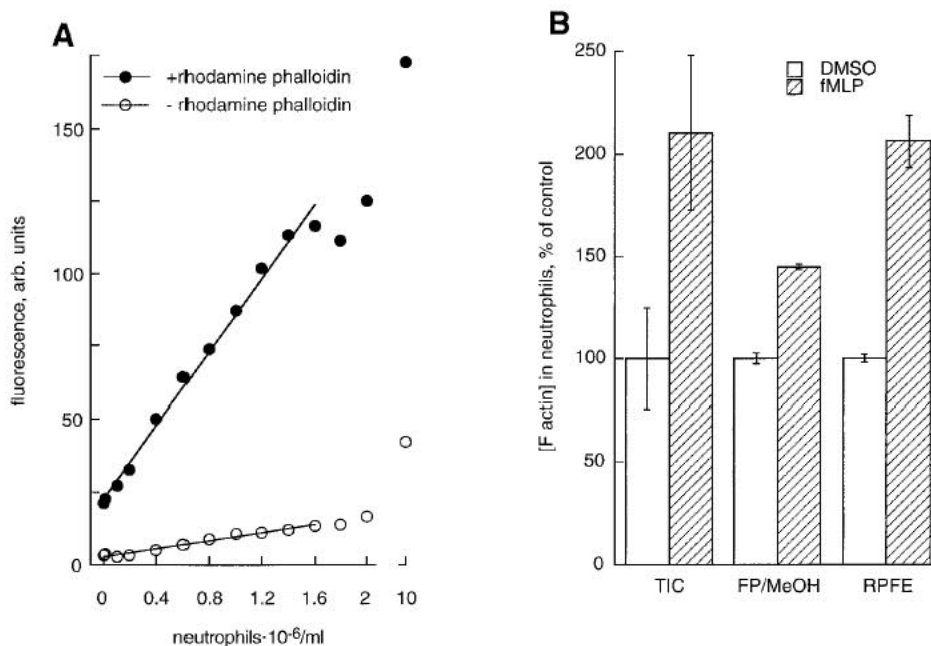
FIG. 3. Cellular F-actin quantification. (A) Human neutrophils were lysed with octyl-β-D-glucopyranoside as described under Materials and Methods and incubated with (closed circles) or without 15 nM rhodamine phalloidin (open circles), followed by fluorescence measurement 30 min later. The data is a representative of two experiments. (B) Human neutrophils were incubated with 0.1% DMSO (empty bars) or 100 nM fMLP (hatched bars) for 15 s, and relative F-actin was measured in parallel by three different methods, namely, quantification of Triton-insoluble cytoskeleton-associated actin (TIC), by fluorescein phalloidin with subsequent methanol extraction of the bound dye (FP/MeOH), and the measurement of rhodamine phalloidin fluorescence enhancement (RPFE). The data are presented in percentage to [F-actin] in DMSO-treated cells, as means ± SE ($n = 3$).

1 are presented in Fig. 2. An important feature of these is the initial region, where fluorescence enhancement is nearly linearly related to the total F-actin concentration (Fig. 2, inset). If desired, this allows the simple determination of absolute F-actin concentrations from the fluorescence enhancement data. For data obtained at equilibrium, Eq. [6] is applied. For nonequilibrium conditions, F-actin can be deduced from ΔF using curves generated with Eq. [8].

An example of such a conversion is presented in the insert of Fig. 1. It is apparent that these data can be well fitted linearly. F-actin values (presented as squares) calculated from the ΔF data show that the region of linearity expands up to 10–15 nM F-actin, allowing reliable F-actin measurements in this region, in a good accordance with the mathematical model (see Fig. 2 and Table 1).

A summary of conditions for F-actin measurements from rhodamine phalloidin fluorescence enhancement is shown in Table 1 and was established on the basis of Eqs. [5]–[8] (see Materials and Methods). To simplify the procedure for the users, the table lists limits of ΔF where [F-actin] is directly proportional to ΔF. The lower limit was arbitrary set to $\Delta F = 0.5F_0$ to ensure a good signal-to-noise ratio. The table can also be used to estimate absolute [F-actin] from ΔF data without further considerations.

Noteworthy, in the presented type of assay of cytosolic F-actin quantification, fluorescence enhancement reflects F-actin changes having happened before exposure of the cytosol to rhodamine phalloidin and not after. Indeed, the presence of 15 μM DNaseI, a high-affinity G-actin-sequestering protein (25), does not affect rhodamine phalloidin fluorescence (data not shown). Protection of the preexisting actin filaments to depolymerization is mostly achieved by the role of F-actin-binding proteins: Stabilization of F-actin by α-actinin (26), myosin subfragment 1, and tropomyosin (16) to depolymerization has been successfully performed. Moreover, Cano and others showed that diluted cell lysates do not depolymerize their F-actin even under prolonged incubation due to the presence of actin-stabilizing proteins (26). Therefore, no special precautions are required when F-actin has to be quantified in cells, cell lysates or cytosolic fractions.

To measure F-actin in cells, the latter are usually lysed with membrane perturbants like lysophosphatidylcholine (0.08–0.1 mg/ml) or Triton X-100 (1%) (13, 18). These compounds interfere, however, with the fluorescence-enhancement assay by causing a 10- to 20-fold increase in rhodamine phalloidin fluorescence by themselves. This effect was observed only when detergent concentrations exceeded the critical micelle concentration (CMC, data not shown), being best ex-

plained by an unspecific hydrophobic interaction of rhodamine phalloidin with the detergent micelles.

Having a high CMC, octyl-β-D-glucopyranoside (OG) was chosen as the membrane-permeabilizing agent. Neutrophils were fixed for 15 min in the presence of 4% p-formaldehyde and 2.5% OG, which is sufficient to lyse cell membranes (27). Subsequently, the cells were diluted to reduce the concentration of OG below CMC (which is 0.64%, (28)) with PBS supplemented with rhodamine phalloidin to give a final concentration of 15 nM, and the fluorescence was read after 30 min incubation at RT. Up to 1.5×10^6 cells/ml, the fluorescence was linearly related to the cell number, but became saturated at about 1×10^7 cells/ml (Fig. 3A). Assuming that a neutrophil contains ca. 50 pg actin, of which ~30% is polymerized in the resting state (29), up to 500 nM of cellular F-actin falls into a region of approximately linear relationship with fluorescence enhancement of 15 nM rhodamine phalloidin. Making actin nonaccesible to phalloidin by formylation, formaldehyde fixation of F-actin increases its apparent dissociation constant for phalloidin to ~400 nM (data not shown). Thus, the obtained results are in a good agreement with theory (see Fig. 2 and Table 1) and define conditions to measure relative F-actin changes in neutrophils.

For comparison, three methods were used to quantify F-actin before and after neutrophil stimulation with fMLP (Fig. 3B): (i) measurement of Triton-insoluble actin (5, 6), (ii) fluorescein phalloidin labeling of cells with subsequent methanol extraction of bound dye and fluorescence measurement (13), and (iii) rhodamine phalloidin fluorescence enhancement method presented here. All detect fMLP-induced actin polymerization, although (ii) yielded a lower relative increase in F-actin, which might be due to an incomplete extraction of the dye achieved after 1 h incubation in methanol used here according to (13, 18) instead of 24–48 h of extraction proposed by Cano and others (30, 14).

In summary, the rhodamine phalloidin fluorescence enhancement assay as presented here is characterized by the following assets: (i) Speed—it takes about 20 min to quantify F-actin in cell lysates and about 45 min in whole cells, compared to several hours–days required by other methods (18, 30). (ii) Simplicity—no washing or extraction steps, no SDS–PAGE, or densitometry analysis are necessary. (iii) Cost—the assay requires 100–1000 times less fluorescently labeled phalloidin than competitors (18, 30) and, most importantly, reduces the sample size by a similar factor.

ACKNOWLEDGMENTS

REFERENCES

1. Huang, Z. J., Haugland, R. P., You, W. M., and Haugland, R. P. (1992) *Anal. Biochem.* **200**, 199–204.
2. Condeelis, J. (1993) *Annu. Rev. Cell Biol.* **9**, 411–444.
3. Pollard, T. D., and Cooper, J. A. (1986) *Annu. Rev. Biochem.* **55**, 987–1035.
4. Blikstad, I., Markey, F., and Carlsson, L. (1978) *Cell* **15**, 935–943.
5. White, J. R., Naccache, P. H., and Sha'afi, R. I. (1982) *Biochem. Biophys. Res. Commun.* **108**, 1144–1149.
6. White, J. R., Naccache, P. H., and Sha'afi, R. I. (1983) *J. Biol. Chem.* **258**, 14041–14047.
7. Cooper, J. A., Walker, S. B., and Pollard, T. D. (1983) *J. Muscle Res. Cell Motil.* **4**, 253–262.
8. Symons, M. H., and Mitchison, T. J. (1991) *J. Cell Biol.* **114**, 503–513.
9. Westphal, M., Jungbluth, A., Heidecker, M., Mühlbauer, B., Heizer, C., Schwartz, J. M., Marriott, G., and Gerisch, G. (1997) *Curr. Biol.* **7**, 176–183.
10. Wieland, T. (1986) Peptides of Poisonous Amanita Mushrooms, pp. 129–180, Springer-Verlag, New York.
11. Cooper, J. A. (1987) *J. Cell Biol.* **105**, 1473–1478.
12. Howard, T. H., and Meyer, W. H. (1984) *J. Cell Biol.* **98**, 1265–1271.
13. Howard, T. H., and Oresajo, C. O. (1985) *Cell Motil.* **5**, 545–557.
14. Cano, M. L., Cassimeris, L., Joyce, M., and Zigmond, S. H. (1992) *Cell Motil. Cytoskel.* **21**, 147–158.
15. Zigmond, S. H., Joyce, M., Borleis, J., Bokoch, G. M., and Devreotes, P. N. (1997) *J. Cell. Biol.* **138**, 363–374.
16. De La Cruz, E. M., and Pollard, T. D. (1994) *Biochemistry* **33**, 14387–14392.
17. Katanaev, V. L., and Wymann, M. P. (1998) *J. Cell Sci.* **111**, 1583–1594.
18. DiNubile, M. J., and Southwick, F. S. (1988) *Methods Enzymol.* **162**, 246–271.
19. Böyum, A. (1968) *Scand. J. Clin. Lab. Invest.* **97**, 77–89.
20. Ward, L. D. (1985) *Methods Enzymol.* **117**, 400–414.
21. Rodbard, D., and Feldman, H. A. (1975) *Methods Enzymol.* **36**, 3–16.
22. Vassent, G., and Jard, S. (1971) *C. R. Acad. Sci.* **272**, 880–883.
23. De La Cruz, E. M., and Pollard, T. D. (1996) *Biochemistry* **35**, 14054–14061.
24. Dancker, P., Low, I., Hasselbach, W., and Wieland, T. (1975) *Biochim. Biophys. Acta* **400**, 407–414.
25. Mannherts, H. G., Leigh, J. B., Leberman, R., and Pfrang, H. (1975) *FEBS Lett.* **60**, 34–38.
26. Cano, M. L., Cassimeris, L., Fechheimer, M., and Zigmond, S. H. (1992) *J. Cell Biol.* **116**, 1123–1134.
27. Hartwig, J. H., Bokoch, G. M., Carpenter, C. L., Janmey, P. A., Taylor, L. A., Toker, A., and Stossel, T. P. (1995) *Cell* **82**, 643–653.
28. Calbiochem Biochemicals (1997) A Guide to the Properties and Uses of Detergents. Biology and Chemistry, Calbiochem Corporation, San Diego.
29. Omann, G. M., Allen, R. A., Bokoch, G. M., Painter, R. G., Traynor, A. E., and Sclar, L. A. (1987) *Physiol. Rev.* **67**, 285–322.
30. Cano, M. L., Lauffenburger, D. A., and Zigmond, S. H. (1991) *J. Cell Biol.* **115**, 677–687.

3. Central role of G protein-couped PI3Kγ in inflammation.

Hirsch E, Katanaev VL, Garlanda C, Azzolino O, Pirola L, Silengo L, Sozzani S, Mantovani A, Altruda F, Wymann MP. Science, in press.

ulations of CD45R$^+$ cells in spleens or of CD45R$^+$ and CD43$^+$ cells in bone marrow (10). Unlike wild-type mice, however, mice lacking PI3Kγ produced few antibodies containing the λ light chain when immunized with T cell–independent (TI) antigen hydroxylnitrophenyl (NP)–Ficoll (Fig. 4A). By contrast, mice lacking both PLC-β2 and PLC-β3 consistently produced larger amount of TI antigen-specific antibodies composed of the immunoglobulin λ light chain (TI-Igλ$_L$) than did wild-type mice (Fig. 4A). It appears that the PLC pathway, in this case, opposes the PI3K pathway. Enhancement in TI-Igλ$_L$ production appeared to be primarily dependent on the PLC-β3 deficiency (Fig. 4A). Neither PLC nor PI3K deficiency affected the production of TI-Igκ (Fig. 4B) or of T cell–dependent (TD) antigen NP–chicken gamma globulin (NP-CCG)–specific antibodies composed of either λ or κ light chains (10). Together these data suggest that the production of TI-Igλ$_L$ may be subjected to regulation by G protein–mediated signaling pathways. Because no differences were detected between wild-type and PI3Kγ-deficient mice in the amount of total serum Igλ$_L$ and in the number of B cells carrying cell surface λ$_L$ (10), we think that PI3Kγ deficiency is more likely to affect antigen-dependent processes than early development of B cells.

Mice lacking PLC-β3 developed spontaneous multifocal skin ulcers usually starting at the age of 6 months or older (Fig. 4C). The lesions were localized mainly behind ears or on the neck, but sometimes also appeared on the face. Similar phenotypes were observed with mice lacking both PLC-β2 and PLC-β3. Histological examination of the lesion tissues revealed hyperinfiltration of leukocytes in the lesion tissues (Fig. 4, D and E). Most of the infiltrated leukocytes had morphological characteristics of macrophages and lymphocytes. No ulcerative lesions were observed in wild-type mice, mice heterozygous for the disrupted PLC-β3 genes, or other transgenic lines including PLC-β2– and PI3Kγ-null mice that were housed in the same rooms under the same conditions. This ulcerative phenotype is consistent with the idea that the PLC pathways act to inhibit some important responses mediated by chemoattractants.

In summary, this study with mouse lines deficient in two prominent chemoattractant-activated signaling pathways confirms that both PI3Kγ and PLC-β2/-β3 have important roles in chemoattractant-induced responses. The study also revealed roles for these proteins in leukocyte functions, including the involvement of PI3Kγ in the production of TI-Igλ$_L$ and the PLC pathway in down-modulation of chemotaxis and production of TI-Igλ$_L$ and in hyperinflammatory conditions.

References and Notes

1. M. Baggiolini, *Nature* **392**, 565 (1998).
2. B. A. Premack and T. J. Schall, *Nature Med.* **2**, 1174 (1996).
3. S. Jung and D. R. Littman, *Curr. Opin. Immunol.* **11**, 319 (1999).
4. D. Wu, G. J. LaRosa, M. I. Simon, *Science* **261**, 101 (1993).
5. B. Stoyanov *et al.*, *Science* **269**, 690 (1995).
6. L. R. Stephens *et al.*, *Cell* **89**, 105 (1997).
7. The PI3Kγ-deficient mouse line was generated by standard protocol (11). An 8-kb genomic DNA was isolated from a mouse 129sv genomic DNA library containing at least the first three exons of mouse PI3Kγ. A part of the first exon and entire second and third exons were replaced by the cDNA encoding GFP, which was fused in frame with the coding sequence of PI3Kγ. In addition, a neomycin–resistant gene expression unit was inserted behind GFP for selection of transfected embryonic stem (ES) cells. Three of the positive ES clones were used to produce chimeras. Mice heterozygous and homozygous for the disrupted PI3Kγ genes were produced by standard mating schemes.
8. The levels of PtdIns (3,4,5)P$_3$ were determined as described (24) with some modification. Mouse neutrophils (1 × 10^7) were labeled with [^{32}P]orthophosphate (1 mCi/ml) for 60 min at 37°C. After washing, cells were treated with 1 μM *f*MLP for 45 s. Lipid was extracted and analyzed on a 20 cm by 20 cm Silica Gel 60 thin-layer chromatography plate (EM Science, Gibbstown, NJ), as described in (24).
9. H. Jiang, Y. Kuang, M. I. Simon, D. Wu, *Proc. Natl. Acad. Sci. U.S.A.* **94**, 7971 (1997).
10. Z. Li *et al.*, data not shown.
11. W. Xie *et al.*, *Proc. Natl. Acad. Sci. U.S.A.* **96**, 10385 (1999).
12. C. J. Vlahos *et al.*, *J. Immunol.* **154**, 2413 (1995).
13. M. Thelen, M. P. Wymann, H. Langen, *Proc. Natl. Acad. Sci. U.S.A.* **91**, 4960 (1994).
14. U. G. Knaus, P. G. Heyworth, T. Evans, J. T. Curnutte, G. M. Bokoch, *Science* **254**, 1512 (1991).
15. A. Abo *et al.*, *Nature* **353**, 668 (1991).
16. G. M. Bokoch, *Curr. Opin. Cell Biol.* **6**, 212 (1994).
17. P. T. Hawkins *et al.*, *Biochem. Soc. Trans.* **25**, 1147 (1997).
18. J. Han *et al.*, *Science* **279**, 558 (1998).
19. J. W. Park and B. M. Babior, *J. Biol. Chem.* **267**, 19901 (1992).
20. L. M. Keranen, E. M. Dutil, A. C. Newton, *Curr. Biol.* **5**, 1394 (1995).
21. J. A. Le Good *et al.*, *Science* **281**, 2042 (1998).
22. D. A. Fruman *et al.*, *Science* **283**, 393 (1999).
23. H. Suzuki *et al.*, *Science* **283**, 390 (1999).
24. A. Ptasznik *et al.*, *J. Biol. Chem.* **271**, 25204 (1996).
25. V. Benard, B. P. Bohl, G. M. Bokoch, *J. Biol. Chem.* **274**, 13198 (1999).
26. The levels of guanosine triphosphate (GTP)–bound Rac were assayed by determining the amount of Rac associated with glutathione S-transferase–protein binding domain (GST-PBD) as described (25), with some modification. Murine neutrophils (1 × 10^7/50 μl) were treated with 4 μM *f*MLP for the durations indicated. The reaction was stopped by adding the same volume of the 2× lysis buffer [50 mM tris-HCl (pH 7.5), 10 mM MgCl$_2$, 200 mM NaCl, 2% NP-40, 10% glycerol, 2 mM phenylmethylsulfonyl fluoride, leupeptin (2 μg/ml), aprotinin (2 μg/ml), 2 mM orthovanadate, and 10 μg of GST-PBD]. The lysates were centrifuged for 3 min at 700g, and the supernatant was incubated with glutathione-Sepharose 4B beads for 1 hour at 4°C after addition of 200 μl of binding buffer [25 mM tris-HCl (pH 7.5), 1 mM dithiothreitol (DTT), 30 mM MgCl$_2$, 40 mM NaCl, and 0.5% Triton X-100]. The beads were washed three times with a washing buffer (the binding buffer with 1% Triton X-100) and washed one time with the binding buffer in the absence of Triton X-100. The beads were resuspended in SDS–polyacrylamide gel electrophoresis sample buffer and analyzed by Western blot with an antibody to Rac.
27. Mice (8 to 12 weeks old) were injected intraperitoneally with 10 μg of Alumn-precipitated NP32-Ficoll (TI) or NP22-CGG (TD). Sera were collected on day 7. Ten μl of serum was added to 100 μl of phosphate-buffered saline. Enzyme-linked immunosorbent assay (ELISA) was carried out in 96-well plates coated with NP30–bovine serum albumin with an ELISA kit from Zymed (South San Francisco, CA).
28. We thank M.-C. Dagher for antibody to p47phox, A. Pahxia for technical help, and A. Satterthwaite and O. Witte for critically reading this manuscript. Supported by grants to D.W. and A.V.S. from NIH and the American Heart Association.

17 September 1999; accepted 16 December 1999

Central Role for G Protein–Coupled Phosphoinositide 3-Kinase γ in Inflammation

Emilio Hirsch,[1]* Vladimir L. Katanaev,[2] Cecilia Garlanda,[3] Ornella Azzolino,[1] Luciano Pirola,[2] Lorenzo Silengo,[1] Silvano Sozzani,[3] Alberto Mantovani,[3,4] Fiorella Altruda,[1]† Matthias P. Wymann[2]*†

Phosphoinositide 3-kinase (PI3K) activity is crucial for leukocyte function, but the roles of the four receptor-activated isoforms are unclear. Mice lacking heterotrimeric guanine nucleotide-binding protein (G protein)–coupled PI3Kγ were viable and had fully differentiated neutrophils and macrophages. Chemoattractant-stimulated PI3Kγ$^{-/-}$ neutrophils did not produce phosphatidylinositol 3,4,5-trisphosphate, did not activate protein kinase B, and displayed impaired respiratory burst and motility. Peritoneal PI3Kγ-null macrophages showed a reduced migration toward a wide range of chemotactic stimuli and a severely defective accumulation in a septic peritonitis model. These results demonstrate that PI3Kγ is a crucial signaling molecule required for macrophage accumulation in inflammation.

Chemoattractant-mediated recruitment of leukocytes is a key step in the progress of acute and chronic inflammation. Chemokines and chemotactic peptides, such as N-formyl-Met-Leu-Phe (*f*MLP), C5a, and interleukin-8 (IL-8), bind to G protein–coupled re-

ceptors (1). Receptor activation induces the release of Gβγ subunits from trimeric G proteins. In phagocytic cells, this triggers a series of signaling events that culminate in directional cell movement, phagocytosis, degranulation, and superoxide generation (1). The production of phosphatidylinositol 3,4,5-trisphosphate [PtdIns $(3,4,5)P_3$] appears to have an essential role, because inhibitors of PI3K prevent these responses (2). Leukocytes express all the four known class I PI3K isoforms (PI3Kα, β, γ, and δ), but it is presently not clear which enzyme(s) relay inflammatory signals (3).

To assess the physiologic role of the PI3Kγ isoform, we generated PI3Kγ-deficient mice by homologous recombination. The targeting vector disrupted the PI3Kγ gene by the insertion of an IRES (internal ribosomal entry site)-LacZ and a neomycin resistance cassette in the first coding exon (exon 2) (4). Embryonic stem (ES) cell clones showing heterozygous gene disruption were used to generate germ line chimeras (5).

Mice homozygous for the PI3Kγ-targeted allele were viable, fertile, and displayed a normal life-span in a conventional mouse facility. Whereas wild-type (WT) mice expressed PI3Kγ in neutrophils, macrophages, and splenocytes, homozygous mutant cells showed no expression of the protein. In the same cells, the lack of PI3Kγ did not alter the expression of other class I PI3Ks (namely α, β, and δ) (Fig. 1A) (6).

Peripheral blood cell counts of PI3Kγ-deficient mice showed no statistically significant differences in the hematocrit or in the distribution of lymphocytes, monocytes, basophils, and eosinophils compared with those in WT animals. By contrast, PI3Kγ-null mice had about twice as many of circulating polymorphonuclear neutrophils (PMNs) as WT mice (Table 1). Microscopic examination of blood smears did not show any morphological abnormality in any leukocyte population.

[1]Department of Genetics, Biology and Biochemistry, University of Torino, Turin, Italy. [2]Institute of Biochemistry, University of Fribourg, CH-1700 Fribourg, Switzerland. [3]Istituto di Ricerche Farmacologiche Mario Negri, Milan, Italy. [4]Section of General Pathology, University of Brescia, Brescia, Italy.

*To whom correspondence should be addressed. E-mail: hirsch@molinette.unito.it and matthiaspaul.wymann@unifr.ch
†These authors contributed equally to this work.

Table 1. Blood parameters. Data are the mean ± SE of 15 mice from each group.

| Parameter	WT	PI3Kγ$^{-/-}$
Hematocrit (%)	47.30 ± 0.72	47.8 ± 1.03
Neutrophils ($10^3/\mu l$)	0.66 ± 0.10	1.23 ± 0.13*
Lymphocytes ($10^3/\mu l$)	2.18 ± 0.29	1.26 ± 0.17
Monocytes ($10^3/\mu l$)	0.08 ± 0.02	0.08 ± 0.02
Eosinophils ($10^3/\mu l$)	0.004 ± 0.001	0.008 ± 0.003
Basophils ($10^3/\mu l$)	0.008 ± 0.002	0.006 ± 0.002
Platelets ($10^3/\mu l$)	415 ± 25	410 ± 35

*$P < 0.001$ (Student's t test).

Fig. 1. PI3K downstream signaling by seven–transmembrane helix receptors. (**A**) Failure of PI3Kγ$^{-/-}$ hematopoietic cells to express PI3Kγ. Murine PI3Kγ was detected in WT bone marrow–derived neutrophils (NØ), thioglycollate-elicited peritoneal macrophages (MØ), macrophage-depleted splenocytes (Spl.), and cells from the upper Percoll layer [light bone marrow fraction (6), LBM; consisting mainly of lymphocytes and monocytes] by immunoblotting with monoclonal antibodies produced against the NH₂-terminal part of human PI3Kγ. PI3Kα, β, and δ were detected with antibodies described in (6). Murine hematopoietic 32D cells (32D) and human embryonic kidney (HEK) 293 cells were applied as positive and negative controls. (**B**) Neutrophil PI3K activity after C5a (10 nM), fMLP (1 μM), and IL-8 (100 nM) stimulation. Lipids were extracted from PMNs labeled with inorganic phosphate ($^{32}P_i$) at the indicated times, deacylated, and separated by HPLC (2). To obtain the kinetic profile in the left panel, peaks as shown in the right panel (15-s stimulation) were integrated, and the ratio of PtdIns$(3,4,5)P_3$/PtdIns$(4,5)P_2$ was calculated as a percentage ($n \geq 3$, mean ± SE). The elution times of the deacylation products of PtdIns$(4,5)P_2$ and PtdIns$(3,4,5)P_3$ are indicated by (4,5) and (3,4,5), respectively. (**C**) PKB phosphorylation in response to heptahelical receptor agonists. Bone marrow–derived PMNs (10^6/ml) of the indicated genotypes were incubated for 10 min at 37°C and subsequently stimulated with 1 μM fMLP, 10 nM C5a, or 10 nM IL-8 for 30 s. Samples were probed for the presence of PI3Kγ, PKB phosphorylated on Ser-473, and total PKB. (**D**) PKB phosphorylation by G protein–independent signaling pathways. Human serum–opsonized zymosan (C3b$_i$ and immunoglobulin G–coated) and GM-CSF (100 ng/ml) were used to stimulate neutrophils for 15 and 5 min, respectively. C5a stimulation was done as in (C). (**E**) G protein–dependent intracellular calcium release. Fura-2–loaded PMNs obtained from wild-type (wt) and PI3Kγ-null mice were stimulated with IL-8 (50 nM), C5a (1 nM), platelet activating factor (PAF, 100 nM), and fMLP (100 nM).
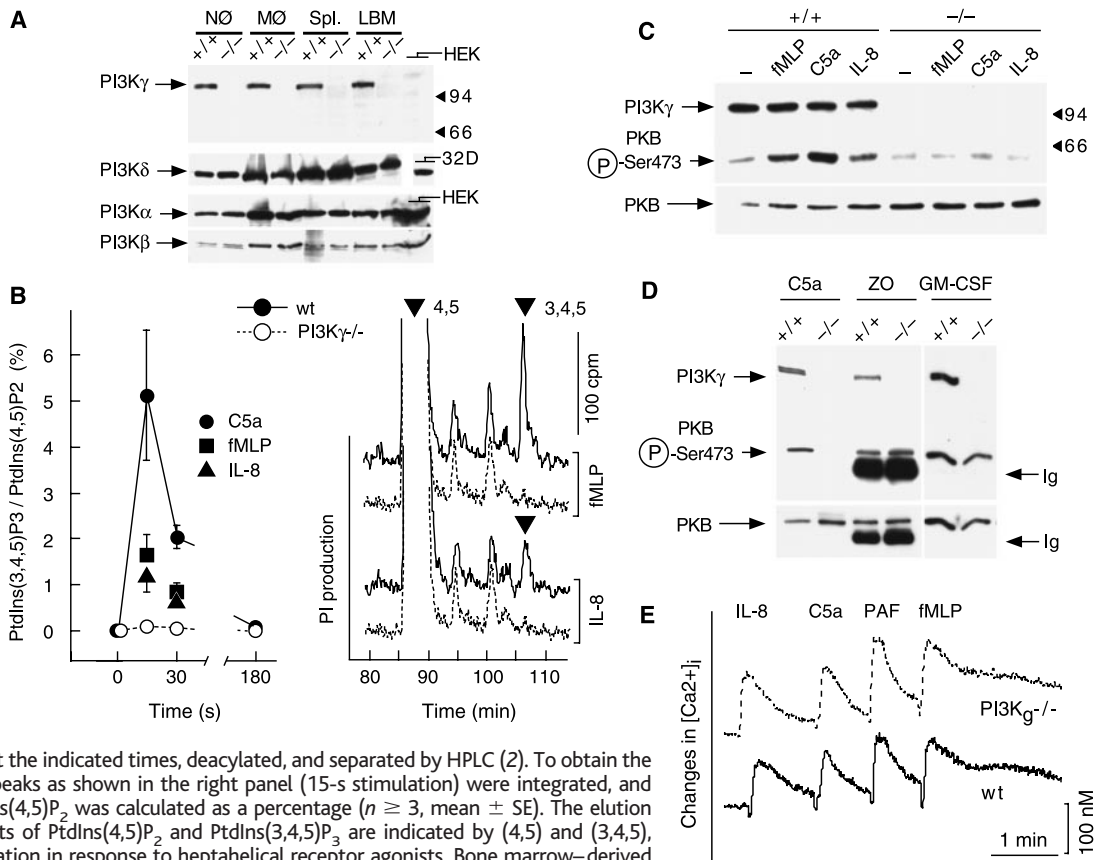
Fluorescence-activated cell sorter (FACS) analysis of bone marrow PMNs and resident peritoneal macrophages with antibodies to distinct cell surface markers (Gr-1 and CD11b for PMNs; CD11b, F4/80, CD80, and CD86 for macrophages) revealed matching cell distribution and expression patterns in WT and PI3Kγ-null mice, indicating that differentiation of myeloid cells is independent of PI3Kγ (7).

The coupling of PI3Kγ to seven–transmem-
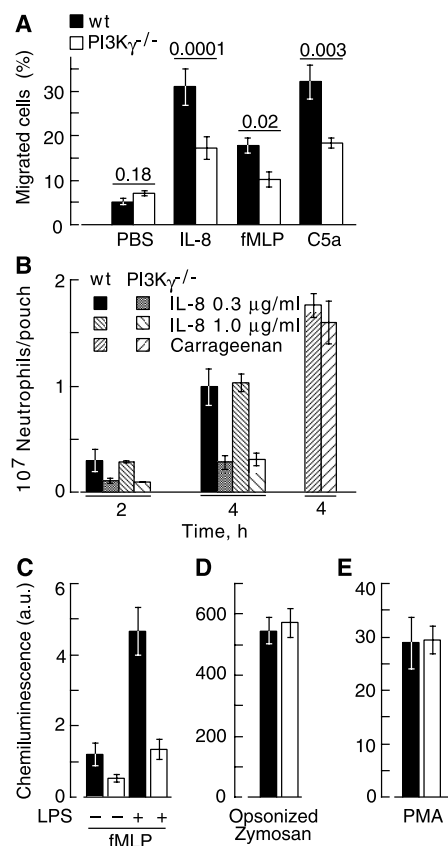
Fig. 2. Chemotaxis and respiratory burst of PMNs. (**A**) Chemotaxis to IL-8 (50 nM), fMLP (100 nM), and C5a (3 nM) was measured with fluorescently labeled cells (18). The data (mean ± SE, n = 6 to 13) are expressed as the percentage of total cells that migrated. Indicated P values were calculated by ANOVA and represent comparisons of WT and PI3Kγ-null populations. (**B**) Migration to air pouches. IL-8 (1 and 0.3 μg/ml in sterile apyrogenic saline) and carrageenan (1% in sterile apyrogenic saline) were injected into 6-day-old air pouches (12). Mice were killed 2 or 4 hours later and the exudate collected in 1 ml of saline. Results are the mean ± SE of PMN counts from five to six different mice per group. (**C** to **E**) Respiratory burst in PMNs. (C) PMNs were preincubated in the absence or presence of lipopolysaccharide (LPS, 100 ng/ml) before stimulation with 1 μM fMLP (mean ± SE; n = 8 to 13). (D) Resting PMNs were stimulated with human serum–opsonized zymosan (mean ± SE; n = 3). (E) Resting PMNs were stimulated with 100 nM PMA (mean ± SE; n = 6). Chemiluminescence was measured according to published methods (19), and data represent integrated responses (fMLP, 3 min; opsonized zymosan, 30 min; PMA, 30 min).

brane receptor signaling was assessed in morphologically mature bone marrow PMNs. Phosphoinositides were analyzed by metabolic labeling with ^{32}P–inorganic phosphate and subsequent analysis of deacylated lipids on high-performance liquid chromatography (HPLC). After stimulation of cells with C5a, fMLP, or IL-8, PtdIns(3,4,5)P$_3$ was produced in WT but not in PI3Kγ$^{-/-}$ cells (Fig. 1B). The serine-threonine protein kinase B (PKB/Akt) is a major target of PI3K (8). Whereas C5a, fMLP, and IL-8 triggered PKB phosphorylation in response to chemoattractants in WT cells, in PI3Kγ-null PMNs PKB phosphorylation did not rise above background levels (Fig. 1C). Serum–opsonized zymosan and granulocyte-macrophage colony-stimulating factor (GM-CSF), by contrast, were still capable of signaling to PKB (Fig. 1D). Therefore, protein tyrosine kinase–dependent processes successfully activate PI3Kα, β, or δ isoforms in PI3Kγ-null cells. The intact calcium release initiated by fMLP-, C5a-, platelet-activating factor (PAF)-, and IL-8 receptors (Fig. 1E) illustrates that PI3Kγ-independent G protein–coupled signaling pathways are not affected. PI3Kγ is thus the sole PI3K isoform coupled to fMLP, C5a, and IL-8 receptors.

PI3Kγ functions in cytoskeletal remodeling and leukocyte mobility (9). In addition, the chemotactic response to agonists of G protein–linked heptahelical receptors is correlated with PI3K-dependent activation of PKB (10). We thus examined the ability of mutant PMNs to adhere and migrate. Mutant cells showed no increase in cell adhesion on fibronectin in response to IL-8 (11). Because adhesion and cytoskeletal remodeling are prerequisites for cell motility, the chemotactic response to IL-8, fMLP, and C5a was assayed. PMNs from PI3Kγ-null mice displayed a reduction in chemotaxis in response to IL-8, fMLP, and C5a in vitro (Fig. 2A). The in vivo impact of this chemotactic defect was assessed by measurement of agonist-induced PMN infiltration into subcutaneous air pouches. IL-8 at doses of 0.3 and 1 μg caused recruitment of 60% fewer PMNs in PI3Kγ-null mice than in WT animals after 2 and 4 hours (Fig. 2B). The response to carrageenan, a pleiotropic inflammatory stimulus (12), was not altered in PI3Kγ-null mice (Fig. 2B). These data indicate that lack of PI3Kγ leads to impaired recruitment of PMNs in response to chemokines.
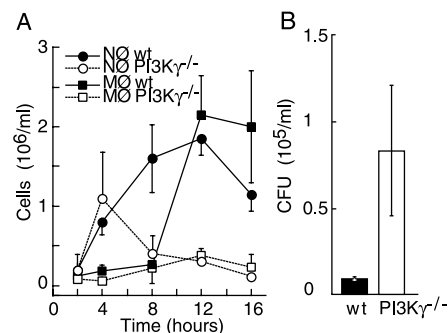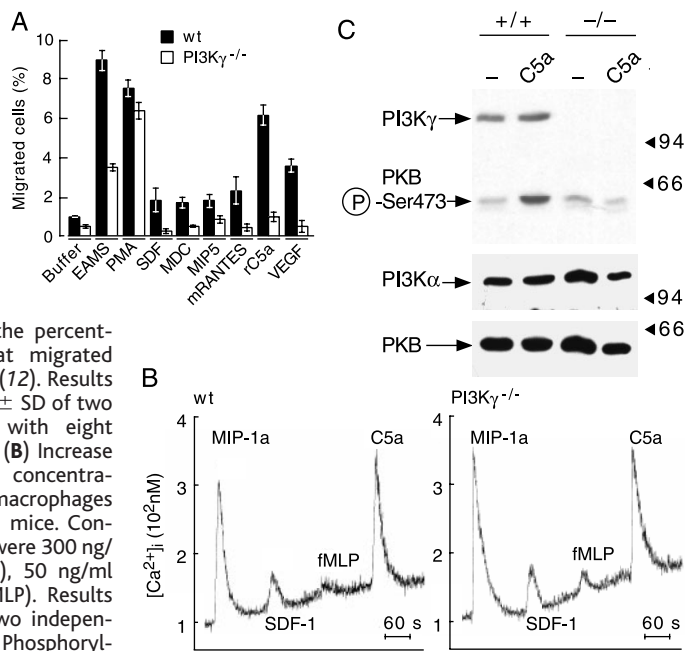
Of the various neutrophil responses, the agonist-induced respiratory burst is the most sensitive to PI3K inhibitors (2). Resting neutrophils only weakly respond with a respiratory burst to seven–transmembrane receptor agonists, but can be "primed" with tumor necrosis factor–α, GM-CSF, or lipopolysaccharide (LPS) to markedly increase their response (13). Consistent with these data, WT murine bone marrow–derived PMNs responded to fMLP

after a prolonged incubation with LPS, whereas PI3Kγ-null cells remained less responsive (Fig. 2C). Prolonged adhesion restored the sensitivity of PI3Kγ-null neutrophils to fMLP in a wortmannin-sensitive manner (7). Activation of the NADPH (nicotinamide adenine dinucleotide phosphate, reduced) oxidase by serum–opsonized zymosan or phorbol 12-myristate 13-acetate (PMA) was intact in PI3Kγ$^{-/-}$ cells (Fig. 2, D and E). These results, and the reported sensitivity of fMLP and zymosan-induced respiratory burst to wortmannin (2), suggest that fMLP triggers PtdIns(3,4,5)P$_3$ production required for the respiratory burst exclusively by way of PI3Kγ. The zymosan signal (complement 3b$_i$-mediated stimulation) or priming events, on the other hand, act by way of protein tyrosine kinases on p85-associated PI3Ks, thus relieving an essential requirement for PI3Kγ (e.g., for the activation of PKB; see Fig. 1D).

PI3Kγ-null macrophages, obtained from peritoneal exudate of thioglycollate-treated mice, were tested in an in vitro chemotaxis assay with various chemoattractants. First, we evaluated the chemotactic response toward endotoxin-activated mouse serum (EAMS) as a source of chemotactic complement fractions. In this assay, the chemotactic response of PI3Kγ-null cells was reduced by 60% (Fig. 3A). In contrast, peritoneal macrophages showed a similar migration toward PMA, indicating that the defect resided in receptor signaling rather than in leukocyte locomotion ability. To further characterize the migratory deficiency observed with EAMS, we stimulated PI3Kγ-deficient macrophages with G protein–coupled serpentine receptor agonists such as RANTES (regulated on activation, normal T cell expressed and secreted), macrophage inflammatory protein–5 (MIP-5), macrophage-derived chemokine (MDC), stromal cell–derived factor–1 (SDF-1), and C5a. Migration toward all of these chemotactic agents was reduced in mutant macrophages. Chemotaxis of PI3Kγ$^{-/-}$ macrophages was decreased in response to C5a (85% reduction), SDF-1 (85%), RANTES (80%), MDC (70%), and MIP-5 (52%) compared with WT cells (Fig. 3A). PI3Kγ$^{-/-}$ peritoneal macrophages also exhibited an 85% reduction in chemotaxis toward vascular endothelial growth factor (VEGF), an agonist known to bind a tyrosine kinase receptor (Fig. 3A) (14). This observation is consistent with the report that VEGF-stimulated migration can be inhibited by pertussis toxin (15) and establishes a crucial role of PI3Kγ in this G protein–mediated response. Upon stimulation with G protein–coupled receptor agonists RANTES, MIP-5, SDF-1, C5a, and fMLP, mutant and WT macrophages showed similar increases in intracellular Ca^{2+} release (Fig. 3B). Consistent with a specific PI3K signaling defect, PI3Kγ$^{-/-}$-purified resting peritoneal macrophages showed no increase in PKB phosphorylation after C5a stimulation (Fig. 3C).

Fig. 3. Role of PI3Kγ in thioglycollate-elicited peritoneal macrophages. (**A**) Chemotaxis was elicited by using optimal concentrations of agonists: 5% EAMS, 16 nM PMA, 100 ng/ml SDF-1, 100 ng/ml MDC, 1 μg/ml MIP-5, 100 ng/ml RANTES, 100 ng/ml C5a, and 10 ng/ml VEGF. Data represent the percentage of total cells that migrated through the filter pores (*12*). Results are shown as the mean ± SD of two triplicate experiments with eight mice of each genotype. (**B**) Increase of intracellular calcium concentration in Fura-2–loaded macrophages from WT and PI3Kγ$^{-/-}$ mice. Concentrations of agonists were 300 ng/ml (MIP-1α and SDF-1), 50 ng/ml (C5a), and 10 μM (*f*MLP). Results are representative of two independent experiments. (**C**) Phosphorylation of PKB after C5a stimulation. Experiments were performed as in Fig. 1C.

major task of present pharmacological research. Our results indicate that PI3Kγ might be a suitable target for development of drugs that could specifically modulate phagocyte functions without generating severe side effects.

References and Notes

1. M. Baggiolini, B. Dewald, B. Moser, *Annu. Rev. Immunol.* **15**, 675 (1997); M. Locati and P. M. Murphy, *Annu. Rev. Med.* **50**, 425 (1999); A. D. Luster, *N. Engl. J. Med.* **338**, 436 (1998); A. Mantovani, *Immunol. Today* **20**, 254 (1999).
2. M. Baggiolini et al., *Exp. Cell Res.* **169**, 408 (1987); A. Arcaro and M. P. Wymann, *Biochem. J.* **296**, 297 (1993); T. Okada, Y. Kawano, T. Sakakibara, O. Hazeki, M. Ui, *J. Biol. Chem.* **269**, 3568 (1994).
3. M. P. Wymann and L. Pirola, *Biochim. Biophys. Acta* **1436**, 127 (1998); B. Vanhaesebroeck, S. J. Leevers, G. Panayotou, M. D. Waterfield, *Trends Biochem. Sci.* **22**, 267 (1997).
4. A genomic DNA fragment of 11 kb encompassing exons 1 through 8 of the mouse PI3Kγ was used to integrate the IRES-LacZ cassette followed by the PGK-neomycin resistance gene from the pWH9 plasmid (provided by R. Fässler, Lund University, Sweden) in exon 2, 105 base pairs downstream of the first coding ATG. Five independently targeted R1 ES cell clones were identified by Southern blot hybridization. No evidence for random integration was detected (*17*).
5. All ES cells clones were injected into C57BL/6 blastocysts. For genotyping of mice, DNA derived from tail biopsies was amplified by polymerase chain reaction with two primers sets (1: 5′-GGAGAACTAT-GAACAACCGG-3′, 5′-CAACTTCCAGTAATGCAGGC-3′; 2: 5′-CTGCTCTTTACTGAAGGCTC-3′, 5′-CAACT-TCCAGTAATGCAGGC-3′) that detect the WT and targeted allele, respectively. Phenotypic analysis was performed on two lines derived from independent clones, and results were confirmed in a 129sv-C57BL/6 mixed and 129sv inbred genetic background. The IRES-LacZ reporter gene under the control of the PI3Kγ promoter was expressed in peripheral blood leukocytes and in spleen macrophages [(*17*); for expression studies see H. G. Bernstein, G. Keilhoff, M. Reiser, S. Freese, R. Wetzker, *Cell Mol. Biol.* **6**, 973 (1998)]. Animal experiments were carried out in accordance with institutional guidelines.
6. Bone marrow cells were flushed from femurs with ice-cold RPMI 1640 medium (Gibco/BRL) supplemented with 10% fetal calf serum and antibiotics. Erythrocytes were removed by isotonic lysis, and white blood cells were loaded onto a Percoll 60/80% discontinuous step gradient. PMNs were collected from the 60/80% interface after a 30-min centrifugation (4°C, 520*g*). Splenocytes were depleted of macrophages (3-hour incubation at 37°C, 5% CO$_2$ in Iscove's modified Dulbecco's medium (IMDM medium, Life Technologies). Macrophages were obtained by washing the peritoneal cavity of mice 5 days after intraperitoneal injection of 1 ml of 3% thioglycollate (Difco). Antibodies to PI3K were from A. Klippel (Berlin, Germany; PI3Kα), R. Wetzker (Jena, Germany; PI3Kγ), B. Vanhaesebroeck (London, UK; PI3Kδ), and St. Cruz Biotechnology (PI3Kβ).
7. E. Hirsch and M. P. Wymann, unpublished data.
8. D. R.. Alessi and P. Cohen, *Curr. Opin. Genet. Dev.* **8**, 55 (1998); L. Stephens et al., *Science*, **279**, 710 (1998); T. Bondeva et al., *Science* **282**, 293 (1998); B. Tilton, M. Andjelkovic, S. A. Didichenko, B. A. Hemmings, M. Thelen, *J. Biol. Chem.* **272**, 28096 (1997).
9. A. D. Ma, A. Metjian, S. Bagrodia, S. Taylor, C. S. Abrams, *Mol. Cell Biol.* **18**, 4744 (1998); A. al-Aoukaty, B. Rolstad, A. A. Maghazachi, *J. Immunol.* **162**, 3249 (1999).
10. R. Meili et al., *EMBO J.* **18**, 2092 (1999).
11. IL-8 (50 nM) stimulated a significant [$P < 0.05$, analysis of variance (ANOVA)] increase in adhesion from 27.1% (SE = 4.8%, $n = 10$; percentage of total administered cells) to 43.5% (SE = 6.0%, $n = 14$) in WT, but not in PI3Kγ-null neutrophils [unstimulated, 27.8 ± 3.3% ($n = 10$) versus 27.0 ± 2.9% ($n = 14$) in the presence of IL-8]. C5a- and *f*MLP-induced

Fig. 4. Impairment of leukocyte recruitment during septic peritonitis in PI3Kγ$^{-/-}$ mice. (**A**) Kinetics of PMN and macrophage recruitment after intraperitoneal administration of 10^7 CFU of *E. coli* [American Type Culture Collection (ATCC) 25922]. Bacteria were grown to exponential phase, and the optical density at 600 nm was used to extrapolate cell number. Cells were washed and resuspended in 200 μl of phosphate-buffered saline before injection. Three to six mice were used for each time point (mean ± SD). (**B**) Clearance of viable *S. aureus* (ATCC 25923) from the peritoneal cavity. The peritoneal cavity was washed with 5 ml of sterile saline and the number of CFU/ml was evaluated. Results represent the mean ± SD of three mice of each genotype.

A model of aseptic peritonitis induced by intraperitoneal injection of thioglycollate was used to evaluate the impact of the lack of PI3Kγ on the onset of an inflammatory response in vivo. The number of thioglycollate-elicited peritoneal leukocytes was measured at various time points in mutant and control mice. There was a 36% decrease in total PI3Kγ$^{-/-}$ peritoneal leukocytes ($n = 7$; $P =$

0.09) at 120 hours, but no differences were present at earlier time points (4 and 48 hours). In contrast, induction of septic peritonitis by injection of Gram-positive and Gram-negative bacteria resulted in an impaired inflammatory response in PI3Kγ-deficient mice. FACS analysis and microscopic inspection of the elicited cell populations indicated that the lack of PI3Kγ affected the recruitment of both neutrophils and macrophages. The number of peritoneal PI3Kγ-null macrophages as early as 12 hours after bacteria administration was reduced by 90% compared with that in WT animals (Fig. 4A). Similar results were obtained with Gram-positive bacteria such as *Staphylococcus aureus* [5 × 10^8 colony-forming units (CFU)]. Microscopic analysis of peritoneal leukocytes revealed that PI3Kγ$^{-/-}$ macrophages did normally phagocytose bacteria. Because macrophage recruitment is essential to purge peritoneal infections, we tested whether PI3Kγ-deficient mice were able to clear peritoneal bacteria after administration of sublethal doses of *S. aureus* (*16*). Forty-eight hours after intraperitoneal injection of 5 × 10^7 CFU per mouse, bacteria persisted in the abdominal cavity of PI3Kγ$^{-/-}$ mice, with a concentration 10 times that of WT mice (Fig. 4B).

Our data are consistent with a central role of PI3Kγ in linking G protein–coupled receptor signaling to PtdIns(3,4,5)P$_3$ production, which in turn rigorously governs cell motility in macrophages and to some extent in neutrophils. The control of macrophage infiltration in chronic inflammatory diseases such as rheumatoid arthritis, pulmonary fibrosis, atherosclerosis, and autoimmune disorders is a

adhesion were not significantly reduced by the loss of PI3Kγ. Teflon-coated 12-well glass slides (Marienfeld) were coated with fibronectin (20 μg/ml; Sigma) solution. Calcein-AM (Molecular Probes)–loaded PMNs (20 μl) were applied to the glass slides. After stimulation, nonadherent cells were removed by washing. Fluorescence of attached cells was measured in a Bio-Tek FL600 fluorescence plate reader (excitation, 485 nm, 20-nm slit; emission, 530 nm, 25-nm slit).

12. M. Romano *et al.*, *Immunity* **6**, 315 (1997).
13. C. Nathan *et al.*, *J. Cell. Biol.* **109**, 1341 (1989); E. Kownatzki, A. Kapp, S. Uhrich, *Clin. Exp. Immunol.* **74**, 143 (1988); F. R. DeLeo *et al.*, *J. Clin. Invest.* **101**, 455 (1998).

14. F. Bussolino, A. Mantovani, G. Persico, *Trends Biochem. Sci.* **22**, 251 (1997).
15. B. Barleon *et al.*, *Blood* **87**, 3336 (1996).
16. Y. Aratani *et al.*, *Infect. Immun.* **67**, 1828 (1999).
17. Supplemental Web data are presented on *Science* Online at www.sciencemag.org/feature/data/1044275.shl.
18. C. W. Frevert, V. A. Wong, R. B. Goodman, R. Goodwin, T. R. Martin, *J. Immunol. Methods* **213**, 41 (1998).
19. S. T. Test and S. J. Weiss, *Methods Enzymol.* **132**, 401 (1986); M. P. Wymann, M. von Tscharner, D. A. Deranleau, M. Baggiolini, *Anal. Biochem.* **165**, 371 (1987).
20. We thank L. Barberis, M. F. Brizzi, G. Bulgarelli-Leva,

Requirement for DARPP-32 in Progesterone-Facilitated Sexual Receptivity in Female Rats and Mice

S. K. Mani,[1]* A. A. Fienberg,[2]† J. P. O'Callaghan,[3] G. L. Snyder,[2] P. B. Allen,[2] P. K. Dash,[4] A. N. Moore,[4] A. J. Mitchell,[1] J. Bibb,[2] P. Greengard,[2] B. W. O'Malley[1]

DARPP-32, a dopamine- and adenosine 3′,5′-monophosphate (cAMP)–regulated phosphoprotein (32 kilodaltons in size), is an obligate intermediate in progesterone (P)–facilitated sexual receptivity in female rats and mice. The facilitative effect of P on sexual receptivity in female rats was blocked by antisense oligonucleotides to DARPP-32. Homozygous mice carrying a null mutation for the DARPP-32 gene exhibited minimal levels of P-facilitated sexual receptivity when compared to their wild-type littermates. P significantly increased hypothalamic cAMP levels and cAMP-dependent protein kinase activity. These increases were not inhibited by a D_1 subclass dopamine receptor antagonist. P also enhanced phosphorylation of DARPP-32 on threonine 34 in the hypothalamus of mice. DARPP-32 activation is thus an obligatory step in progestin receptor regulation of sexual receptivity in rats and mice.

Progesterone (P) and dopamine (DA) facilitation of sexual receptivity in female rats requires intact, intracellular progestin receptors (PRs) (*1*). Wild-type female mice exhibit high levels of P- and DA-facilitated lordosis, whereas homozygous females carrying a null mutation for the PR gene show minimal reproductive behavior (*2, 3*). These observations substantiate a critical role for the PR as a transcriptional mediator for the signal transduction pathways initiated by P and DA.

DA, signaling through the D_1 subclass of receptors in the neostriatum, induces increases in the levels of adenosine 3′,5′-monophosphate (cAMP) and activates cAMP-dependent protein kinase (PKA) (*4*). Dopamine- and cAMP-regulated phosphoprotein-32 (DARPP-32) is phosphorylated by PKA. In its phosphorylated state, this molecule, by inhibiting the activity of protein phosphatase–1 (PP-1), increases the state of phosphorylation of many substrate proteins, leading to the induction of physiological responses (*4*). To determine whether DARPP-32 might be involved in P and DA actions on the hypothalamus, we examined its role in the facilitation of sexual receptivity in female rats and mice (*5*).

Antisense oligonucleotides to the PR inhibit P-facilitated lordosis in female rats (*6, 7*). We used a similar strategy to examine the role of DARPP-32 in P- and DA-facilitated sexual receptivity. Ovariectomized, estradiol benzoate (EB)–primed, Sprague-Dawley female rats with stereotaxically implanted stainless steel cannulae in the third cerebral ventricle (*5*) exhibited high levels of P-facilitated lordosis in the presence of males (Fig.

1A). This P-facilitated lordosis response was significantly reduced in the animals that received antisense oligonucleotides to DARPP-32 but not in control animals receiving sense oligonucleotides to DARPP-32 (Fig. 1A).

In a parallel experiment, intracerebroventricular (icv) administration of the selective D_1 agonist SKF 38393 also facilitated a lordosis response in EB-primed rats. The response was reduced by antisense but not by sense oligonucleotides to DARPP-32 (Fig. 1A). In contrast, antisense oligonucleotides to DARPP-32 had no effect on serotonin-facilitated sexual receptivity in these animals (Fig. 1B). These results were confirmed with two separate sets of oligonucleotides to DARPP-32 mRNA and their matched sense oligonucleotide controls.

DA and P facilitation of sexual receptivity were also examined in mice carrying a null mutation for the gene encoding DARPP-32 (*8*). Wild-type and DARPP-32 knockout mice show similar levels of hypothalamic PRs (*9*). Ovariectomized wild-type, heterozygous, and homozygous female mice were tested for a lordosis response in the presence of wild-type DARPP-32 males 30 min after P administration (*3, 5*). Icv P after EB priming resulted in high levels of lordosis in wild-type and heterozygous mice, whereas homozygous mice exhibited significantly lower levels of lordosis (Fig. 2A). The lordosis response of the wild-type mice to the treatments did not differ from those of the parental mouse strains C57BL/6 and 129SvEv, indicating that the behavioral alterations observed in knockout mice were not due to variations in genetic background.

Icv administration of SKF 38393 48 hours after EB priming also facilitated a reliable lordosis response in the parental strains and in wild-type and heterozygous female mice. Homozygous mutant mice, however, responded to the icv injection of SKF 38393 with minimal levels of lordosis (Fig. 2B). The lordosis response did not significantly differ between wild-type, heterozygous, and homozygous mice upon icv injection of serotonin (Fig. 2B), corroborating the DARPP-32 antisense experiments in rats indicating that DARPP-32 is not an integral part of the serotonin signaling pathway. This is consis-

[1]Department of Molecular and Cellular Biology, Baylor College of Medicine, Houston, TX 77030, USA. [2]Laboratory of Molecular and Cellular Neuroscience, Rockefeller University, New York, NY 10021, USA. [3]Centers for Disease Control and Prevention, National Institute for Occupational Safety and Health, Morgantown, WV 26505, USA. [4]Department of Neurobiology and Anatomy, The University of Texas Medical School, Houston, TX 77030, USA.

*To whom correspondence should be addressed. E-mail: smani@bcm.tmc.edu
†Present address: The Novartis Institute for Functional Genomics, San Diego, CA, USA.

4. Unpublished observations.

1. Towards the morphological analysis of the actin cytoskeleton induced by Rho proteins in the neutrophil cytosol. Role of Arp2/3 complex.

GTPγS stimulates actin polymerization in the neutrophil cytosol (Zigmond *et al.*, 1997; Katanaev and Wymann, 1998a). In addition to this, massive cross-linking of newly polymerized filaments is observed (Katanaev and Wymann, 1998a). α-actinin, ABP-280 (filamin), and other actin-binding proteins are responsible for this phenomenon (Katanaev and Wymann, 1998a). To visualise GTPγS-induced actin-rich structures with high resolution, together with Carine Galli (Institute of Experimental Physics, University of Fribourg) we applied atomic force microscopy (AFM, for a review see Engel *et al.*, 1999). Individual actin filaments were detected by this approach (Fig. 1A-F) with length ranging from <0.1 to >1 μm. Several actin structures were repeatedly observed in numerous images, including bundles (Fig. 1A) and cross-links of actin filaments at different angles (Fig. 1B-E).

Two-headed rod-like structures of α-actinin dimers (Djinovic-Carugo *et al.*, 1999) may be responsible for formation of F-actin bundles as those seen on Fig. 1A. Interestingly, examination at higher resolution identified some filaments which were densely decorated with short rods going perpendicular to the filament (Fig. 1F, marked as "α-actinin?"). The length of the rods measured by AFM was 22.9 ± 2.6 nm (mean ± sem, n=8), very close to that predicted by the analysis of α-actinin segment crystal structure (Djinovic-Carugo *et al.*, 1999). Moreover, belobed structures seen on the tips of some rods are very similar to those observed at certain angles with electron microscopy analysis of α-actinin (Winkler *et al.*, 1997).

Various forms of actin filament cross-links were repeatedly observed by AFM (Fig. 1B-E). These included X- and Y-like intersections of filaments. Quite frequently the latter were formed by two filaments branching out from the same point on the stem filament (Fig. 1C). Y-like branches are also seen at a higher resolution on Fig. 1F. Cross-section analysis revealed that most of the branchings observed lied in the same plane and were not formed by a simple overlap of two independent filaments. This indicates an involvement of actin binding proteins which cross-linked the filaments. About 40% of cross-links in macrophages were attributed to ABP-280 (Hartwig and Shevlin, 1986). This is a dimeric protein whose flexible "leaf spring" configuration allows high angle branching of the filaments (Gorlin *et al.*, 1990). Its characteristic short needle-like structure forming an angle between two actin filaments as that viewed by electron microscopy in (Hartwig *et al.*, 1980) was frequently observed in our AFM images (Fig. 1F, marked as "ABP-280?"). The dimensions of this structure, ca. 70 nm in length and ca. 4 nm in width, is very close to those of ABP-280 seen in (Hartwig *et al.*, 1980).

In addition to ABP-280, Arp2/3 complex may be responsible for formation of Y-like intersections presented on Fig. 1 D-F (Mullins *et al.*, 1998b). Arp2/3 is enriched in the leading edge of migrating cells, where it is proposed to function in either initiation or branching of filaments (Mullins *et al.*, 1997; Svitkina and Borisy, 1999; Weiner *et al.*, 1999).To test whether Arp2/3 complex is enriched in the GTPγS-induced F-actin networks, low speed sediments of the cytosol treated with or without GTPγS were probed with anti-Arp3 antiserum after separation on polyacrylamide gels. As described previously (Katanaev and Wymann, 1998a), 3-5 times more actin is found in the precipitates obtained from GTPγS-treated cytosol than from control ones. When amount of the sample from the control-treated cytosol loaded on the gel was increased to obtain equal quantities of actin in both samples, no difference in the association of Arp3 with the samples was seen (Fig. 1G). Moreover, there was clearly more Arp3 per actin in the cytosol itself than in the low speed precipitates. This is in a sharp contrast with the association of e.g. α-actinin and ABP-280 with the actin cytoskeleton. These proteins are clearly enriched in the GTPγS-induced low speed precipitates in comparison with untreated cytosol or the precipitates from control-treated cytosol (Katanaev and Wymann, 1998a). These data demonstrate that GTPγS does not enrich the Arp2/3 complex in newly formed actin cytoskeleton. The fact that the complex is nevertheless present in the cytosolic cytoskeleton suggests that Arp2/3 may still play a role in the GTPγS-induced actin polymerization.

The AFM analysis of the cytosolic actin cytoskeleton may prove to be very promising. In order to identify the molecular nature of these or those structures in the actin filament networks induced by Rho proteins in cell lysates, comparison with AFM images of purified actin binding proteins and their complexes with actin would have to be done. This could give insights into the mechanisms controlling cellular actin polymerization.

Fig. 1. GTPγS-induced actin cytoskeleton. Cytosols from human neutrophils were incubated for 20 min in the presence of GTPγS unless indicated otherwise, and centrifuged at low speed. Samples were subsequently resuspended in 1/10th of the original volume before application to silicium plates and AFM analysis (A-F) or washed, separated with SDS-PAGE and transferred to a membrane (G). (A-E) Representative F-actin structures observed with 2 nm resolution: a bundle of filaments (A), an X-like intersection (B), a Christmas tree-like structure (C), and Y-like branchings (D,E). Scale bar, 20 nm. The colour scale represents the vertical dimension. (F) Three-dimensional reconstitution of actin cytoskeleton observed with the resolution of 1.2 nm. Scale bar, 100 nm. Big spheres to the left-bottom and right-top of the image are contaminations. Short rods decorating a filament to the top-right have shapes and dimensions of α-actinin. A thin link connecting two actin filaments in the lower part of

the image has a shape and dimensions of ABP-280. (G) Anti-Arp3 antiserum (Machesky *et al.*, 1997; kindly provided by A. Segal, University College London) or Coomassie staining were used to visualize Arp3 and actin, respectively. Three times more material from the sediment of control- than of GTPγS-treated cytosol was loaded on the gel to equalize the amount of actin from the two sediments. Total protein applied before sedimentation (T) contains half actin as that loaded with the sediments.

2. CIP4 inhibits GTPγS-induced actin polymerization in the neutrophil cytosol.

In a search for the GTPase(s) mediating GTPγS-induced actin polymerization in the neutrophil cytosol, we tested the effects of recombinant CIP4, a 545-amino acid-long protein identified in a yeast two-hybrid screen as a candidate binding partner of Cdc42 and, to a less extent, Rac (Aspenström, 1997). In cultured fibroblasts, CIP4 dissociates stress fibres and antagonizes the effects of serum, PDGF, or bradykinin on stress fibre formation (Aspenström, 1997). CIP4 at 2 µM inhibited the GTPγS-induced actin polymerization in the neutrophil cytosol by ca. 50% (Fig. 2A). This inhibition was mediated by the central region of CIP4 (amino acids 293-481), known to contain the Cdc42-binding sequence as well as the site of homology to the erzin/radixin/moesin (ERM) proteins (for a review see Mangeat *et al.*, 1999). The N-terminal half of the protein was ineffective in the inhibition of actin polymerization. When higher concentrations of CIP4 were used (8 µM), an insignificant increase in the inhibitory capacity of the protein was found. In contrast to CIP4, the Cdc42-binding region of WASP (Symons *et al.*, 1996) did not affect GTPγS-induced actin polymerization (Fig. 2, see also Katanaev and Wymann, 1998a). Noteworthy, neither the full-length CIP4 nor its domains tested could induce actin polymerization on their own (not shown).

In contrast to its inhibitory effect on GTPγS-induced actin polymerization in the cytosol alone, CIP4 did not interfere with the GTPγS response in the cytosol supplemented with plasma membranes (Fig. 2B). These data might mean that different signalling pathways are activated by GTPγS in the cytosol and in the cytosol/membrane interface. A CIP4-sensitive protein would then be involved in actin polymerization initiated in solution, but another protein would play the role in the presence of plasma membranes. Alternatively, plasma membranes migh somehow compensate for the inhibitory action of CIP4 on the GTPγS-induced actin polymerization.

The partial inhibition of GTPγS-induced cytosolic actin polymerization by CIP4 was also seen when SDS-PAGE analysis of low speed sediments was performed (Fig. 2C). Together with a ca. 50% reduction of the actin band in the sediments, a concomitant decrease in α-actinin and ABP-280 content was seen. Surprisingly, CIP4 induced a strong increase of another high molecular weight protein cosedimenting with actin (Fig. 2C), which co-migrated with myosin (not shown). Approximately 20 times

more myosin per actin was present in the sediments of neutrophil cytosol stimulated with GTPγS in the presence of CIP4.

The presented results indicate that a CIP4-binding protein mediates GTPγS-induced actin polymerization in the cytosol of neutrophils. Affinity purification with CIP4 may be used to identify this protein(s).

Fig. 2. CIP4 inhibits GTPγS-induced actin polymerization in the neutrophil cytosol. GTPγS was added to the neutrophil cytosol in the presence of 2 mM EDTA (A,C) or $MgCl_2$ + 0.1 mg/ml plasma membranes (B). Recombinant WASP CRIB (Cdc42/Rac interactive binding) domain to 30 µM (hatched bars) or full-length CIP4 or its N-terminal or central domains to 2-8 µM (double hatch) were included. GTPγS-induced actin polymerization was measured by rhodamine phalloidin fluorescence enhancement and expressed as % of control, where recombinant proteins were omitted (buffer, open bars). Alternatively, actin cytoskeletons induced by GTPγS in the absence or presence of 2 µM central domain of CIP4 were analyzed by low speed sedimentation and SDS-PAGE (C). Proteins cosedimenting with actin are marked. GST fusions of CIP4 variants were bacterially expressed and kindly provided by P. Aspenström, Ludwig Institute for Cancer Research, Uppsala. GST-CRIB of WASP (amino acids 237-268) was expressed in bacteria using an expression plasmid kindly provided by U. Franke, Stanford University.

3. Rho as a candidate GTPase for GTPγS-induced actin polymerization.

As noted previously in (Katanaev and Wymann, 1998a), high concentrations of recombinant C3 transferase could reduce by 40% GTPγS-induced actin polymerization in the cytosol. Moreover, the toxin was able to inhibit by ca. 70% the response to GTPγS initiated in the presence of plasma membranes (Fig. 3A). These data put forward Rho as a possible target of GTPγS in the neutrophil cytosol, and may indicate differential use of this protein in the induction of actin polymerization depending on whether plasma membranes are present or not.

At concentrations up to 10 µg/ml, recombinant RhoA could not induce significant actin polymerization in the cytosol (Katanaev and Wymann, 1998a). However, when longer incubation times (1 hour, not shown) or higher concentrations of RhoA (20-30 µg/ml) were used, actin polymerization was stimulated (Fig. 3B). This effect of recombaninat RhoA was reproduced with different preparations of the protein and was abolished upon heat-inactivation of RhoA (data not shown). However, RhoA could induce actin polymerization equally well in the GTPγS- and GDPβS- loaded forms (Fig. 3B).

The paradox that GTPγS-induced actin polymerization is sensitive to C3 transferase but recombinant Rho induces actin polymerization in a GTP-independent manner can be reconciled in the following way. RhoGDI associates about ten times stronger with GDP- than GTP-bound Rho (Sasaki *et al*., 1993). Additionally, phosphatidylinositol 5-kinase (PI5K), unlike many other Rho binding proteins, binds Rho and Rac independently from their nucleotide (Tolias *et al*., 1995; Ren *et al*., 1996; Tolias *et al*., 1998). ADP-ribosylation of Rho by C3 transferase is known to increase strongly the affinity of PI5K for Rho (Ren *et al*., 1996). Finally, GDP-Rac has been shown to form *in vivo* a complex comprising RhoGDI, PI5K, and diacylglycerol kinase (Tolias *et al*., 1998). If Rho could also exist in such a complex in neutrophil cytosol, GTPγS addition might lead to Rho activation and liberation from the complex due to weaker affinity of GTP-Rho for RhoGDI. GTP-loading of Rho in a complex with RhoGDI requires, in addition to an exchange factor, ERM proteins which are able to interact directly with RhoGDI (Takahashi *et al*., 1997). One might speculate that Rho, when liberated from the complex, is able to induce actin polymerization independently from whether it is bound to GTP or GDP. The binding of Rho to GTP might thus be necessary only for the dissociation of Rho from the complex.

Fig. 3. Rho may mediate the effect of GTPγS on actin. (A) GTPγS-induced actin polymerization in cytosol or cytosol supplemented with plasma membranes was analyzed as above after 30 min pretreatment without (open bars) or with (double hatched bars) 100 μg/ml C3 transferase in the presence of 20 μM NAD$^+$. Recombinant C3 transferase was purified as in (Dillon and Feig, 1995) using an expression plasmid kindly provided by L.A. Feig, Tufts University, Boston. (B) Actin polymerization was induced in the cytosol by increasing concentrations of recombinant V14RhoA (kindly provided by A. Ridley, Ludwig Institute for Cancer Research, London) preloaded with GTPγS or GTPβS as described (Self and Hall, 1995). The experiment was performed in the presence of 2 mM MgCl$_2$, condition where GTPγS alone does not induce actin polymerization (Katanaev and Wymann, 1998a). In the presence of 2 mM EDTA, GTPγS (black bar) stimulated actin polymerization comparable to that induced by high concentrations of Rho.

4. An attempt to purify an actin polymerization stimulatory activity from the neutrophil cytosol.

As described in (Katanaev and Wymann, 1998a), GTPγS induces actin polymerization in the neutrophil cytosol only when the concentration of free magnesium ions is low. Otherwise, the presence of neutrophil plasma membranes is required to

allow the GTPγS-induced actin polymerization. These data are explained by possible membranous localization of the guanine nucleotide exchange factor (GEF) for the cytosolic Rho protein mediating the effect of GTPγS.

We found conditions which allowed preparation of the neutrophil cytosol capable of GTPγS-induced actin polymerization even in the presence of 2 mM $MgCl_2$. These conditions include neutrophil breakage at higher cell concentration ($2*10^8$ cells/ml) and the presence of 2 mM $MgCl_2$ in the breakage buffer. Addition of aliquots of this cytosol (called "donor cytosol" hereafter) resulted in restoration of the GTPγS-induced actin polymerizing activity in the cytosol previously inactive in the presence of 2 mM $MgCl_2$ (called "recipient cytosol" hereafter; data not shown).

The donor cytosol was used in an attempt to purify the actin polymerization stimulatory activity (APSA). The scheme of purification is shown on Fig. 4A. Donor cytosol protein (5 mg) precipitation with ammonium sulphate was used as the first step to enrich the APSA. The pellet obtained after precipitation with 40% saturated ammonium sulphate contained most of the APSA of the donor cytosol. The pellet was dissolved in 10 mM Tris-HCl pH 7.5 in the volume to obtain the ammonium sulphate concentration of 5 mM and loaded onto DEAE-sepharose equilibrated with 5 mM ammonium sulphate, 10 mM Tris-HCl, pH 7.5 (Buf A). Bound material was eluted with continuous gradient of 0-500 mM KCl in Buf A (Fig. 4B). Most proteins were eluted by 100-200 mM KCl. When the elution fractions were tested for the APSA in the recipient cytosol in the presence of 2 mM $MgCl_2$, the APSA activity was localized to the material eluted with ca. 40 mM KCl and containing relatively low protein (Fig. 4B).

To our surprise, we found that the APSA eluted from the DEAE column may not be a protein. First, the activity was resistant to heat treatment (100°C, 10 min, not shown). Second, the activity passed through 10 kD cut-off pores during ultrafiltration (not shown). These properties of the APSA were used to further purify it: after incubation at 100°C and centrifugation, the supernatant was ultrafiltered. The flowthrough was loaded onto an HPLC Partisil SAX 10 micron column equilibrated with water, and eluted with a continuous gradient of 0-1 M KH_2PO_4 (Fig. 4C). Fractions absorbing at 260 nm were collected. Two peaks of absorbency were seen in the eluate: the first corresponding to the material eluted at ca. 680 mM , and the second- 750 mM KH_2PO_4. The second peak was found to contain the APSA (Fig. 4C).

To assess the purity of the APSA preparation and molecular weights of substances present in it, the preparation was analyzed by electro-spray mass-spectrometry after proton ionization (performed by Prof. T. Yenni, Institute of Organic Chemistry, Univ. Fribourg). The results are presented on Fig. 4D. Among the substances present in the APSA preparation, four were absent in the sample from peak 1 of the HPLC (see Fig. 4C). Their molecular weight are 445.8, 581.7, 679.7, and 717.7. After

search in public databases, some candidate molecules were found with such molecular weights and properties which could allow them to be purified from the neutrophil cytosol by the procedures applied in our experiments.

The presented results describe a partial purification of a low molecular weight activity stimulating GTPγS-induced actin polymerization in the presence of magnesium ions. The starting material used in the purification was cytosol of human neutrophils. These cells were isolated in several steps, including several washings (see Protocol III-1), which makes it unlikely, although not completely impossible, that the activity is a contamination coming from extracellular milieu or from blood collection equipment. We can not be sure that the activity comes from one of the molecules detected by the mass-spectrometry and does not escape the detection. Further purification and more analysis with different techniques would have to be done to identify the active substance. It is very unlikely that the substance is some agent chelating $MgCl_2$ and thus allowing GTPγS-induced actin polymerization, since millimolar concentrations of such a chelator would be required, while relatively low amount of material was used in purification, and low signals were detected after DEAE-chromatorgaphy, HPLC, and mass-spectrometry. Noteworthy, the APSA did not induce any actin polymerization on its own in the cytosol. This excludes an involvement of some ions, like Ca^{2+}, which induces strong pointed-end actin polymerization (data not shown; DiNubile, 1998).

In conclusion, the presented results might indicate an involvement of a low molecular weight substance in stimulating Rho protein-induced actin polymerization in the neutrophil cytosol. The molecular nature of the substance is not clear yet.

Fig. 4. Partial purification of the actin polymerization stimulatory activity (APSA) from neutrophil cytosol. (A) Purification scheme. (B) Ion-exchange chromatography on DEAE-sepharose. After loading in 5 mM ammonium sulphate, 10 mM Tris-HCl, pH 7.5 (Buf A), the material was eluted in a gradient of 0-500 mM KCl in Buf A. Protein concentration in elution fractions is shown in empty circles, APSA in black squares. (C) APSA preparation from previous steps was loaded on the HPLC Partisil SAX column and eluted with a gradient of 0-1 M KH_2PO_4. Eluate absorbing at 260 nm was collected. Peak 2 of the eluate contained APSA. (D) ES-MS analysis of the material in the HPLC peak 2. Mass-to-charge values of four substances present in peak 2 but absent in peak 1 are encircled.
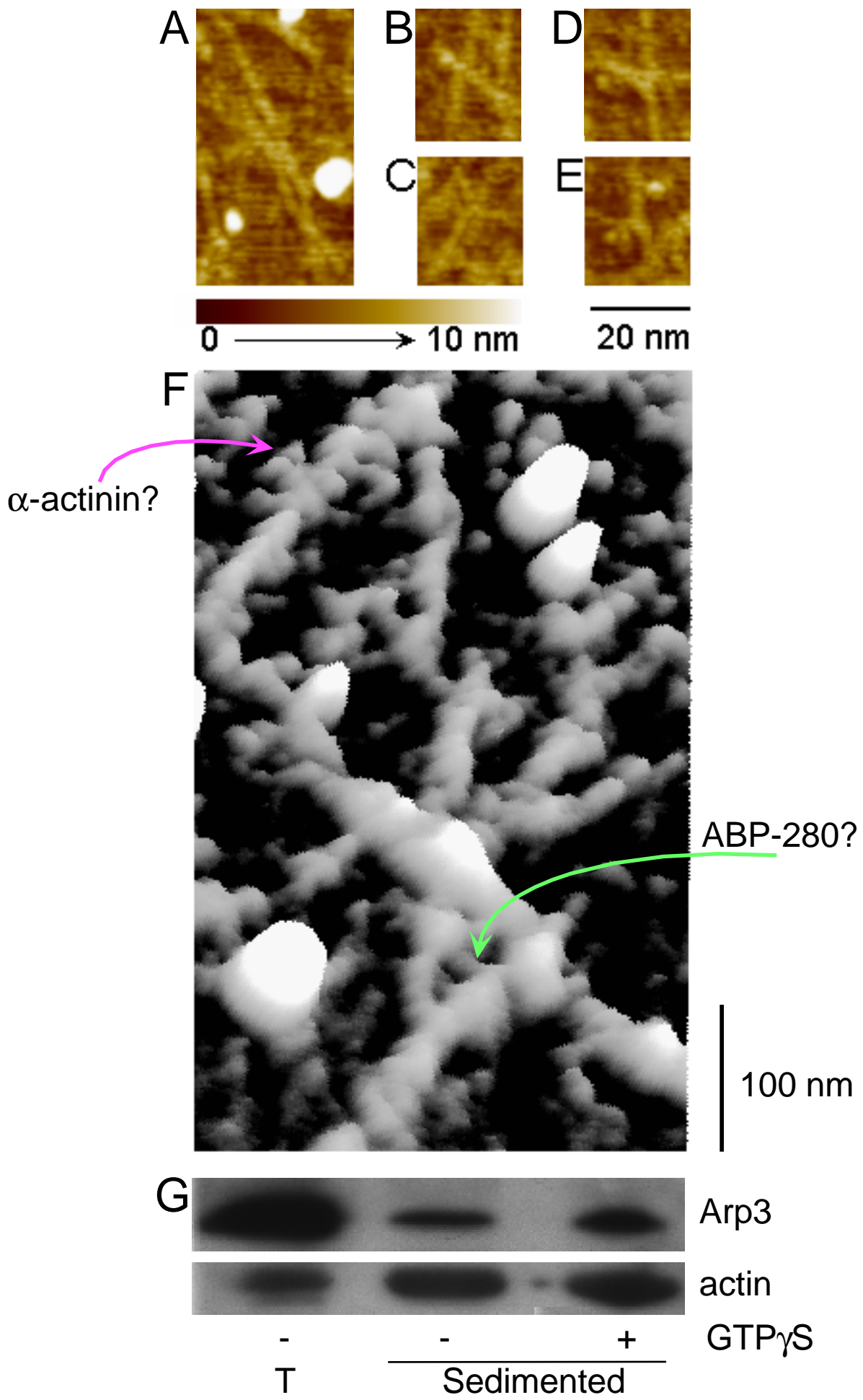
Fig. 1.

A

B
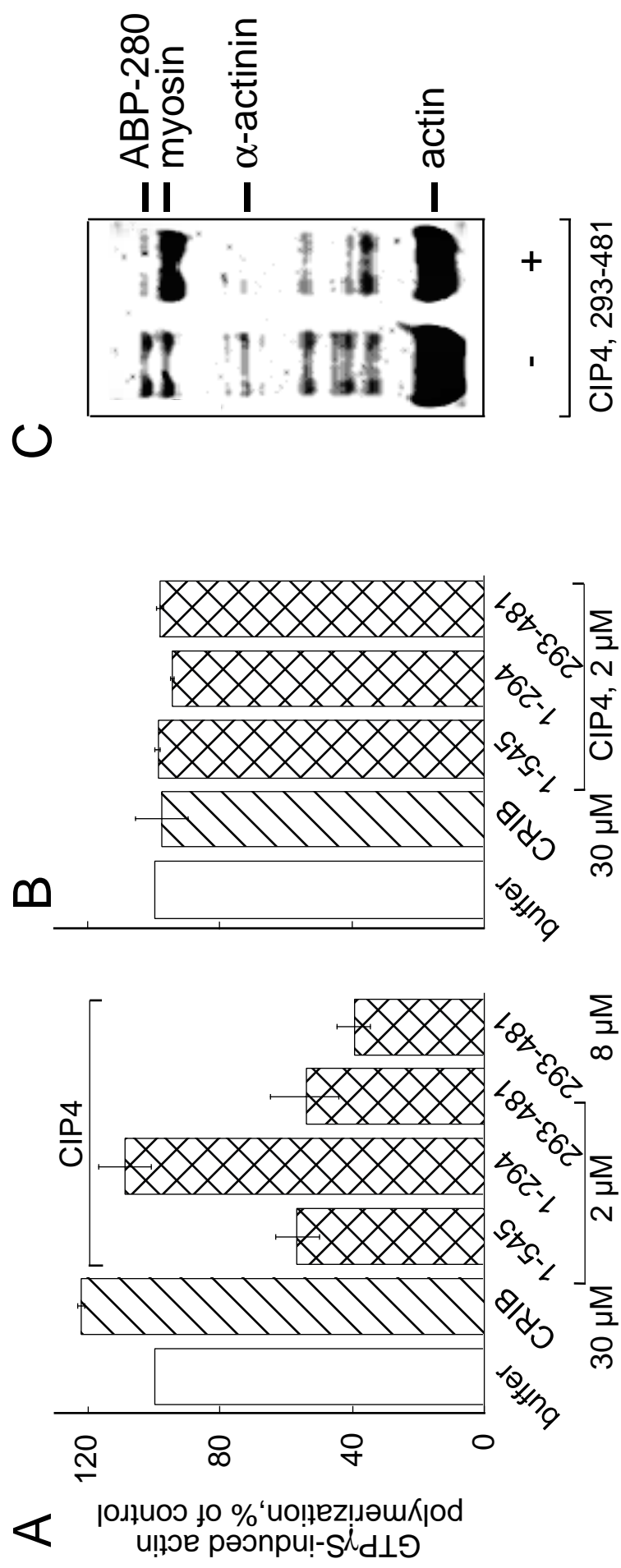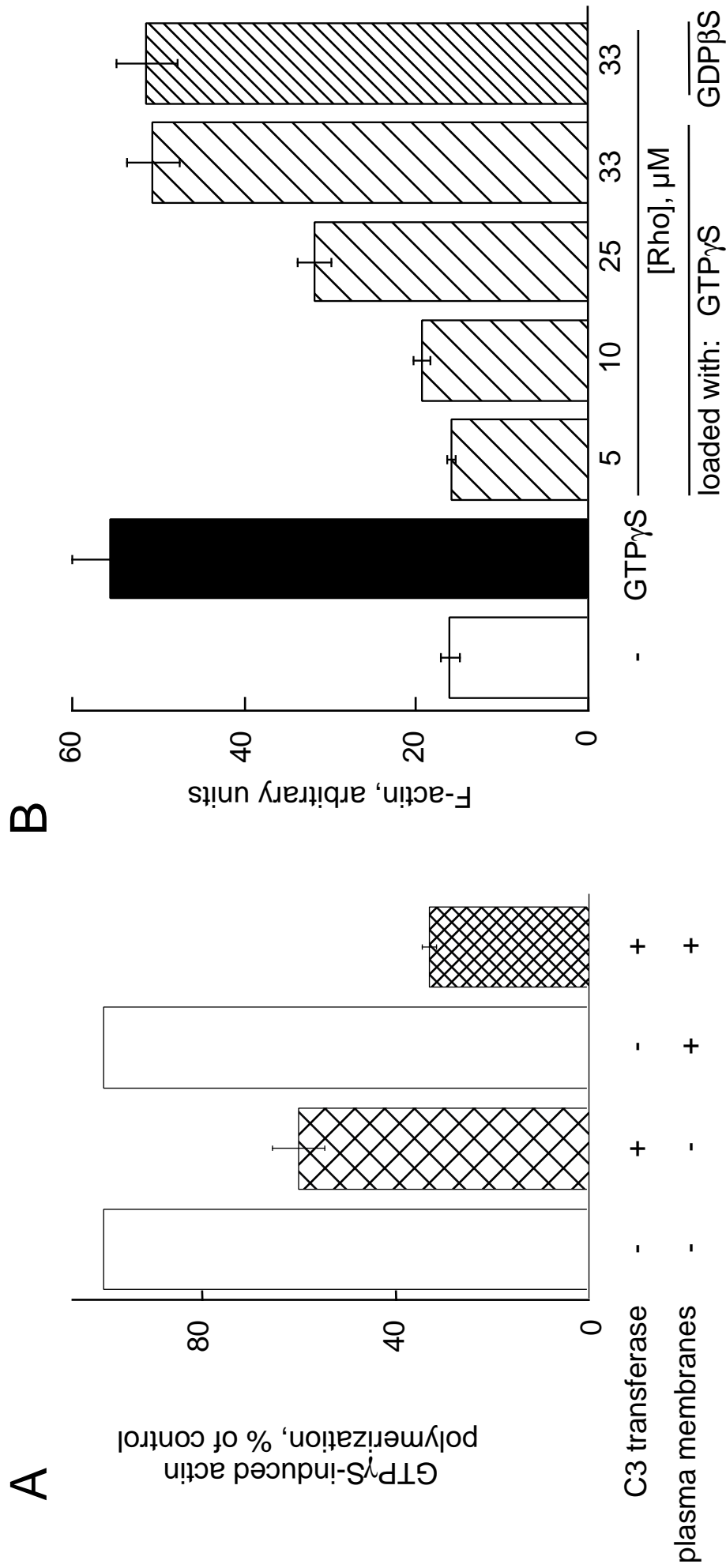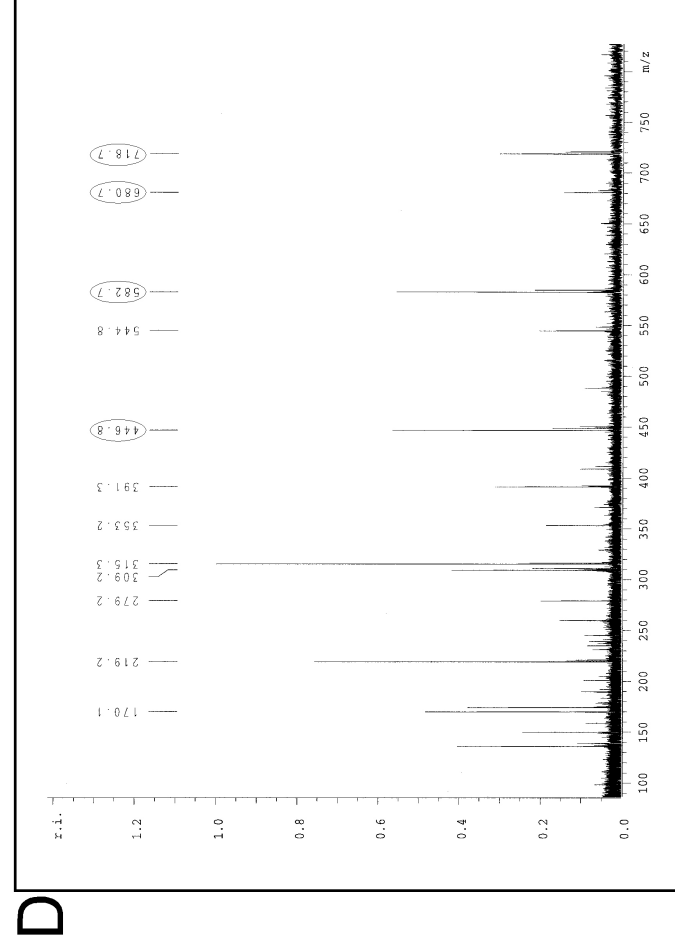
C

D

E

0 ⟶ 10 nm

20 nm

F

α-actinin?

ABP-280?

100 nm

G

Arp3

actin

-          -   +   GTPγS

T   Sedimented

Fig. 2

Fig. 3
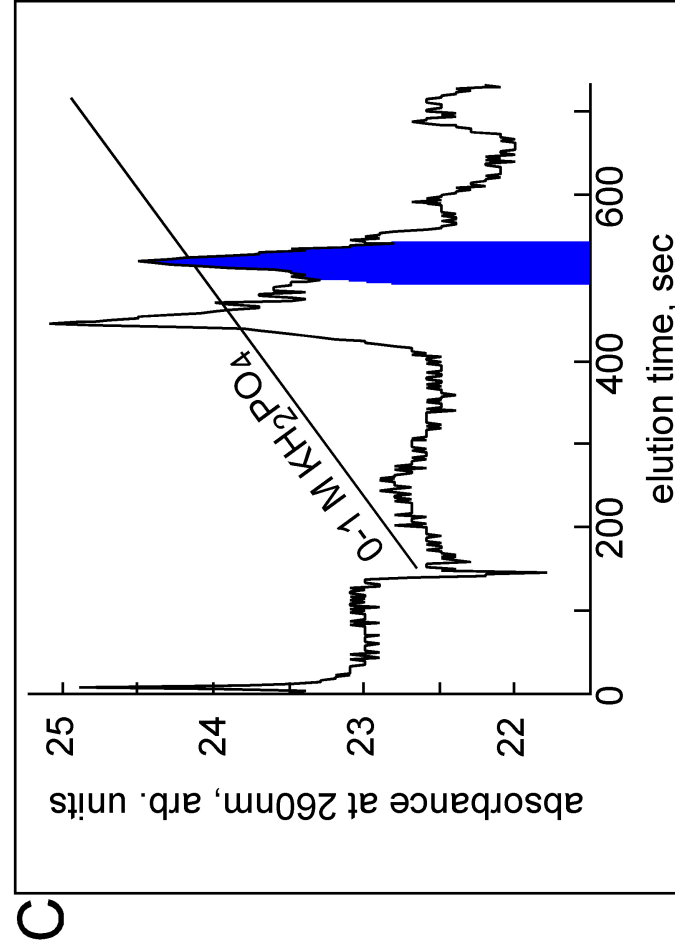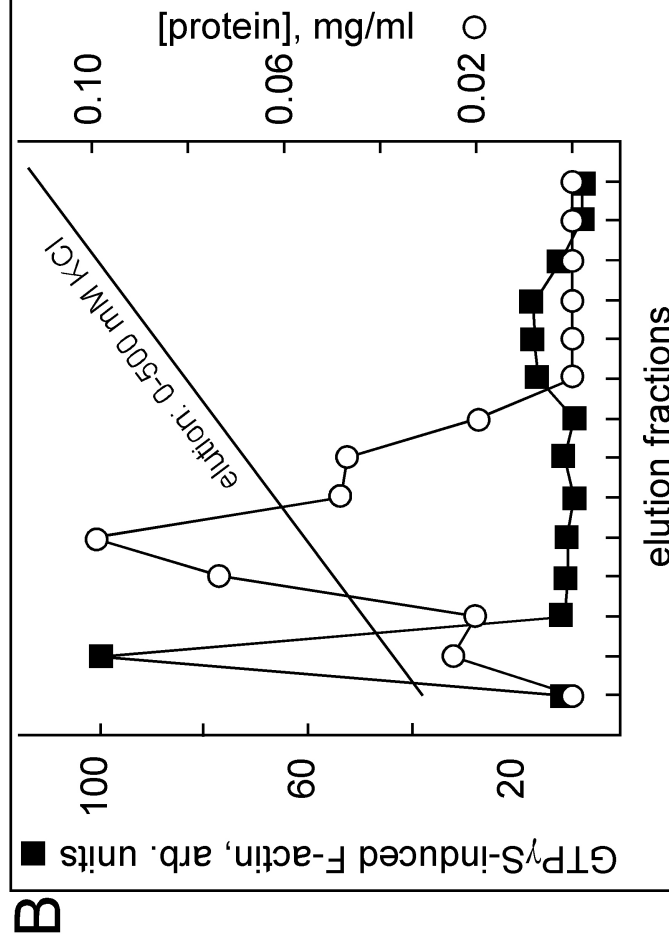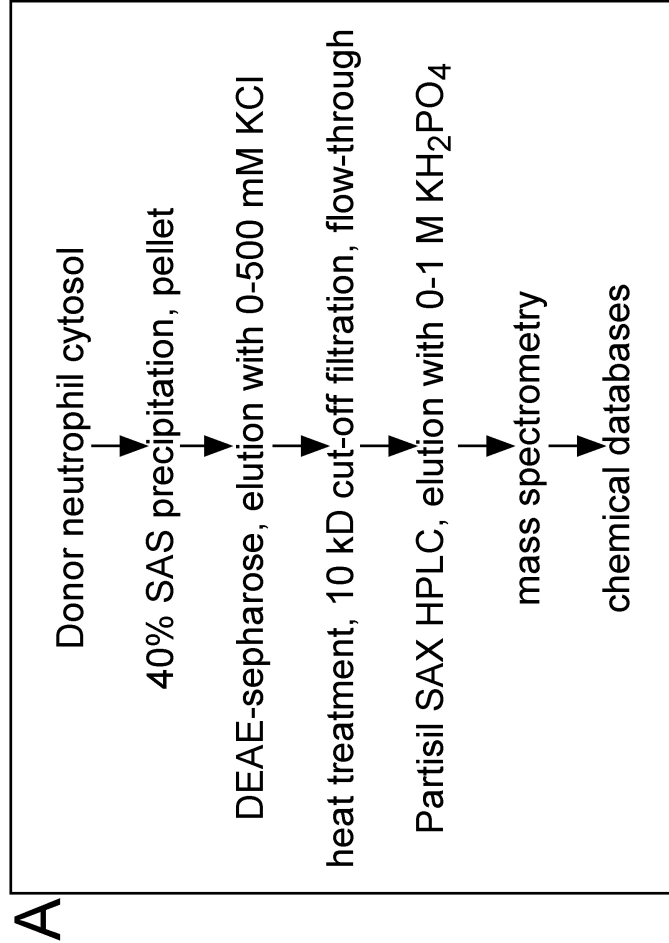
Fig. 4

PROTOCOLS

I. Molecular biology techniques.

1. Restriction endonuclease digests

1) Mix: 2 µl 10x buffer (see enzyme charts), 1 µl enzyme (2-3 U/µg DNA), 1-4 µg DNA, water to 20 µl. Glycerol must be at ≤5% (see star activity charts in e.g. NEB catalogue).

2) Incubate 1-3 h 37°C. When high temperatures or prolonged incubations are used, evaporation must be prevented (mineral oil, tube lead heating).

3) If necessary inactivate the restriction enzyme by heating at 65°C for 20 min or/and by phenol/chloroform extraction. For the latter, add equal volume of phenol, stir rigorously, and centrifuge 12000 g 2 min 4°C. Repeat the liquid phase extraction with phenol: chloroform (1:1) and chloroform. Adjust NaCl to 200 mM or Na-acetate to 300 mM. Precipitate DNA by 2 vol ethanol, ≥15 min ≤4°C. Centrifuge 12000 g 10 min 4°C. Carefully rinse the DNA pellet with 75% ethanol. Dissolve DNA.

4) Analyse the efficiency of digestion by agarose gel-electrophoresis (see I-4).

2. Dephosphorylation of 5' DNA ends with calf intestinal alkaline phosphatase (CIP).

1) Suspend ca. 0.5 µg DNA in 1mM $ZnCl_2$, 1mM $MgCl_2$, 10 mM Tris-HCl pH 8.3.

2) Incubate at 37°C after addition of CIP: 1U CIP per 100 pmoles of protruding 5' termini for 30 min, or for 15 min per 2 pmoles of blunt or recessed 5' termini, for which 1U more is added for further 45 min at 55°C. Note: 2 µg of a linearized plasmid DNA 5kb in length contains ca. 1.4 pmoles of 5'-ends.

3) Add EDTA/SDS to 5 mM/ 0.5% for 1h 65°C. Extract with phenol/ chloroform, precipitate/ wash with ethanol.

3. Blunting DNA ends.

1) Mung-bean nuclease (MBN) can be used to remove ss extensions: dissolve DNA in 50 mM Na-acetate, 30 mM NaCl, 1 mM $ZnCl_2$; add 0.5-1 U MBN/ µg DNA, incubate 30 min 37°C. Note: high [MBN] or long incubation will increase the risk of ds DNA end loss.

2) Klenow DNA polymerase (KDP) can be used to fill up 5'-overhands: DNA at ca. 50 µg/ml in 10 mM Tris-HCl pH 7.5, 5 mM $MgCl_2$, 7.5 mM DTT (KDP is also 50% active in standard restriction buffers) is mixed with 1U KDP per µg DNA and 200 µM each dNTPs. New sticky ends may be created omitting some dNTPs. Incubate 30 min 25°C. Stop by transfer to 75°C in 10 mM EDTA, 300 mM NaCl.

3) Other enzymes such as T4 DNA polymerase or nuclease S1 can be also used.

4. Agarose gel-electrophoresis.

1) Prepare 0.8-2% agarose gels (0.8% for 1000-5000 bp, 2% for 100-1000 bp DNA). Melt the weighed amount of agarose in TAE (40 mM Tris-acetate pH 8.0, 1mM EDTA) and 0.3 µg/ml ethidium bromide. Pour on glass plates and put in the combs before agarose solidifies. Keep pre-made gels at 4°C in himudity for weeks.

2) Mix DNA samples with ca. 1/10th of 0.4% bromphenol blue, 0.4% xylene cyanol FF, 50% glycerol and load on the gel. >2 ng and <500 ng DNA has to be present in one band for the sake of resolution. Also load a DNA marker.

3) Add ca. 10 µl of 10 mg/ml ethidium bromide to the negative electrode of the tank. Run the electrophoresis at 80V before and at 100-120V after the samples have entered the gel. When the gel is devided into 3 approx. equal parts by the two dyes, stop the run. Visualize DNA under UV.

4) Work very clean when preparative electrophoresis is done. A gel with big slots is used. When finished with the electrophoresis, cut out in a minimal volume the band of interest. Mince in pieces. Put in a 0.5-ml tube with a hole in the bottom onto a clot of glass wool. Insert the tube into 1.5-ml tube, centrifuge 12000 g ≥10 min untill all liquid arrives to the lower tube. Extract with phenol/ chloroform and precipitate DNA as in I-1.

5) Alternatively, low-melting point agarose can be used for preparative electrophoresis. The tube with agarose is frozen in liquid nitrogen for 2-3 min and centrifuged for 15 min 12000 g RT. Precipitate DNA from the liquid as in I-1.

5. Ligation.

1) DNA fragments should be present in equimolar concentrations (ca. 0.5 fmole/µl).

2) Additionally, 20 µl of ligation mixture should contain 1 mM ATP, 1 mM DTT, 10 mM Tris-HCl pH 7.5, 10 mM $MgCl_2$, 0.2 mg/ml BSA, 0.4-0.8 U T4 DNA ligase.

3) To ligate sticky ends, incubate at 0-4°C for 3h-ON.

4) To ligate blunt ends, incubate at 10-16°C ON-24h.

5) To improve the efficiency of blunt end ligation, decrease [ATP] to 0.5 mM, or include condensing agents like 15% PEG (polyethylene glycol) 8000 or 1-1.5 µM hexamminecobalt chloride.

6. Preparation of competent bacteria.

1) Transfer a colony of freshly grown bacteria from an LB-agar plate to 50 ml LB medium and grow ON at 37°C with agitation (300 cycles/min).

2) Add a ml from above to a fresh 50 ml LB flask. Grow until OD_{600}=0.8 (≤10^8 cells/ml).

3) Transfer to centrifugation bottles, precool on ice, 10 min. Centrifuge 5300 g 10 min 4°C.

4) Resuspend the pellet in 20 ml ice-cold sterile 50 mM CaCl$_2$, store on ice, 20 min-1.5h.

5) Centrifuge 5300 g 10 min 4°C.

6) Resuspend the pellet very gently in 4 ml ice-cold 50 mM CaCl$_2$, store on ice for ≤ 48h.

7) Add ice-cold sterile glycerol to 15%, freeze 200 µl aliquots in liquid nitrogen, store at -80°C. The expected transformation efficiency is ≥5∗10^6 colonies/µg supercoiled DNA.

7. Bacterial transformation

1) Add ≤50 ng DNA (≤10 µl) to 200 µl competent bacteria. Gently swirl to mix.

2) Incubate for 30 min on ice.

3) Heat shock for 90 sec in a 42°C-warm water bath. Incubate on ice for 10 min.

4) Optional: gently mix with 800 µl 37°C-warm LB (no antibiotics), incubate 1h 37°C.

5) Plate ≤200 µl bacteria per LB-agar plate with antibiotic. Grow ON 37°C.

8. Minipreparation of plasmid DNA.

1) Inoculate 15-ml tubes with 2 ml LB- antibiotic by single bacterial colonies.

2) Grow for several hours at 37°C with agitation. Put to 1.5 ml tubes. Centrifuge*.

3) Resuspend the pellet in 200 µl STET (8% sucrose, 0.1% Triton X-100, 50 mM EDTA, 50 mM Tris-HCl pH 8.0), mix intensively. Add RNase (DNase-free) to 10 µg/ml.

4) Add 20 µl of 20 mg/ml lysozyme, keep 5 min RT.

5) Boil for 45 sec, centrifuge*. Take away the genomic DNA pellet with a toothpin.

6) Add 8 µl of 5% cetyltrimethylammonium bromide to the liquid. Mix and centrifuge*.

7) Add 300 µl 1.2 M NaCl to the pellet, keep 15 min RT. Precipitate/ wash with ethanol.

8) Dissolve dried pellet in 50 µl TE (10 mM Tris-HCl, 1 mM EDTA, pH 8.0). Verify the correct clone by electrophoresis and restriction analysis.

9) * All centrifugations are done at RT for 10 min at 12000 g.

10) As an alternative to this minipreparation method, the plasmid maxipreparation technique described below can be scaled down.

9. Plasmid maxipreparation by LETR.

1) LETR buffer (keep in aliquots at -20°C for months): 2 mg/ml lysozyme, 100 mM EDTA, 50 mM Tris-HCl pH 8.0, 0.1 mg/ml RNase (DNase-free).

2) Grow bacteria in 500 ml LB-antibiotic in 5 lt flasks ON. Centrifuge 5300 g 15 min 4°C.

3) Resuspend the pellet in 20 ml LETR. Transfer to 50ml tubes. Incubate at RT for 30 min.

4) Add 200 µl 10% Triton X-100, incubate 10-30 min RT. Centrifuge 1400 g 30 min 4°C.

5) Phenol-chloroform extraction as in I-1. Precipitate with 0.1 volume 3M NaCl and 0.6 volume isopropanol. Rinse with 75% and then 100% ethanol. Dry, dissolve in 0.5 ml TE.

6) Determine DNA concentration: one unit of OD_{260} = 50 µg/ml ds DNA. Measure OD_{260}/ OD_{280}, if it is less than 2, some protein, phenol, or chloroform contamination is present.

10. DNA sequencing.

1) Denature ds DNA: Mix 5 µg DNA with 100 µl TE and 10 µl 2M NaOH/ 2mM EDTA, incubate 30 min 37°C. Add 1/10th of 3M Na-acetate, precipitate/wash with ethanol. Dissolve in 7 µl water.

2) Anneal DNA with primers: Mix 7 µl DNA with 2 µl reaction buffer (5x stock: 200 mM Tri-HCl pH 7.5, 100 mM $MgCl_2$, 250 mM NaCl) and 1µl 1µM primer (e.g. T3 or T7). Heat 2 min 65°C, then cool slowly to <35°C over 15-30 min. Chill on ice.

3) Prepare 4 termination mixtures. ddA mix: 80 µM each of dATP, dGTP, dCTP, dTTP, 50 µM NaCl, 8 µM ddATP. Similarly prepare ddG, ddC, and ddT mixtures. Put 2.5 µl of each mixtrure to a separate tube. Prewarm at 37°C.

4) Labelling reaction: To ice-cold annealed DNA mixture (10µl) add:

1µl 0.1 M DTT

2 µl prediluted labeling mix (from a 5x stock: 7.5 µM each of dGTP, dCTP, dTTP)

0.5 µl [^{35}S] dATP (e.g. 10 mCi/ml)

2 µl 1.6 U/µl Sequenase (e.g. from USB). Mix and incubate at RT for 2-5 min.

5) Termination reactions: Transfer 3.5 µl of the labeling reaction to each of the 2.5-µl termination mixtures, mix, incubate 5 min 37°C.

6) Stop the reactions by 4 µl Stop Solution (95% formamide, 20 mM EDTA, 0.05% bromphenol blue, 0.05% xylene cyanol FF).

7) Heat the samples for 2 min 75°C immediately before loading onto sequencing gel.

8) Prepare 50 ml solution of 8M Urea, 6% acrylamide, 0.3% N,N'-methylene-bis-acrylamide (MBA) in TBE (90 mM Tris-borate, 2 mM EDTA, pH 8.0). Degaz.

9) Add 1/100th of 10% APS (ammonium persulphate, freshly prepared) and 1/2000th of TEMED. Pour the solution into the glass plates, keeping them in a semivertical poistion.

10) Prerun 30 min 34-40 W in TBE.

11) Load samples for the long run, 3 µl each, in the order: GATC. Run at 50 W, until the bromphenol blue leaves the gel (ca. 1h).

12) Load the samples for the short run in the neibouring wells. Run for ca. 1h more (until bromphenol blue has run 3 quaters of the gel).

13) Stop the run. Take away the upper glass. The gel on the lower glass is put to a tank and carefully poured with water: acetic acid: methanol (85:10:5) for 20 min. Lay a filter paper onto the gel, revert the sandwich and remove the remaining glass.

14) Cover the gel with a Saran rap and dry. Mount for autoradiography or phosphoimaging. Read the sequence.

11. Mouse PCR genotyping for the PI3Kγ gene (see Malumbres*et al.*, 1997; Hirsch *et al.*, in press).

1) Clip 3mm of mouse tail tip. Keep at -20°C if not used immediately.

2) Add 200 μl of the extraction buffer: 50 mM KCl, 1.5 mM MgCl$_2$, 10 mM Tris-HCl pH 8.5, 0.45% Nonidet P-40 , 0.45% Tween 20, 100 μg/ml proteinase K. Incubate 2h 55°C. Heat 15 min 95°C to inactivate proteinase K. Spin down briefly.

3) Take 2.5 μl for a 50μl- PCR mixture containing:

H$_2$O	10 μl
10x PCR Buffer*	5 μl
dNTPs 25 mM each	0.5 μl
PI3KgUP primer** 5 μM	10 μl
PI3KgDN primer** 5 μM	10 μl
NEOPA primer** 5 μM	10 μl
0.5 U/ml Taq Polymerase (Pharmacia)	2 μl***

*composition: 500 mM KCl, 100 mM Tris pH 8.8, 1 mg/ml BSA, 0.5% Tween 20, 15 mM MgCl$_2$.

**primers: PI3KgUP: 5'-GGA GAA CTA TGA ACA ACC GG-3'
            PI3KgDN: 5'-CAA CTT CCA GTA ATG CAG GC-3'
            NEOPA: 5'-CTG CTC TTT ACT GAA GGC TC-3'.

***Add the enzyme only after the PCR mixtures are prewarmed to 95°C (hot start).

4) Run the PCR using the following cycle profile (Biometra UNO-Thermoblock; slope=2°C/sec; lid temp=99°C; use thin-wall PCR tubes):

     95°C, pause;

10 cycles:(95°C, 30 sec/ 65°C-1°C each cycle, 30 sec/ 72°C, 30 sec);

25 cycles:(94°C, 30 sec/ 55°C, 30 sec/ 72°C, 30 sec);

     72°C, 2 min;

     4°C, pause.

5) Load on a 2% agarose gel. Wild type and mutant alleles give 378 and 530 bp bands, respectively.

II. Protein biochemistry techniques.

1. Protein SDS-polyacrylamide gel-electrophoresis (SDS-PAGE).

1) Use 15% (w/v) acrylamide gels to separate low molecular weight proteins (10-30 kDa), and 7.5% for heavy proteins (>100 kDa). Additionally, separation gels contain: 650 mM Tris-HCl pH 8.8, 0.1% SDS, MBA being 3% of acrylamide. Before gel pouring, add APS to 0.07% and TEMED to 0.03%.

2) Gradient separation gels are prepared using a gradient former with solutions of 15/0.45% and 5/0.15% acrylamide/MBA containing 375 mM Tris-HCl pH 8.8, 0.1% SDS, 0.01% APS, 0.1% TEMED. Heavy gel (15%) also contains 25% glycerol.

3) Stacking gel composition: 4% acrylamide, 0.12% MBA, 125 mM Tris-HCl pH 6.8, 0.1% SDS, 0.1% APS, 0.1% TEMED. Keep prepared gels at 4°C in humidity.

4) Mix the protein sample with the sample buffer to final concentrations of glycerol=10%, Trid-HCl pH 6.8=60 mM, SDS=2.5%, β-mercaptoethanol=5%, and bromphenol blue= 0.1%. Boil the mixture for 5 min before loading onto the gel. Optionally, include 4M Urea to the sample buffer or prolong boiling for up to 30 min.

5) Run electrophoresis in 200 mM glycine, 25 mM Tris, 0.1% SDS with the current of 10-20 mA (per a 8cmX 5cmX 0.8mm gel) before the sample enters the stacking gel, 20-40 mA before it enters the separating gel, and 40-80 mA untill the dye exits the gel.

6) Stain with Coomassie: soak for 5-15 min in a solution of Comassie Blue R-250 in water: methanol: acetic acid 43:50:7.

7) Destain the gel in water: methanol: acetic acid with several changes each 10-20 min.

8) Silver staining can be done alternatively to Coomassie staining or after it as follows:

fix the gel in 40%methanol/ 10% acetic acid for 30 min,

fix in 10% ethanol/ 5% acetic acid for 15 min,

repeat (this is the first step to be used after Coomassie staining/ destaining),

oxidize in 3.4 mM $K_2Cr_2O_7$ and 3.2 N HNO_3 for 5 min (use the solution once),

soak in water several times untill the yellow colour is removed from the gel,

soak in the silver reagent (12 mM $AgNO_3$, freshly dilute from stock, light sensitive),

soak in water for 1 min,

develop in 0.28 M Na_2CO_3/0.6 mM formaldehyde till the colour changes (ca. 30 sec),

change the developer twice for 5 min, stop the reaction with 5% acetic acid.

2. Western blotting.

1) Activate PVDF membrane with methanol for 1 min and preincubate in the transfer buffer (25 mM Tris, 192 mM glycine, 20% methanol, pH 8.3) for >10 min together with 6 pieces of Whatmann 3MM filter paper.

2) After SDS-PAGE, put the gel on the membrane, 3 layers of filter below and above them.

3) Electrotransfer in semi-dry mode for 1 h, 60 mA per 1 cm^2.

4) Agitate the membrane in the blocking solution (3% dry milk or BSA, 0.1% PEG 35000 in PBS- 0.05% Tween 20) for 45 min. Stain the gel by Coomassie as in II-1.

5) Wash the membrane 3 times for 5 min in PBS-Tween.

6) Incubate the membrane for 45 min in 8 ml PBS-Tween with the primary antibodies, diluted normally 1000- if polyclonal, and 2000-fold if monoclonal. The diluted antibodies can often be reused after storage at 4°C in 0.02% NaN_3. Wash the membrane 3 times.

7) Incubate the membrane for 45 min in 8 ml PBS-Tween with normally 2000-fold diluted commercial secondary antibodies, peroxidase coupled.

8) Wash thrice for 5 min in PBS-Tween, once more for 15 min.

9) Agitate for 1-2 min in the SuperSignal^{TM} Substrate (Pierce): mix 2.5 ml of nanopure water, Luminol/Enhancer, and Stable Peroxide Solution.

10) Expose the membrane for 1-10 min to the Hyperfilm^{TM} ELC^{TM} (Amersham). Develop for ≥1 min, fixate for ≥1 min.

11) To reuse with another antibody: incubate the membrane 30 min 50°C in strip buffer (62.5 mM Tris pH 6.7, 2% SDS, 0.1 M β-mercaptoethanol) with agitation, follow by several washes in PBS-Tween before addition of antibodies.

12) Stain 1-2 min in Coomassie, destain 2-3 min in 80% methanol, 2% acetic acid.

3. Purification of GST-WASP proteins as an example of affinity protein purification.

1) Inoculate a 5-lt flask with 500 ml LB-100 µg/ml ampicillin by 50 ml ON culture of M15 bacteria transformed with pGEX5-WASP48-325 (see Symons *et al* ., 1996).

2) Grow until OD$_{600}$ reaches 0.6-0.8 (ca. 2 h). Add isopropyl β-D-thiogalactopyranoside to 1 mM. Grow for additional 2-6 h.

3) Prepare 1 ml of 50% Glutathione Sepharose 4B in PBS: resuspend the sepharose stock, take 0.67 ml to a 50 ml Falcon tube, centrifuge 500 *g* 5 min 4°C, aspirate the supernatant, resuspend in 30 ml PBS, centrifuge, repeat with fresh PBS, add to the drained sepharose 0.5 ml <u>PBS</u> (8 mM Na_2HPO_4, 1.4 mM KH_2PO_4, 2.6 mM KCl, 136 mM NaCl).

4) Transfer the bacterial culture to a 0.5 lt tube and centrifuge 7700 *g* 10 min 4°C.

5) Discard the supernatant. Resuspend the pellet in 25 ml of ice-cold PBS (50 µl PBS per 1 ml of the culture).Transfer to a 50 ml Nalgene tubes.

6) Sonicate the suspension using a rod-sonifier in 6 bursts of 1 min interrupted by ≥1 min intervals of staying on ice. Ensure the suspension is not warmed up during sonication. Check the completeness of cell lysis microscopically; continue sonication if necessary.

7) Add Triton X-100 to 1% to the lysate, incubate 30 min 4°C on a rotatory shaker.

8) Centrifuge 12000 g 10 min 4°C. Trasfer the supernatant to a 50 ml Falcon tube.

9) Add 500 µl 50% slurry of Glutathione Sepharose 4B equilibrated with PBS to the sonicate. Incubate on a rotary shaker, 4°C 1.5 h.

10) Centrifuge 500 g 5 min 4°C. Wash the sepharose pellet twice with 25 ml PBS.

11) To the sedimented matrix, add 250 µl of the Glutathione Elution Buffer (10 mM reduced glutathione, 0.5 mM EDTA, 1 mM DTT, 50 mM Tris-HCl, pH 8.0). Mix gently to resuspend the matrix. Incubate on a rotary shaker at 4°C for 20 min.

12) Centrifuge 500 g 5 min 4°C. Keep the supernatant in a separate tube on ice.

13) Repeat the elution and centrifugation steps twice. Pool the three eluates. Determine the concentration by Bradford. Concentrate if necessary by ultrafiltration or as in II-4.

14) Similarly to the purification of GST-fused proteins (the system provided by Promega), the Quagen-system based purification of (His)$_6$-tagged recombinant proteins is achieved. In this case Ni-NTA-agarose is used as the resin for affinity purification.

4. Purification of plasma gelsolin (brevin) (see Kurokawa *et al.*, 1990).

1) Collect fresh bovine blood and allow blood clotting for 1h at RT. Centrifuge 5000 g 15 min, collect the serum, which can be stored at -20°C for months.

2) Prepare saturated ammonium sulphate (SAS) by mixing 1kg ammonium sulphate (AS) with 1 lt of water. Heat up to 60°C for 1h with occasional mixing. Cool to RT and let stay ≥12h before use. Keep at RT. AS concentration in SAS is about 4M and is changed very little between 0°C and 25°C.

3) Add to 400 ml serum Tris-HCl pH 8.0 to 50 mM, NaN$_3$ to 0.02%, DTT to 1 mM.

4) Add dropwise SAS to a saturation of 35%, and continue stirring for 30 min on ice.

5) Centrifuge 1000 g 15 min 4°C. Add to the supernatant SAS to 50%, stir 30 min on ice.

6) Centrifuge 1000 g 15 min 4°C, wash the pellet twice with SAS 50%/Tris 25 mM pH 8.0.

7) Resuspend the pellet in a minimal volume of buf A (NaCl 45 mM, Tris-HCl 25 mM pH 8.0, 1 mM EGTA, 0.02% NaN$_3$, 1 mM DTT) and dialyze at 4°C with three changes of buf A untill removal of AS is complete (confirm by BaCl$_2$).

8) Load sample on equilibrated DE-52 column (Whatman, approx. 2.5 x 20-30 cm) and wash column with buf A until the absorption returns to background (ca. 8 bed

volumes). <u>All buffers for the chromatography must be filtered through 0.2 μm pore filters and cooled to 4°C before use</u>.

9) Wash the column with two bed volumes of buf B (30 mM NaCl, 25 mM Tris-HCl pH 8.0, 0.1 mM EGTA, 0.02% NaN_3, 1 mM DTT).

10) Elute brevin with buf C (30 mM NaCl, 25 mM Tris-HCl pH 8.0, 2 mM $CaCl_2$, 0.02% NaN_3, 1 mM DTT, ca. 4 bed volumes). Expected yield: 15 mg of brevin/400 ml of serum. 1.538 OD_{280}= 1 mg/ml of brevin.

11) Wash the column with buf D (1 M NaCl, 25 mM Tris-HCl pH 8.0, 1 mM EGTA, 0.02% NaN_3, 1 mM DTT, 5 bed volumes) and reequilibrate with buf A. Store column in buf A + 10% methanol + 0.02% NaN_3 at 4°C.

12) Concentrate brevin with PEG if necessary. The solution is placed into a dialysis sac with an appropriate pore size. The sac is rapped in the powder of PEG 35000 and incubated with agitation for 1-2h. PEG will take up the fluid from the sac (be sure not to dry it).

5. Determination of ammonium sulphate (AS) concentration in protein samples.

1) Add 200 μl of 100 mM $BaCl_2$ solution to each cuvette (a reference cuvette, 7 cuvettes for the standard curve, and the sample cuvette(s)) to end up with 20 mM solutions after all components are combined.

2) Add 800 μl or less of 50 ppm antifoam A to the cuvettes. The volume to be added is calculated so that the final volume in all cuvettes after addition of all components is 1 ml. Mix the content of the parafilm-closed cuvettes by inversions.

3) Add 0-1-2-4-8-16-32 μl of the 100 mM AS solution to the cuvettes to end up with 0-0.1-0.2-0.4-0.8-1.6-3.2 mM AS, or the necessary volume of the sample (1-15 μl). Mix the content of the cuvettes by inversions immediately after addition of AS or the sample.

4) Measure OD_{450} of the cuvettes after equal time intervals (15-30 min), mixing each cuvette by 3 inversions immediately before the measurement.

5) Build a standard curve of OD_{450} dependence on [AS]. Calculate [AS] in the sample.

6) Note: It is critical to add a small - below 30 μl - volume of the AS or the sample solution to a big (ca. 800 μl) volume of 20 mM $BaCl_2$. Changes in the order or the relative volumes of the additions may lead to deviation of the standard curve from the straight line.

7) Note: The presence of antifoam A allows a closer match of the results obtained with protein-containing AS solutions to the standard curve built on protein-free AS serial dilutions. BSA to the final concentrations up to 200 μg/ml could be added to the cuvettes with a negligible effect on AS concentration measurement under these conditions.

6. Preparation of muscle acetone powder.

1) Do all procedures at 4°C and using cool solutions and equipment.

2) Excise dorsal lateral muscles and hind leg muscles of a freshly sacrificed rabbit and chill them on ice. Wash the muscles in water and grind them.

3) Extract the minced muscles stirring for 10 min with 1 lt of KCl 0.1 M, 0.15 M KH_2PO_4 pH 6.5. Filter through four layers of cheese-cloth. Discard the filtrate.

4) Extract with 2 lt of $NaHCO_3$ 0.05 M for exactly 10 min, filter.

5) Extract with EDTA 1 mM, pH 7.0, 1 lt, for 10 min. Filter.

6) Two extractions with water (2 lt each for 5 min.). Extract five times with acetone.

7) Dry the extracted residue obtaining the "acetone powder". Store for months at -20°C.

7. Purification of actin from acetone powder (see Pardee and Spudich, 1982; MacLean-Fletcher and Pollard, 1980).

1) Extract 10 g of the acetone powder by stirring in 200 ml water, 4°C, 30 min.

2) Centrifuge the extract 5000 g 10 min 4°C. Reextract the residue in 100 ml of water, centrifuge and pool the supernatants.

3) Centrifuge at 10-20'000 g for 1h at 4°C. Collect carefully the supernatant.

4) Add to 9 parts of the supernatant 1 part of Pol. 10x (Tris-HCl 20 mM, 500 mM KCl, 20 mM $MgCl_2$, 10 mM ATP, 10 mM DTT). Actin should start to polymerize (apparent increase in solution viscosity). Polymerize for 2h-ON at 4°C.

5) High salt wash to remove tropomyosin: solid KCl is slowly added to a concentration of 0.6 M and the solution is gently stirred for exactly 30 min at 4°C.

6) Ultracentrifuge* F-actin. Homogenize the pellet into 120 ml of 0.6 M KCl, 2 mM $MgCl_2$, 1 mM ATP and ultracentrifuge*. Rince the F-actin pellet with water.

7) Add 1ml water and keep on ice for 1h. Homogenize F-actin in 30 ml water totally. Dialize at 4°C with three changes of buf G (0.1 mM ATP-Tris pH ca.7).

8) Ultracentrifuge*, keep the supernatant.

9) To obtain pure actin monomers depleted from dimers or other oligomers, run on a gel-filtration (Sephadex-150) column equilibrated with buf G at 4°C.

10) Use G-actin within 2 weeks or keep it at -80°C (with a loss of acivity).

11) Measure actin concentration in solution by absorbance, $OD_{290}= 0.65$ cm^{2}mg^{-1}.

12) For long storage, repolymerize G-actin: to 9 parts add 1 part of Pol. 10x. Polymerize for 24-48h. Ultracentrifuge*. Keep F-actin at 4°C.

13) * Ultracentrifugations are carried out for 1.5h at 150'000 g, 4°C.

8. Labelling actin with pyrenyl (see DiNubile and Southwick, 1988).

1) Polymerize actin as above but without DTT.

2) Dropwise, with constant stirring of 10 ml F-actin, add 200 µl N-pyrenyliodoacetamide (Molecular Probes, dissoled in DMSO to 14 mg/ml).

3) Incubate ON RT on a rotatory shaker. Quench the labelling reaction by 50 μl 0.2 M DTT.

4) Centrifuge twice 2500 g 15 min 4°C. Save the supernatant.

5) Centrifuge 150,000 g 1.5h 4°C, store the pellet at 4°C, protected from light.

6) Depolymerize pyrenyl F-actin, purify actin monomers by gel-filtration as in II-7. Measure actin concentration as follows: 1 mg/ml pyrenyl G-actin= [OD_{290}-(0.33∗OD_{344})] / 0.637 (see Carson *et al.*, 1986).

9. Determination of concentrations of free and protein-bound ATP.

1) Measure free ATP in solution by luciferase bioluminescence kit (Boehringer Mannheim).

2) Total ATP in complex solutions (neutrophil cytosol, actin samples) is measured releasing the protein-bound nucleotides with 400 mM perchloric acid followed by centrifugation and adjustment of the supernatant pH with KOH.

3) Protein-bound ATP is calculated as the difference between total and free ATP.

10. Purification of low-molecular weight actin polymerization- stimulatory activity (APSA) from neutrophil cytosol.

1) In contrast to normal conditions of neutrophil cytosol preparation (see IV-2), to prepare the cytosol-donor for the APSA, higher cell concentration ($2*10^8$ neutrophils/ml) and the presence of 2 mM $MgCl_2$ in the breaking buffer are required. The resulting cytosol (protein concentration: 5-6 mg/ml) is able to polymerize actin in response to GTPγS even in the presence of Mg^{2+} (see Katanaev and Wymann, 1998a).

2) Treat 1 ml donor cytosol with 40% SAS for 40 min at 4°C on rotary shaker, centrifuge 1800 g 10 min 4°C.

3) Dissolve the precipitate in 300 μl 10 mM Tris-HCl, pH 7.5, keep 40 min on ice, centrifuge 1000 g 10 min 4°C.

4) Determine [AS] as in II-5, dilute the supernatant with 10 mM Tris pH 7.5 to 5 mM AS.

5) Load the sample onto a DEAE-sepharose column (bed volume ca. 50 ml) pre-equilibrated with buf A: 10 mM Tris-HCl pH 7.5, 5 mM AS.

6) Run the chromatography with the flow rate 0.1 ml/min. Use a conductivity meter to assess the gradient. Wash the column with: 5 ml buf A; 10-ml gradient of buf A to 50% buf B (buf A + 1mM KCl); 3 ml 50% buf B; step to 100% buf B; 5 ml buf B; step to 0% buf B; 20 ml buf A. Collect 1-ml fractions.

7) Analyze the collected fractions for the APSA: 10 μl of fractions per 35 μl of the actin polymerization reaction mixture containing 2mM $MgCl_2$ using normal neutrophil cytosol as the recipient (see IV-9). Ensure that the final concentration of KCl in the

reaction mixtures is the same (115 mM) knowing the [KCl] of each fraction by the conductivity meter.

8) Boil the active fraction for 5 min. Centrifuge 10000 g 10 min RT. Ultrafiltrate the supernatant through a Microcon membrane (cut-off 10 kDa). Collect the flow-through.

9) Load the sample onto the water-equilibrated Partisil SAX 10 micron HPLC column (bed volume ca. 4 ml).

10) Run the HPLC using freshly 0.2 μm-filtered buffers (buf A= water, buf B= 1M KH_2PO_4 pH 4.0): 2 min 100% buf A, 10 min the gradient of 0-100% buf B, 2 min 100% buf B. Flow rate- 2.1 ml/min. Collect fractions adsorbing at 260 nm. Analyze the activity.

11) Analyze the purity and molecular mass(es) of the active fraction using ES-MS after proton ionization (run on the FT-ICR Bruker Daltonics Bio APEX II mass spectrophotometer, Spectrospin AG, by Prof. Yenni, Inst. Organic Chemistry, Univ. Fribourg).

12) To assess the possible chemical nature of the substances present in the active HPLC fraction, address public chemical databases (www.chemfinder.com/; www.matrixscience.com/cgi/index.pl?page=/search_form_select.html; www.americanpeptide.com/). Purchase the candidate chemicals and analyze them for the APSA in the neutrophil cytosol.

III. Hematology techniques.

1. Isolation of human blood neutrophils (see Böyum, 1968).

1) Buffy Coats were prepared at the Swiss Red Cross Transfusion Centre, Hôpital Cantonale, Fribourg.

2) Solutions: all besides Lymphoprep should be filter sterile; ensure their osmolarity is 290-300 mosmols. Keep at 4°C.

ACD (acid citrate dextrose: 10.1 mM glucose, 30 mM citric acid, 0.63% NaCl, pH 6.5 by 3M NaOH);

Shock solution 10x: 1.55 M NH_4Cl, 100 mM $KHCO_3$, 1 mM EGTA, pH 7.4;

Ficoll: 500 ml Lymphoprep^{TM} (Nycomed Pharma AS, Oslo, Norway) + 29 ml 3.2% trisodium citrate (to 0.186%).

3) Add one half (ca. 30 ml) of a ≤24h-old Buffy Coat to 10 ml of ACD, mix by inversion.

4) Centrifuge 1000 g 5 min RT. Remove platelet-rich plasma. Collect light red layer on top of red pellet: add 7 ml to 11 ml of PBS with 13.64 U/ml heparin, mix by inversion.

5) Overlay on top of 10 ml Ficoll. Centrifuge 500 *g* 20 min 18°C, swing-out rotor, brake off. Erythrocytes and granulocytes are precipitated by this technique; lymphocytes are concentrated as one layer in Ficoll. Completely remove them.

6) Resuspend the pellets in 2 ml ice-cold 1x Shock solution, transfer to new tubes, fill up with Shock solution to 40 ml. Keep on ice for 10 min.

7) Centrifuge 400 *g* 5 min 4°C. Repeat the osmotic shock if erythrocyte lysis is incomplete: 20 ml Shock solution, 3 min on ice.

8) Wash neutrophils twice with 0.9% NaCl, 50 µM $CaCl_2$ (or PBS), 300 *g* 5 min 4°C.

9) Count cells with a hemocytometer, estimate viability by Trypan Blue (0.1%) exclusion. Keep the cells in an appropriate buffer, 10°C, up to 10h.

2. Mouse bone marrow isolation.

1) Kill a mouse by cervical dislocation. Cut out intact femurs and humeri. Remove the flesh. Cut the bones with scissors at the two ends.

2) Fill a sterile 2ml syringe with a thinnest needle (27G3/4, 0.4x19 mm, grey mark, Microlance) with ca. 1.5 ml RPMIc (RPMI from GibcoBRL, completed with 10% foetal calf serum [GibcoBRL, heat-inactivated: 30 min 56°C], 100 U/ml penicilline, and 100 µg/ml streptomycine). Flush the inner space of the bones with this, moving the needle to and fro inside the bone, collect the wash-out into an ice-cold tube.

3) Centrifuge 1200 *g* 4 min 4°C. Resuspend each pellet in 150 µl ice-cold shock solution (see III-1). Pool the suspensions from the same mouse. Wash each tube with 50 µl shock solution, add to the pool. Keep on ice for 5 min. Centrifuge. Resuspend in 1 ml PBS.

3. Mouse peritoneal exudate collection.

1) Seize a mouse tightly in your left hand, its belly up. It should not be able to move at all when you sting it with the neddle!

2) Injection. Fill a 1ml syringe with a medium needle (21G2 0.8 x 50 mm, green mark, Microlance) with 1 ml thioglycolate broth (25 g/lt water, boil and dissolve completely, sterilise, heat to boiling and cool just before use). Keeping the needle at ca. 30° to the mouse belly, pierce by some mm avoiding the bladder in the middle of the belly. Move the needle gently further, no resistance should be met if the peritoneum is reached. Inject the broth at steady pace. Remove the needle: no blood nor broth should go out.

3) Sacrifice the mouse by cervical dislocation after ca. 1 day if neutrophils, and after 3-5 days if macrophages are needed.

4) Spray the body with 70% ethanol, dry. Open the belly's skin without breaking the peritoneum wall. Inject 5ml of PBS with a 5ml syringe and green needle into mouse' peritoneum. Remove the needle and massage the mouse' belly. Picking up the

peritoneum wall with a pincer, make a little hole into the peritoneum with scissors. Deepen a 1ml syringe, no needle, into the cut, and collect the liquid to a fresh tube kept on ice. At least 4.5 ml should be obtained.

5) Centrifuge 1200 *g* 4 min 4°C. Resuspend in 1 ml PBS.

4. Mouse whole blood collection.

1) Kill a mouse by servical dislocation. Immediately open the peritoneum and reveal the *vena cava*, which is the thickest blood vessel going vertically close to the dorsal part of the animal between the two kidneys.

2) With a 1ml sterile syringe armed by 21G2 0.8x50 mm needle (green mark, Microlance), prewashed with 13.64 U/ml heparin solution in PBS, pierce the vessel to the direction of the mouse' tail. The needle should be located within the vessel. Start gently collecting the blood. The *vena* can close if the heart is not beating. Put ca. 1 ml blood to a RT sterile 15 ml Falcon tube containing ca. 0.3 vol of the heparin solution. Mix immediately.

3) Centrifuge the blood 650 *g* 2 min RT, swing-out rotor, brake off. Collect platelet-rich plasma. Collect leukocyte-containig light red layer on top of the red pellet, keep on ice.

4) Lyse the contaminating erythrocytes as in III-2. Centrifuge 400 *g* 5 min 4°C and resuspend the pellet in the desired buffer, e.g. PBS.

5. Purification of mouse neutrophils and macrophages by percoll gradient centrifugation.

1) 80% Percoll: 8 vol of Percoll (Pharmacia) are mixed with 1 vol sterile PBS, and 1 vol of sterile sodium phosphate buffer (0.2 M, pH 7.4) containing 1.49 M NaCl (see Watt *et al.*, 1979). 60% and 40% Percoll are prepared from 80% Percoll and PBS.

2) Load 1ml of the bone marrow from III-2 or peritoneal exudate from III-3 on top of 3ml 60% Percoll on top of 3ml 80% Percoll in a 15-ml Falcon tube, if neutrophils are needed. If macrophages are required, use 40%/60% Percoll instead. All solutions are ice-cold.

3) Centrifuge 540 *g* 30 min 4°C, swing-out rotor, brake off.

4) Collect mature neutrophils between the 80 and 60% Percoll layers; collect peritoneal macrophages between 40% and 60% layers. The Percoll gradient for the collection of mature neutrophils was chosen after analysis of actin polymerization in response to fMLP in cells isolated from more narrow discontinious Percoll density centrifugation and confirmed by cell colouration.

5) Wash the cells thrice in PBS, count, resuspend in RPMIc, $3-5*10^6$ cells/ml. Keep on ice.

6. Colouration of blood cells.

1) Put a drop of cell suspension on a very clean glass. Distribute this drop evenly over the glass with a single strike of a cover slip. Dry the cells on fire, don't burn them!

2) Pour and distribute evenly over the glass 1-2 ml of the May-Grünwald or 10% Giemsa solution in PBS. Leave for 1-2 min. Wash away the unbound dye with water.

3) Wait till the glass dries, analyse under the microscope.

7. Mouse platelet aggregation assay.

1) Recentrifuge platelet-rich plasma (PRP, see III-4) 1500 g 20-30 min RT. Collect the platelet-poor plasma (PPP) to a separate tube and keep at RT.

2) With a hemocytometer determine cell concentration in PRP diluting it ca. 100 times with buffer. Add PPP to PRP to adjust platelet concentration.

3) To concentrate platelets or remove plasma proteins, centrifuge PRP 500 g 10 min RT, resuspend the pellet in 138 mM NaCl, 6 mM KCl, 0.66 mM KH_2PO_4, 0.64 mM K_2HPO_4, 1.2 mM $MgCl_2$, 5.6 mM glucose, 20 mM Hepes-NaOH pH 7.4 (see DiNubile and Southwick, 1988) + 1.2 mM $CaCl_2$ + 0.5% BSA.

4) Prewarm the platelet aggregometer (normal spectrophotometer with a magnetic stirrer) and the platelet suspension (not less than $0.1*10^9$/ml, ideal is $0.5-0.6*10^9$/ml) or PRP to 37°C. Record the basal line for 3-5 min.

5) Stimulate the stirred suspension with 1-2 U/ml thrombin, 10-20 μM ADP, or others. Measure light transmittance for ca. 10 min. The read-out system has to be equilibrated to allow high sensitivity in-scale measurements. The best is to adjust 100% transmittance to that of PPP or the buffer, if the signal is expected to be sufficiently high.

8. Quantifying actin polymerization in neutrophils (see Katanaev and Wymann, 1998b).

1) Human neutrophils prepared as in III-1 or mouse neutrophils or macrophages prepared as in III-5 are resuspended to $1-5*10^6$ cells/ml HTBG (138 mM NaCl, 4.6 mM KCl, 20 mM Hepes-NaOH pH 7.5, 10 mM glucose). 10^5 cells are prewarmed for 10 min at 37°C.

2) Add the stimulus in HTBG as 1/10th of cellular volume. Mix gently.

3) For human neutrophils, stimulation is stopped by adding together *p*-formaldehyde to 4% (from 10% stock) and octyl-β-D-glucopyranoside (OG, from 4% stock) to 1%. The suspension is immediately vortexed and kept at RT for 15 min.

4) For mouse cells, *p*-formaldehyde is added first, while OG is added 15 min later.

5) PBS to 600 μl and rhodamine phalloidin to 15 nM are added for 30-40 min.

6) Fluorescence is measured in a 1ml quartz cuvette on a Perkin-Elmer fluorescence spectrophotometer LS50B (ex. 552/5 nm; em. 580/20 nm). HTBG + *p*-formaldehyde/OG + PBS/rhodamine phalloidin is measured as the background.

9. Visualizing F-actin in neutrophils.

1) Control or stimulated neutrophils were mixed with an equal volume of the staining solution (7.3% p-formaldehyde, 183 µg/ml L-α-lysophosphatidylcholine, 1.2 µM rhodamine phalloidin, 18% methanol in the neutrophil buffer).

2) Incubate on ice, protected from light, for 4-20h. Apply 5-10 µl to a coverslip.

3) Mount for fluorescence or confocal microscopy. Use rhodamine filters.

10. Analysis of actin-gelsolin complexes in neutrophils (see Howard *et al.*, 1990).

1) Resuspend neutrophils in 25 mM HEPES-NaOH, 50 mM NaH_2PO_4, 150 mM NaCl, 4 mM KCl, 1 mM $MgCl_2$, 1.2 mM $CaCl_2$, 10 mM glucose, pH 7.15 - a hypertonic buffer. In isotonic buffers neutrophils have no actin-gelsolin complexes.

2) Vortex control or stimulated cells with an equal volume of 2x Lysis buffer (20 mM imidasole-HCl, 2% Triton X-100, 80 mM KCl, 20 mM EGTA, 7 mM diisopropyl fluorophosphate, pH 7.15). Put on ice.

3) Centrifuge the lysate 12000 g 15 min 4°C. The supernatant can be kept at -80°C. Recentrifuge before use in this case.

4) Add ca. 1/50th of the 50% suspension of CNBr beeds coupled to monoclonal anti-gelsolin antibodies (clone 2C4 (Chaponnier *et al.*, 1986)).

5) Incubate at 4°C on a rotatory shaker for 2h. Centrifuge 12000 g 2 min 4°C.

6) Wash successively with 1x Lysis buffer, TBS (10 mM Tris-HCl pH 7.4, 100 mM NaCl) supplemented with 0.3 M $MgCl_2$ and 1 mM EGTA, and TBS alone.

7) Solubilyze the bead-bound proteins with Urea-containing sample buffer and analyse on 10% SDS-PAGE as described in II-1.

11. Measuring leukocyte adhesion to protein-coated glass surfaces.

1) Incubate human neutrophils at $5*10^7$/ml HTBG or mouse neutrophils at $5*10^6$/ml RPMIc with 2 µg/ml calcein AM for 30 min. Wash and resuspend in RPMIc to $3*10^6$ (mouse) and $1*10^7$ (human) cells/ml. Keep the calcein-loaded cells at RT before use.

2) Study cell adhesion on 12-well glass slides (Marienfeld, well diameter = 7 mm). Precoat the wells with 20 µl fibronectin (20 µg/ml, ON 4°C) or fibrinogen (1 mg/ml, 1-2h 37°C) in PBS. To coat with fibrin, refill fibrinogen-coated wells with 20 µl 1U thrombin/ml PBS, incubate 10 min 37°C. Drain the glass slides with a tissue and prewarm to 37°C.

3) Apply 20 µl calcein-loaded cells per well. Incubate 8-10 min 37°C, 5% CO_2 in humidity.

4) Stimulate the cells for 3 min with 1 µl stimulus. Transfer the slides to a container with 138 mM NaCl, 4.6 mM KCl, 20 mM Hepes-NaOH pH 7.5, 2 mM $MgCl_2$, 2 mM $CaCl_2$ and wash at 20 rpm on a horizontal shaker for 8 min at RT.

5) Before complete drying, the slides are put to the microplate-sized holder. The holder is home-made of aluminium, and has the size of a typical microplate. It allows simultaneous measurements of 4 slides, or 48 wells in total. Holder parameters (to be used with the KC4 program of the reader): length 127.0 mm, width 85.4 mm, top left X 14.4 mm, top left Y 10.9 mm, bottom right X 114.5 mm, bottom right Y 55.7 mm, number of columns 12, number of rows 6, well diameter 6 mm.

6) Measure the fluorescence of remaining cells (F_r) from the bottom in a Bio-Tek FL600 Fluorescence Plate Reader, Bio-Tek Instruments, Inc., ex. 485/20 nm, em. 530/25 nm. Also measure before as well as immediately after cell application to detect the background fluorescence (F_b) and the fluorescence of 100% loaded cells (F_{100}), respectively. The percent of adherent cells is quantified as $100 * (F_r-F_b) / (F_{100}-F_b)$.

12. Measuring leukocyte chemotaxis (see Frevert *et al.*, 1998).

1) Load neutrophils with calcein AM as in III-11.

2) Load 29-30 µl buffer or chemoattractants into the wells of the NeuroProbe chemotactic chambers (3.2 µm diameter sites, 30 µl 96-well). Load 20 µl of cells or cell medium into some wells to measure 100% and 0% of migrated cells, respectively.

3) Load a 3µm-pore track-etched polycarbonate membrane (8 mm^2 exposed filter areas) above the chamber. If the wells are filled with the correct volume (27-31 µl), the menisci of the loaded liquid will form an aquaous seal between the chamber and the membrane.

4) Overlay 20 µl cells ($1-5*10^6$ / ml) per each filter site as a liquid drop. If chemokinesis is studied, add to the cells chemoattractants at the same concentration as in the lower wells.

5) Chemotaxis is run during 1.5 h at 37°C, 5% CO_2 in humidity.

6) Remove nonmigrated cells from the membrane with a cell scraper.

7) Measure the number of migrated cells fluorometrically (see III-7) for the unassambled set of the chamber and the membrane.

8) To follow cell migration <u>into</u> vs <u>through</u> the membrane, centrifuge the chemotaxis set 300 *g* 5 min RT, desassemble and measure separately the lower chamber and the membrane.

13. Mouse neutrophil priming with LPS and the respiratory burst measurements (see Wymann *et al.*, 1987).

1) Isolate mouse bone marrow neutrophils as in III-5. Bring to 10^7 cells per ml <u>RPMIc</u> (with serum!!). Keep on ice.

2) Dissolve LPS (lipopolysaccharide, from *Salmonella typhosa*, Sigma (cat.n. L-7136, lot n. 121H4025), prepared by TCA extraction) in water to 10-20 µg/ml, keep at -20°C (stable for several months).

3) Incubate 20 µl neutrophils (200,000 cells) with water or 100 ng/ml LPS in 880 µl <u>RPMI</u> (without serum!!) for 50 min at 38°C. Important: the incubation must be done in <u>polypropylene</u> tubes (Treff, 1.5 ml). Incubation in polystyrene chemiluminescence tubes will lead to strong cell priming due to cell-surface interactions.

4) Continue the incubation for 10 min adding 100 µl of fresh 10x Reaction Buffer (in HTBG, 20 U/ml horseradish peroxidase, 0.2 mM luminol from a 20 mM stock in DMSO [keep at -20°C protected from light]). Meanwhile prewarm the chemiluminescence tubes in the 37°C-warm luminescence reader (Lumicon, Hamilton).

5) Transfer the cell suspension to polystyrene chemiluminescence tubes immediately before starting respiratory burst measurements. Measure not more than two tubes at once with stimuli like fMLP; for PMA or zymozan all six tubes can be measured at the same time. Add fMLP with a 10 µl syringe while recording chemiluminescence. Add PMA and zymozan by a pipette "off-line". Shake cell suspensions with zymozan occasionally.

6) Set 3-5 sec as the counting interval, don't forget to set the multiple (M) measurement regime. The respiratory burst is detected as luminol-dependent chemiluminescence which reflects the instantaneous levels of H_2O_2. Relatively high amounts of peroxidase are included to i) catalyze H_2O_2- induced oxidation of luminol to luminescent 3-aminophthalate and ii) rapidly remove the peroxide, increasing the time resolution of respiratory birst measurements.

14. Free intracellular $[Ca^{2+}]$ measurements with fura-2 in mouse neutrophils (see Grynkiewicz *et al.*, 1985).

1) Isolate mouse bone marrow neutrophils as in III-5. Bring them to 10^7 cells per ml HTBG. Load with 5µM fura-2 (from freshly prepared 5 mM stock in DMSO) for 45 min at RT on a rotary shaker. Wash the cells thrice with warm HTBG and keep at RT before use.

2) Take 10^6 cells per 4 ml plastic fluorescence cuvette; add HTBG to 3ml; add $CaCl_2$ to 1 mM. Omitting $CaCl_2$ will lead to inability of repeated stimulations to effectively induce $[Ca^{2+}]$ rises in mouse neutrophils. Preincubate in the 37°C- warm fluorescence spectrophotometer (Perkin Elmer LS 50 B) for 5 min with magnetic stirring.

3) Start one-wavelength fluorescence recording, ex. 340/15 nm, em. 380/20 nm, in the time drive regime with the minimal increment time. Stir the cell suspension with a magnet.

4) Stimulate the cells with the following sequence of agonists (another sequence will lead to no $[Ca^{2+}]_i$ rises after the 3rd or 2nd stimulus): 50 nM IL-8, 1 nM C5a, 100 nM PAF, 1 μM fMLP. Clear rises in fluorescence should be observed.

5) Before finishing the recording, lyse the cells by 1% Triton X-100. This will lead to liberation of intracellular fura-2 and its immediate complexing with extracellular Ca^{2+}, giving maximal fluorescence F_{max}. Afterwards, add EDTA to 4 mM to complex all Ca^{2+}, giving the minimal fluorescence F_{min}. Determine F_{max} and F_{min} for each experiment.

6) Calculate the free intracellular Ca^{2+} concentration at each time point by the formula $[Ca^{2+}]_i = K_d [(F - F_{min}) / (F_{max} - F)]$, where F is the fluorescence at each time point, and K_d is the dissociation constant for the fura-2 / Ca^{2+} interaction and equals 224 nM.

15. MAPK activation in neutrophils.

1) Resuspend mouse bone marrow neutrophils to $1*10^6$/ml of HTB-glucose. Prewarm 10^6 cells for 10 min at 37°C before stimulation with DMSO or fMLP for 30 sec.

2) Transfer the cells to ice for 1-2 min and centrifuge 10000 g 1 min 4°C. The pellet can be kept at -80°C after freezing in liquid nitrogen.

3) Dissolve the pellets in 15 μl of Urea-containing sample buffer and boil 20 min with occasional mixing, before loading all material for 12% SDS-PAGE (see II-1).

4) Western blot (see II-2) using Anti-ACTIVE^{TM} MAPK pAb (Promega) as the primary antibody (recognizing dually phosphorylated Thr^{183}GluTyr sequence in p44/ERK1 and p42/ERK2) and Anti-Rabbit peroxidase coupled IgG (Sigma) as the secondary antibody.

16. Statistical analysis with ANOVA (ANalysis Of VAriance).

1) ANOVA is used to analyse the data coming from experiments giving different absolute values but similar tendencies. For example, wild type and PI3Kγ knock-out neutrophils in many independent experiments chemotax differently, although the absolute chemotaxis values are not always the same due to unequivalency of different cell preparations. In this case, simple analysis like T tests may show high P values. ANOVA, in contrast, can better resolve the significance of this kind of data.

2) Different programs can be used to run ANOVA, StatView is one of them. To compare different chemotaxis experiments, arrange the data in the following way:

	exp. N	genotype	IL-8 50 nM
Type:	String	Category	Real
Source:	User Entered	User Entered	User Entered
Class:	Nominal	Nominal	Continuous
Format:			Free Format Fixed
Dec. Places:			3
1	exp.1	+/+	8.731
2	exp.1	+/+	9.373
3	exp.2	+/+	34.348
4	exp.2	+/+	37.456

5	exp.1	-/-	4.956
6	exp.1	-/-	5.016
7	exp.2	-/-	14.477
8	exp.2	-/-	16.247

Unpaired or paired T test analysis will estimate the difference between the chemotaxis of wild-type and knock-out neutrophils from these data as P value = 0.1907 or P value = 0.0816, respectively; nonsignificant.

3) To run the ANOVA, ANOVA post-hoc tests should be chosen from the analysis menu. In the appearing table, the "IL-8 50nM" column has to be chosen as the "Dependent Variable", while the columns "genotype" and "exp. N" have to be assigned as "Factor(s)". For the sake of presentation, the "genotype" column should be put first as "Factor(s)". In the resultant view window, the results of the analysis are nicely presented in the following way, showing the P value = 0.0002, or the difference being extremely significant:

Interaction Line Plot for Column 3
Effect: Column 2 * Column 1
Error Bars: ± 1 Standard Error(s)
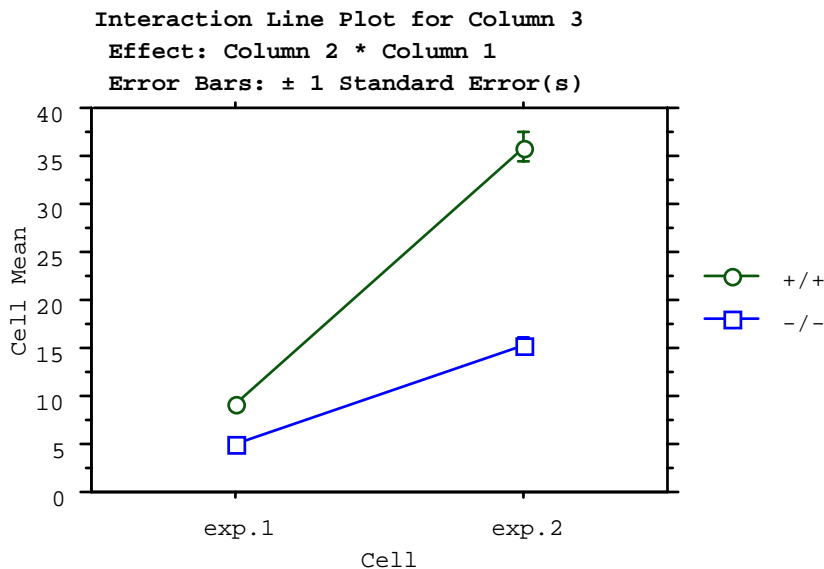
Fisher's PLSD for Column 3
 Effect: Column 2
 Significance Level: 5 %

	Mean Diff.	Crit. Diff	P-Value	
+/+, -/-	12.303	2.523	.0002	S

4) ANOVA can be used not only to compare sets of data for one certain condition (e.g. chemotaxis to 50 nM IL-8), but also to compare whole ranges of responses (e.g. chemotaxis of wild-type and knock-out neutrophils to different concentrations of one or more attractants). To answer whether chemotaxis of knock-out and wild-type cells to increasing concentrations of IL-8 is statistically different, all the data have to be put to one column, respective genotypes to another, and the types of experiments (exp.1: 10nM, exp.1: 50 nM, exp. 2: 10 nM, exp.2: 200 nM, etc) to the third. Running the

analysis like above for the chemotaxis data coming from seven independent experiments with three different IL-8 concentrations gives the folowing results:

Interaction Line Plot for IL8 all
Effect: genotype * exp. N
Error Bars: ± 1 Standard Error(s)
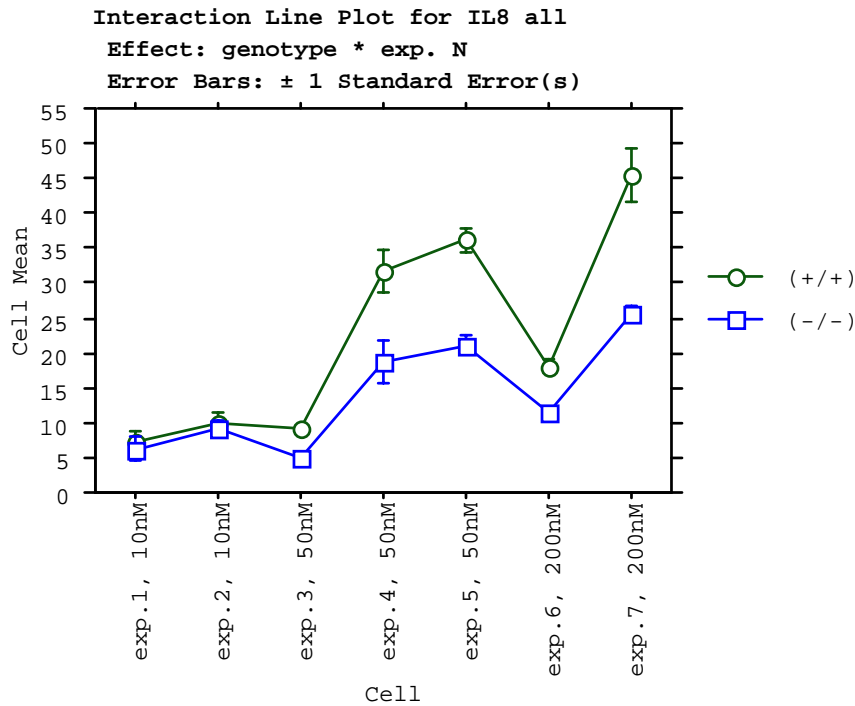
Fisher's PLSD for IL8 all
 Effect: genotype
 Significance Level: 5 %

	Mean Diff.	Crit. Diff	P-Value	
(+/+), (-/-)	9.450	2.233	<.0001	S

, proving that besides variations in the absolute chemotaxis values and chemoattractant concentration from one experiment to the other, the difference between chemotaxis of wild-type and PI3Kγ knock-out neutrophils to IL-8 is extremely significant.

IV. Cell biology techniques.

1. Testing effects of *Clostridium* toxins on fibroblast cultures.
1) An 1ml aliquot of NIH3T3 cells from -80°C is rapidly defrozen in the 37°C-warm water bath with vigirous shaking and immediately mixed with 1 ml of the medium (DMEM completed with 10% foetal calf serum [GibcoBRL, heat-inactivated: 30 min 56°C], 100 U/ml penicilline, 100 μg/ml streptomycine, and 2 mM glutamine), and put to a 50ml cell culture bottle together with 4 ml more of DMEMc.
2) After ca. 3h of growth (37°C, 5% CO_2) when ca. 80% cells are attached, the medium is changed and the cells are grown until confluence.

3) To split the cells, aspirate the medium and rinse the bottle with 2 ml PBS. Add 500 µl trypsin/EDTA (0.5/0.2 mg/ml) to the cells, incubate for 3-5 min at 37°C. When detached, transfer the cells to a sterile tube, rinse the bottle with 2 ml DMEMc, transfer it to the same tube. Rinse the bottle with 2 ml PBS, discard. Put 1/10th of the cell suspension from the tube to the original bottle, grow till confluence (ca. 2 days).

4) Split again, load also $5\text{-}8*10^4$ cells to wells of the 24-well plate. Grow for ca. 2 days to semiconfluence. Change the medium (0.5 ml) before the experiment.

5) Load 1-10-100-1000 ng/ml *Clostridium difficile* toxin B (see Just *et al.*, 1995) or *C. sordellii* (strain 6018) lethal toxin (see Just *et al.*, 1996) to each well. The toxins were kindly supplied in dry ice by Prof. I. Just, Univ. Freiburg, Germany, and diluted in 50 mM Tris-HCl pH 7.5, 500 mM NaCl.

6) Count the percentage of cells becoming round after 1-15 h treatment.

2. Preparation of human neutrophil cytosol, plasma membranes, and granules (see Katanaev and Wymann, 1998a).

1) Human neutrophils prepared as in III-1 are resuspended to 10^8 cells per ml Hepes-potassium buffer (<u>HKB</u>, 135 mM KCl, 10 mM NaCl, 10 mM Hepes, 2 mM EDTA, pH 7.0) supplemented with 1 mM PMSF, 0.5 mM diisopropyl fluorophosphate, 20 mM leupeptin, 18 mM pepstatin, 12.5 U/ml benzone nuclease, and 5% glycerol.

2) Disrupt the cells by nitrogen cavitation (40 min/35 bar) on ice. Centrifuge 1300 *g* 10 min.

3) Ultracentrifuge the supernatant 121,000 *g* 45 min 4°C, producing the neutrophil cytosol.

4) To prepare crude neutrophil membranes, loade the cells on top of 30% (w/w) sucrose on top of 50% sucrose. Centrifuge 200,000 *g*, brake off, at the slowest acceleration rate.

5) To purify plasma membranes and granules, use 15%, 34%, and 45% sucrose layers. Collect the cytosol on top of sucrose, plasma membranes at 15/34% interphase, and granules at 34/45% interphase (see Abo and Segal, 1995).

6) Freeze the preparations in aliquots in liquid nitrogen and keep at -80°C for months.

3. Measuring cell-free NADPH oxidase activity.

1) Calibrate appropriately the reader (Unicam SP 1700 Ultraviolet Spectrophotometer), set the wavelength to 550 nm.

2) Prewarm the Reaction buffer (10 µM FAD, 100 µM oxidized cytochrome C, 10 mM Hepes-NaOH, 10 mM NaCl, 135 mM KCl, 1 mM EGTA, 1 mM $MgCl_2$, pH 8.0) to 25°C.

3) Preincubate cytosol or cytosol + membranes as and if necessary.

4) Add, mixing after each addition, to 1 ml plastic cuvettes:

950 µl Reaction buffer

15 µl 10 mM SDS (to 150 µM)

1 µl 10 mM GTPγS (to 10 µM)

1.3 µl 10% NaN$_3$ (to 2 mM)

20 µl crude membranes (to 100 µg/ml)

15 µl cytosol (to 50 µg/ml). Preincubate at RT for 2-5 min.

5) Add to the reference cuvettes (already containing all the components present in sample cuvettes) 5 µl 10mg/ml superoxide dismutase (to 50 µg/ml).

6) Start the reaction by adding 12 µl of NADPH stock (to 120 µM), mix the contents of the cuvettes and immediately start the measurement.

7) Measure the initial rate of superoxide production (ca. 10 min of measurement).

4. Measuring [^{14}C]-UDPG incorporation into Rho-proteins by *Clostridium* toxins as an example of assaying covalent binding of small molecules to proteins in complex mixtures.

1) Dry the necessary amount of [^{14}C]-UDPG (254 mCi/mmol) under vacuum.

2) Incubate the cytosol with 10 µg/ml toxin B or lethal toxin (see IV-1) (add Mn^{2+} in case of lethal toxin), 10 µM [^{14}C]-UDPG and 40 µM cold UDPG for 30 min.

3) Mix the tubes, take aliquots of 10 µl and put them to the centers of 1.5∗1.5 cm^2 labelled squares predrawn on a sheet of Whatmann 3MM paper. Let the paper dry at RT.

4) Soak the paper for 10 min in 10% TCA (trichloroacetic acid, w/v) on a shaker. Repeat with fresh TCA. Repeat again for 5 min.

5) Repeat with acetone. Let the paper dry at RT.

6) Cut the paper into the predrawn squares, put into liquid scincillator and count the radioactivity in a liquid scintillation analyzer (2200CA Tri-CARB, Packard).

5. Actin polymerization in the cell-free system from neutrophil cytosol (see Katanaev and Wymann, 1998a).

1) The cell-free system (20-100 µl) contains the following components:

neutrophil cytosol protein-   1.6-1.8 mg/ml

Hepes-NaOH pH 7.0-   10 mM

NaCl-   10 mM

KCl-   115 mM

EDTA-   2 mM free.

2) In certain experiments MgCl$_2$ to 2 mM free (instead of EDTA) and plasma membranes to 0.1 mg protein/ml can be added.

3) Stimulate actin polymerization by 50 μM GTPγS or other agents for 5-30 min at 37°C.

6. Analysis of actin-gelsolin interaction in the cell-free systen from neutrophil cytosol.

1) 1 μM recombinant (His)$_6$-tagged or GST-tagged gelsolin prepared basically as explained in II-3 is added to the cell-free system (100 μl).

2) After the required preincubations at 37°C, 20 μl 50% suspension of Ni-NTA agarose (to bind His$_6$-tag) or GSH-sepharose (to bind GST-tag) are added. Alternatively, 10 μl 50% suspension of anti-gelsolin beads described in III-10 are added.

3) After 2h incubation at 4°C on a rotatory shaker and 2 min centrifugation, 12000 g 4°C, the beads are washed successingly with 1ml buf A (10 mM Tris-HCl pH 7.5, 100 mM KCl, 10 mM EGTA), buf B (10 mM Tris, 100 mM KCl, 1 mM EGTA, 300 mM MgCl$_2$), and buf C (10 mM Tris, 100 mM KCl), denatured, and analyzed on 12% SDS-PAGE gels.

7. Analyzing actin cross-linking in the cell-free system.

1) Treat the mixtures as above and centrifuge 9000 g 5 min RT. Wash the sediments twice with HKB, denature and apply to 10% SDS-PAGE gels. Analyze actin bands by densitometry after Coomassie staining. Major proteins cosedimenting with actin are identified by peptide-mass fingerprinting with MALDI-TOF-MS on a PerSeptive Biosystem Voyager Elte mass spectrophotometer after in-gel trypsin digestion (see Cottrell and Sutton, 1996). The MALDI-TOF-MS was run by G.Hughes and S. Frutiger, Univ. Geneva.

2) Alternatively, resuspend the sediments in 1/10th of the original volume and apply 20 μl to AFM (atomic force microscope) -grade silicium plates for 1 min. After 4 brief washes with buffer and one with water, the samples are analyzed in air by AFM (Digital Instruments Inc., Santa Barbara, USA) by C. Galli, Inst. Experimental Physics, Univ. Fribourg. The analysis is performed in Tapping Mode™ (Zhong *et al*., 1993) in order to minimise the force applied to proteins by the microscope's tip.

3) For the fluorescence or confocal microscopy, the actin polymerization is stopped by incubation with 10% *p*-formaldehyde on ice, 10 min, before staining with 0.6 μM rhodamine phalloidin for ≥1h, protected from light.

8. Assaying free actin filament barbed ends in the neutrophil cytosol.

1) GTPγS is used to stimulate the cell-free system for optimally 15 min.

2) Add 20 μl aliquots to 600 ml prewarmed HKB with 0.5 mM pyrenyl G-actin (see II-8).

3) Immediately measure the kinetics of pyrenyl actin fluorescence at 27 °C (ex. 365/3 nm; em. 387/10 nm) on a Perkin-Elmer fluorescence spectrophotometer LS50B.

4) Under these conditions the initial rate of fluorescence increase is the measure of amount of free barbed ends added (Carson *et al..*, 1986).

9. Measuring actin polymerization in the cell-free system.
1) Briefly vortex the mixture from IV-6, add 10 µl to 600 µl HKB (or PBS) containing 15 nM rhodamine phalloidin, vortex briefly.
2) Keep at RT for 20 min.
3) Fluorescence (F) is measured as in III-8. Buffer with rhodamine phalloidin alone is also measured for the background fluorescence (F_0). F-actin levels are related to $\Delta F = F - F_0$. Absolute F-actin concentrations can also be calculated as explained in (Katanaev and Wymann, 1998b).

REFERENCES

Abo A, Segal AW. Reconstitution of cell-free NADPH oxidase activity by purified components. Methods Enzymol 1995: 256: 268-278.

Adelstein RS, Conti MA, Anderson W Jr. Phosphorylation of human platelet myosin. Proc Natl Acad Sci U S A 1973: 70: 3115-3119.

Ahuja SK, Lee JC, Murphy PM. CXC chemokines bind to unique sets of selectivity determinants that can function independently and are broadly distributed on multiple domains of human interleukin-8 receptor B. Determinants of high affinity binding and receptor activation are distinct. J Biol Chem 1996: 271: 225-232.

Aizawa H, Sutoh K, Yahara I. Overexpression of cofilin stimulates bundling of actin filaments, membrane ruffling, and cell movement in Dictyostelium. J Cell Biol 1996: 132: 335-344.

Alessi DR, James SR, Downes CP, Holmes AB, Gaffney PR, Reese CB, Cohen P. Characterization of a 3-phosphoinositide-dependent protein kinase which phosphorylates and activates protein kinase Balpha. Curr Biol 1997: 7: 261-269.

Alessi DR, Kozlowski MT, Weng QP, Morrice N, Avruch J. 3-Phosphoinositide-dependent protein kinase 1 (PDK1) phosphorylates and activates the p70 S6 kinase in vivo and in vitro. Curr Biol 1998: 8: 69-81.

Allen WE, Jones GE, Pollard JW, Ridley AJ. Rho, Rac and Cdc42 regulate actin organization and cell adhesion in macrophages. J Cell Sci 1997: 110: 707-720.

Allen WE, Zicha D, Ridley AJ, Jones GE. A role for Cdc42 in macrophage chemotaxis. J Cell Biol 1998: 141: 1147-1157.

Amano M, Ito M, Kimura K, Fukata Y, Chihara K, Nakano T, Matsuura Y, Kaibuchi K. Phosphorylation and activation of myosin by Rho-associated kinase (Rho-kinase). J Biol Chem 1996: 271: 20246-20249.

Anderlini P, Przepiorka D, Champlin R, Korbling M. Biologic and clinical effects of granulocyte colony-stimulating factor in normal individuals. Blood 1996: 88: 2819-2825.

Arai H, Tsou CL, Charo IF. Chemotaxis in a lymphocyte cell line transfected with C-C chemokine receptor 2B: evidence that directed migration is mediated by betagamma dimers released by activation of Galphai-coupled receptors. Proc Natl Acad Sci U S A 1997: 94: 14495-14499.

Arber S, Barbayannis FA, Hanser H, Schneider C, Stanyon CA, Bernard O, Caroni P. Regulation of actin dynamics through phosphorylation of cofilin by LIM-kinase. Nature 1998: 393: 805-809.

Arcaro A, Wymann MP. Wortmannin is a potent phosphatidylinositol 3-kinase inhibitor: the role of phosphatidylinositol 3,4,5-trisphosphate in neutrophil responses. Biochem J 1993: 296: 297-301.

Aspenstrom P, Lindberg U, Hall A. Two GTPases, Cdc42 and Rac, bind directly to a protein implicated in the immunodeficiency disorder Wiskott-Aldrich syndrome. Curr Biol 1996: 6: 70-75.

Aspenstrom P. A Cdc42 target protein with homology to the non-kinase domain of FER has a potential role in regulating the actin cytoskeleton. Curr Biol 1997: 7: 479-487.

Aspenstrom P. Effectors for the Rho GTPases. Curr Opin Cell Biol 1999b: 11: 95-102.

Aspenstrom P. The Rho GTPases have multiple effects on the actin cytoskeleton. Exp Cell Res 1999a: 246: 20-25.

Azuma T, Witke W, Stossel TP, Hartwig JH, Kwiatkowski DJ. Gelsolin is a downstream effector of rac for fibroblast motility. EMBO J 1998: 17: 1362-1370.

Babior BM. The respiratory burst oxidase. Curr Opin Hematol 1995: 2: 55-60.

Baggiolini M, Dewald B, Schnyder J, Ruch W, Cooper PH, Payne TG. Inhibition of the phagocytosis-induced respiratory burst by the fungal metabolite wortmannin and some analogues. Exp Cell Res 1987: 169: 408-418.

Baggiolini M. Chemokines and leukocyte traffic. Nature 1998: 392: 565-568.

Baldwin JM. The probable arrangement of the helices in G protein-coupled receptors. EMBO J 1993: 12: 1693-1703.

Bamburg JR, McGough A, Ono S. Putting a new twist on actin: ADF/cofilins modulate actin dynamics. Trends Cell Biol 1999: 9: 364-370.

Baranski TJ, Herzmark P, Lichtarge O, Gerber BO, Trueheart J, Meng EC, Iiri T, Sheikh SP, Bourne HR. C5a receptor activation. Genetic identification of critical residues in four transmembrane helices. J Biol Chem 1999: 274: 15757-15765.

Barrett K, Leptin M, Settleman J. The Rho GTPase and a putative RhoGEF mediate a signaling pathway for the cell shape changes in Drosophila gastrulation. Cell 1997: 91: 905-915.

Bazzoni F, Beutler B. The tumor necrosis factor ligand and receptor families. N Engl J Med 1996: 334: 1717-1725.

Becker EL, Davis AT, Estensen RD, Quie PG. Cytochalasin B. IV. Inhibition and stimulation of chemotaxis of rabbit and human polymorphonuclear leukocytes. J Immunol 1972: 108: 396-402.

Becker EL, Kermode JC, Naccache PH, Yassin R, Marsh ML, Munoz JJ, Sha'afi RI. The inhibition of neutrophil granule enzyme secretion and chemotaxis by pertussis toxin. J Cell Biol 1985: 100: 1641-1646.

Belham C, Wu S, Avruch J. Intracellular signalling: PDK1--a kinase at the hub of things. Curr Biol 1999: 9: R93-96.

Benard V, Bohl BP, Bokoch GM. Characterization of rac and cdc42 activation in chemoattractant-stimulated human neutrophils using a novel assay for active GTPases. J Biol Chem 1999: 274: 13198-13204.

Bengtsson T, Rundquist I, Stendahl O, Wymann MP, Andersson T. Increased breakdown of phosphatidylinositol 4,5-bisphosphate is not an initiating factor for actin assembly in human neutrophils. J Biol Chem 1988: 263: 17385-17289.

Bernstein HG, Keilhoff G, Reiser M, Freese S, Wetzker R. Tissue distribution and subcellular localization of a G-protein activated phosphoinositide 3-kinase. An immunohistochemical study. Cell Mol Biol (Noisy-le-grand) 1998: 44: 973-983.

Bockaert J, Pin JP. Molecular tinkering of G protein-coupled receptors: an evolutionary success. EMBO J 1999: 18: 1723-1729.

Bokoch GM, Bohl BP, Chuang TH. Guanine nucleotide exchange regulates membrane translocation of Rac/Rho GTP-binding proteins. J Biol Chem 1994: 269: 31674-31679.

Bokoch GM. Regulation of the human neutrophil NADPH oxidase by the Rac GTP-binding proteins. Curr Opin Cell Biol 1994: 6: 212-218.

Bondeva T, Pirola L, Bulgarelli-Leva G, Rubio I, Wetzker R, Wymann MP. Bifurcation of lipid and protein kinase signals of PI3Kgamma to the protein kinases PKB and MAPK. Science 1998: 282: 293-296.

Bottomley MJ, Salim K, Panayotou G. Phospholipid-binding protein domains. Biochim Biophys Acta 1998: 1436: 165-183.

Boulay F, Naik N, Giannini E, Tardif M, Brouchon L. Phagocyte chemoattractant receptors. Ann N Y Acad Sci 1997: 832: 69-84.

Bourne HR. How receptors talk to trimeric G proteins. Curr Opin Cell Biol 1997: 9: 134-142.

Boyum A. Isolation of mononuclear cells and granulocytes from human blood. Isolation of monuclear cells by one centrifugation, and of granulocytes by combining centrifugation and sedimentation at 1 g. Scand J Clin Lab Invest Suppl 1968: 97: 77-89.

Brenner B, Gulbins E, Busch GL, Koppenhoefer U, Lang F, Linderkamp O. L-selectin regulates actin polymerisation via activation of the small G-protein Rac2. Biochem Biophys Res Commun 1997: 231: 802-807.

Butty AC, Pryciak PM, Huang LS, Herskowitz I, Peter M. The role of Far1p in linking the heterotrimeric G protein to polarity establishment proteins during yeast mating. Science 1998: 282: 1511-1516.

Carlier MF, Pantaloni D. Control of actin dynamics in cell motility. J Mol Biol 1997: 269: 459-467.

Carlson SA, Chatterjee TK, Fisher RA. The third intracellular domain of the platelet-activating factor receptor is a critical determinant in receptor coupling to phosphoinositide phospholipase C-activating G proteins. Studies using intracellular domain minigenes and receptor chimeras. J Biol Chem 1996: 271: 23146-23153.

Carpenter CL, Tolias KF, Van Vugt A, Hartwig J. Lipid kinases are novel effectors of the GTPase Rac1. Adv Enzyme Regul 1999: 39: 299-312.

Carson M, Weber A, Zigmond SH. An actin-nucleating activity in polymorphonuclear leukocytes is modulated by chemotactic peptides. J Cell Biol 1986: 103: 2707-2714.

Carter SB. Effects of cytochalasins on mammalian cells. Nature 1967: 213: 261-261. Norgauer J, Kownatzki E, Seifert R, Aktories K. Botulinum C2 toxin ADP-ribosylates actin and enhances O2- production and secretion but inhibits migration of activated human neutrophils. J Clin Invest 1988: 82: 1376-1382.

Cerione RA, Zheng Y. The Dbl family of oncogenes. Curr Opin Cell Biol 1996: 8: 216-222.

Chaponnier C, Janmey PA, Yin HL. The actin filament-severing domain of plasma gelsolin. J Cell Biol 1986: 103: 1473-1481.

Cheng X, Ma Y, Moore M, Hemmings BA, Taylor SS. Phosphorylation and activation of cAMP-dependent protein kinase by phosphoinositide-dependent protein kinase. Proc Natl Acad Sci U S A 1998: 95: 9849-9854.

Choi KY, Satterberg B, Lyons DM, Elion EA. Ste5 tethers multiple protein kinases in the MAP kinase cascade required for mating in S. cerevisiae. Cell 1994: 78: 499-512.

Chong LD, Traynor-Kaplan A, Bokoch GM, Schwartz MA. The small GTP-binding protein Rho regulates a phosphatidylinositol 4-phosphate 5-kinase in mammalian cells. Cell 1994: 79: 507-513.

Chou MM, Hou W, Johnson J, Graham LK, Lee MH, Chen CS, Newton AC, Schaffhausen BS, Toker A. Regulation of protein kinase C zeta by PI 3-kinase and PDK-1. Curr Biol 1998: 8: 1069-1077.

Clapham DE, Neer EJ. G protein beta gamma subunits. Annu Rev Pharmacol Toxicol 1997: 37: 167-203.

Clore GM, Appella E, Yamada M, Matsushima K, Gronenborn AM. Three-dimentional structure of interleukin 8 in solution. Biochemistry 1990: 29: 1689-1696.

Coates TD Behavioral aspects of neutrophil motility. Curr Opin Hematol 1996: 3: 41-47.

Condeelis J. Life at the leading edge: the formation of cell protrusions. Annu Rev Cell Biol 1993: 9: 411-444.

Cottrell JS, Sutton CW. The identification of electrophoretically separated proteins by peptide mass fingerprinting. Methods Mol Biol 1996: 61: 67-82.

Crooks SW, Stockley RA. Leukotriene B4. Int J Biochem Cell Biol 1998: 30: 173-178.

Currie RA, Walker KS, Gray A, Deak M, Casamayor A, Downes CP, Cohen P, Alessi DR, Lucocq J. Role of phosphatidylinositol 3,4,5-trisphosphate in regulating the activity and localization of 3-phosphoinositide-dependent protein kinase-1. Biochem J 1999: 337: 575-583.

Daniels RH, Bokoch GM. p21-activated protein kinase: a crucial component of morphological signaling? Trends Biochem Sci 1999: 24: 350-355.

De Lozanne A, Spudich JA. Disruption of the Dictyostelium myosin heavy chain gene by homologous recombination. Science 1987: 236: 1086-1091.

Dharmawardhane S, Brownson D, Lennartz M, Bokoch GM. Localization of p21-activated kinase 1 (PAK1) to pseudopodia, membrane ruffles, and phagocytic cups in activated human neutrophils. J Leukoc Biol 1999: 66: 521-527.

Dillon ST, Feig LA. Purification and assay of recombinant C3 transferase. Methods Enzymol 1995: 256: 174-184.

DiNubile MJ, Southwick FS. Contractile proteins in leukocytes. Methods Enzymol 1988: 162: 246-271.

DiNubile MJ. Nucleation and elongation of actin filaments in the presence of high speed supernate from neutrophil lysates: modulating effects of Ca2+ and phosphatidylinositol-4,5-bisphosphate.Biochim Biophys Acta 1998: 1405: 85-98.

Djinovic-Carugo K, Young P, Gautel M, Saraste M. Structure of the alpha-actinin rod: molecular basis for cross-linking of actin filaments. Cell 1999: 98: 537-546.

Dutil EM, Toker A, Newton AC. Regulation of conventional protein kinase C isozymes by phosphoinositide-dependent kinase 1 (PDK-1). Curr Biol 1998: 8: 1366-1375.

Edwards DC, Sanders LC, Bokoch GM, Gill GN. Activation of LIM-kinase by Pak1 couples Rac/Cdc42 GTPase signalling to actin cytoskeletal dynamics. Nat Cell Biol 1999: 1: 253-259.

Elson EL, Felder SF, Jay PY, Kolodney MS, Pasternak C. Forces in cell locomotion. Biochem Soc Symp 1999: 65: 299-314.

Engel A, Lyubchenko Y, Muller D. Atomic force microscopy: a powerful tool to observe biomolecules at work. Trends Cell Biol 1999: 9: 77-80.

Fackler OT, Luo W, Geyer M, Alberts AS, Peterlin BM. Activation of Vav by Nef induces cytoskeletal rearrangements and downstream effector functions. Mol Cell 1999: 3: 729-739.

Farrens DL, Altenbach C, Yang K, Hubbell WL, Khorana HG. Requirement of rigid-body motion of transmembrane helices for light activation of rhodopsin. Science 1996: 274: 768-770.

Featherstone C. The many faces of WAS protein. Science 1997: 275: 27-28.

Fechheimer M, Zigmond SH. Changes in cytoskeletal proteins of polymorphonuclear leukocytes induced by chemotactic peptides. Cell Motil 1983: 3: 349-361.

Frangiskakis JM, Ewart AK, Morris CA, Mervis CB, Bertrand J, Robinson BF, Klein BP, Ensing GJ, Everett LA, Green ED, Proschel C, Gutowski NJ, Noble M, Atkinson DL, Odelberg SJ, Keating MT. LIM-kinase1 hemizygosity implicated in impaired visuospatial constructive cognition. Cell 1996: 86: 59-69.

Franke K, Gruler H. Directed cell movement in pulsed electric fields. Z Naturforch [C] 1994: 49c: 241-249.

Franke TF, Kaplan DR, Cantley LC, Toker A. Direct regulation of the Akt proto-oncogene product by phosphatidylinositol-3,4-bisphosphate. Science 1997: 275: 665-668.

Frevert CW, Wong VA, Goodman RB, Goodwin R, Martin TR. Rapid fluorescence-based measurement of neutrophil migration in vitro. J Immunol Methods 1998: 213: 41-52.

Fukuda M, Kojima T, Kabayama H, Mikoshiba K. Mutation of the pleckstrin homology domain of Bruton's tyrosine kinase in immunodeficiency impaired inositol 1,3,4,5-tetrakisphosphate binding capacity. J Biol Chem 1996: 271: 30303-30306.

Gaudry M, Caon AC, Gilbert C, Lille S, Naccache PH. Evidence for the involvement of tyrosine kinases in the locomotory responses of human neutrophils. J Leukoc Biol 1992: 51: 103-108.

Gayle RB 3d, Sleath PR, Srinivason S, Birks CW, Weerawarna KS, Cerretti DP, Kozlosky CJ, Nelson N, Vanden Bos T, Beckmann MP. Importance of the amino terminus of the interleukin-8 receptor in ligand interactions. J Biol Chem 1993: 268: 7283-7289.

Gerard C, Gerard NP. C5A anaphylatoxin and its seven transmembrane-segment receptor. Annu Rev Immunol 1994: 12: 775-808.

Goldman DW, Chang FH, Gifford LA, Goetzl EJ, Bourne HR. Pertussis toxin inhibition of chemotactic factor-induced calcium mobilization and function in human polymorphonuclear leukocytes. J Exp Med 1985: 162: 145-156.

Goodson HV, Anderson BL, Warrick HM, Pon LA, Spudich JA. Synthetic lethality screen identifies a novel yeast myosin I gene (MYO5): myosin I proteins are required for polarization of the actin cytoskeleton. J Cell Biol 1996: 133: 1277-1291.

Gorlin JB, Yamin R, Egan S, Stewart M, Stossel TP, Kwiatkowski DJ, Hartwig JH. Human endothelial actin-binding protein (ABP-280, nonmuscle filamin): a molecular leaf spring. J Cell Biol 1990: 111: 1089-1105.

Grynkiewicz G, Poenie M, Tsien R. A new generation of Ca2+ indicators with greatly improved fluorescence properties. J Biol Chem 1985: 260: 3440-3450.

Gullberg U, Andersson E, Garwicz D, Lindmark A, Olsson I. Biosynthesis, processing and sorting of neutrophil proteins: insight into neutrophil granule development. Eur J Haematol 1997: 58: 137-153.

Haines KA, Kolasinski SL, Cronstein BN, Reibman J, Gold LI, Weissmann G. Chemoattraction of neutrophils by substance P and transforming growth factor-beta 1 is inadequately explained by current models of lipid remodeling. J Immunol 1993: 151: 1491-1499.

Hall A. Rho GTPases and the actin cytoskeleton. Science 1998: 279: 509-514.

Hamm HE, Gilchrist A. Heterotrimeric G proteins. Curr Opin Cell Biol 1996: 8: 189-196.

Han J, Luby-Phelps K, Das B, Shu X, Xia Y, Mosteller RD, Krishna UM, Falck JR, White MA, Broek D. Role of substrates and products of PI 3-kinase in regulating activation of Rac-related guanosine triphosphatases by Vav. Science 1998: 279: 558-560.

Hanahan DJ. Platelet activating factor: a biologically active phosphoglyceride. Annu Rev Biochem 1986: 55: 483-509.

Hannigan M, Zhan L, Ai Y, Huang CK. The role of p38 MAP kinase in TGF-beta1-induced signal transduction in human neutrophils. Biochem Biophys Res Commun 1998: 246: 55-58.

Harakawa N, Sasada M, Maeda A, Asagoe K, Nohgawa M, Takano K, Matsuda Y, Yamamoto K, Okuma M. Random migration of polymorphonuclear leukocytes induced by GM-CSF involving a signal transduction pathway different from that of fMLP. Leukoc Biol 1997: 61: 500-506.

Harrington WF, Rodgers ME. Myosin. Annu Rev Biochem 1984: 53: 35-73.

Hart MJ, Jiang X, Kozasa T, Roscoe W, Singer WD, Gilman AG, Sternweis PC, Bollag G. Direct stimulation of the guanine nucleotide exchange activity of p115 RhoGEF by Galpha13. Science 1998: 280: 2112-2114.

Hartman RS, Lau K, Chou W, Coates TD. The fundamental motor of the human neutrophils is not random: evidence for local non-Markov movement in neutrophils. Biophys. J. 1994: 67: 2535-2545.

Hartwig JH, Bokoch GM, Carpenter CL, Janmey PA, Taylor LA, Toker A, Stossel TP. Thrombin receptor ligation and activated Rac uncap actin filament barbed ends through phosphoinositide synthesis in permeabilized human platelets. Cell 1995: 82: 643-653.

Hartwig JH, Shevlin P. The architecture of actin filaments and the ultrastructural location of actin-binding protein in the periphery of lung macrophages. J Cell Biol 1986: 103: 1007-1020.

Hartwig JH, Tyler J, Stossel TP. Actin-binding protein promotes the bipolar and perpendicular branching of actin filaments. J Cell Biol 1980: 87: 841-848.

Hasleton PS, Roberts TE. Adult respiratory distress syndrome - an update. Histopathology 1999: 34: 285-294.

Heiss SG, Cooper JA. Regulation of CapZ, an actin capping protein of chicken muscle, by anionic phospholipids. Biochemistry 1991: 30: 8753-8758.

Hirsch E, Katanaev VL, Garlanda C, Azzolino O, Pirola L, Silengo L, Sozzani S, Mantovani A, Altruda F, Wymann MP. Central role for the G protein-coupled PI3Kgamma in inflammation. Science, in press.

Hofman P, d'Andrea L, Guzman E, Selva E, Le Negrate G, Far DF, Lemichez E, Boquet P, Rossi B. Neutrophil F-actin and myosin but not microtubules functionally regulate transepithelial migration induced by interleukin 8 across a cultured intestinal epithelial monolayer. Eur Cytokine Netw 1999: 10: 227-236.

Howard T, Chaponnier C, Yin H, Stossel T. Gelsolin-actin interaction and actin polymerization in human neutrophils. J Cell Biol 1990: 110: 1983-1991.

Huang R, Lian JP, Robinson D, Badwey JA. Neutrophils stimulated with a variety of chemoattractants exhibit rapid activation of p21-activated kinases (Paks): separate signals are required for activation and inactivation of paks. Mol Cell Biol 1998: 18: 7130-7138.

Hubbard SR. Structural analysis of receptor tyrosine kinases. Prog Biophys Mol Biol 1999: 71: 343-358.

Ihle JN, Witthuhn BA, Quelle FW, Yamamoto K, Silvennoinen O. Signaling through the hematopoietic cytokine receptors. Annu Rev Immunol 1995: 13: 369-398.

Isakoff SJ, Cardozo T, Andreev J, Li Z, Ferguson KM, Abagyan R, Lemmon MA, Aronheim A, Skolnik EY. Identification and analysis of PH domain-containing targets of phosphatidylinositol 3-kinase using a novel in vivo assay in yeast. EMBO J 1998: 17: 5374-5387.

Janmey PA, Iida K, Yin HL, Stossel TP. Polyphosphoinositide micelles and polyphosphoinositide-containing vesicles dissociate endogenous gelsolin-actin complexes and promote actin assembly from the fast-growing end of actin filaments blocked by gelsolin. J Biol Chem 1987: 262: 12228-12236.

Janmey PA. Phosphoinositides and calcium as regulators of cellular actin assembly and disassembly. Annu Rev Physiol 1994: 56: 169-191.

Janmey PA. The cytoskeleton and cell signaling: component localization and mechanical coupling. Physiol Rev 1998: 78: 763-781.

Jiang H, Kuang Y, Wu Y, Xie W, Simon MI, Wu D. Roles of phospholipase C beta2 in chemoattractant-elicited responses. Proc Natl Acad Sci U S A 1997: 94: 7971-7975.

Jin T, Amzel M, Devreotes PN, Wu L. Selection of gbeta subunits with point mutations that fail to activate specific signaling pathways in vivo: dissecting cellular responses mediated by a heterotrimeric G protein in Dictyostelium discoideum. Mol Biol Cell 1998: 9: 2949-2961.

Just I, Selzer J, Hofmann F, Green GA, Aktories K. Inactivation of Ras by Clostridium sordellii lethal toxin-catalyzed glucosylation. J Biol Chem 1996: 271: 10149-10153.

Just I, Selzer J, Wilm M, von Eichel-Streiber C, Mann M, Aktories K. Glucosylation of Rho proteins by Clostridium difficile toxin B. Nature 1995: 375: 500-503.

Katada T, Kurosu H, Okada T, Suzuki T, Tsujimoto N, Takasuga S, Kontani K, Hazeki O, Ui M. Synergistic activation of a family of phosphoinositide 3-kinase via G-protein coupled and tyrosine kinase-related receptors. Chem Phys Lipids 1999: 98: 79-86.

Katan M. Families of phosphoinositide-specific phospholipase C: structure and function. Biochim Biophys Acta 1998: 1436: 5-17.

Katanaev VL, Wymann MP. GTPgammaS-induced actin polymerisation in vitro: ATP- and phosphoinositide-independent signalling via Rho-family proteins and a plasma membrane-associated guanine nucleotide exchange factor. J Cell Sci 1998a: 111: 1583-1594.

Katanaev VL, Wymann MP. Microquantification of cellular and in vitro F-actin by rhodamine phalloidin fluorescence enhancement. Anal Biochem 1998b: 264: 185-190.

Kaukonen J, Lahtinen I, Laine S, Alitalo K, Palotie A. BMX tyrosine kinase gene is expressed in granulocytes and myeloid leukaemias. Br J Haematol 1996: 94: 455-460.

Kent JD, Sergeant S, Burns DJ, McPhail LC. Identification and regulation of protein kinase C-delta in human neutrophils. J Immunol 1996: 157: 4641-4647.

Kimura K, Ito M, Amano M, Chihara K, Fukata Y, Nakafuku M, Yamamori B, Feng J, Nakano T, Okawa K, Iwamatsu A, Kaibuchi K. Regulation of myosin phosphatase by Rho and Rho-associated kinase (Rho-kinase). Science 1996: 273: 245-248.

Kitayama C, Sugimoto A, Yamamoto M. Type II myosin heavy chain encoded by the myo2 gene composes the contractile ring during cytokinesis in Schizosaccharomyces pombe. J Cell Biol 1997: 137: 1309-1319.

Klippel A, Kavanaugh WM, Pot D, Williams LT. A specific product of phosphatidylinositol 3-kinase directly activates the protein kinase Akt through its pleckstrin homology domain. Mol Cell Biol 1997: 17: 338-344.

Knall C, Worthen GS, Johnson GL. Interleukin 8-stimulated phosphatidylinositol-3-kinase activity regulates the migration of human neutrophils independent of extracellular signal-regulated kinase and p38 mitogen-activated protein kinases. Proc Natl Acad Sci U S A 1997: 94: 3052-3057.

Knall C, Young S, Nick JA, Buhl AM, Worthen GS, Johnson GL. Interleukin-8 regulation of the Ras/Raf/mitogen-activated protein kinase pathway in human neutrophils. J Biol Chem 1996: 271: 2832-2838.

Knecht DA, Loomis WF. Antisense RNA inactivation of myosin heavy chain gene expression in Dictyostelium discoideum. Science 1987: 236: 1081-1086.

Kolluri R, Tolias KF, Carpenter CL, Rosen FS, Kirchhausen T. Direct interaction of the Wiskott-Aldrich syndrome protein with the GTPase Cdc42. Proc Natl Acad Sci U S A 1996: 93: 5615-5618.

Korchak HM, Vienne K, Wilkenfeld C, Roberts C, Rich AM, Weissmann G. The first seconds of neutrophil activation: phosphoinositides, protein kinase C, and calcium movements. Trans Assoc Am Physicians 1985: 98: 224-232.

Kozasa T, Jiang X, Hart MJ, Sternweis PM, Singer WD, Gilman AG, Bollag G, Sternweis PC. p115 RhoGEF, a GTPase activating protein for Galpha12 and Galpha13. Science 1998: 280: 2109-2111.

Kozma R, Ahmed S, Best A, Lim L. The Ras-related protein Cdc42Hs and bradykinin promote formation of peripheral actin microspikes and filopodia in Swiss 3T3 fibroblasts. Mol Cell Biol 1995: 15: 1942-1952.

Kozma R, Sarner S, Ahmed S, Lim L. Rho family GTPases and neuronal growth cone remodelling: relationship between increased complexity induced by Cdc42Hs, Rac1, and acetylcholine and collapse induced by RhoA and lysophosphatidic acid. Mol Cell Biol 1997: 17: 1201-1211.

Krugmann S, Hawkins PT, Pryer N, Braselmann S. Characterizing the interactions between the two subunits of the p101/p110gamma phosphoinositide 3-kinase and their role in the activation of this enzyme by G beta gamma subunits. J Biol Chem 1999: 274: 17152-17258.

Kuczmarski ER, Spudich JA. Regulation of myosin self-assembly: phosphorylation of Dictyostelium heavy chain inhibits formation of thick filaments. Proc Natl Acad Sci U S A 1980: 77: 7292-7296.

Kureishi Y, Kobayashi S, Amano M, Kimura K, Kanaide H, Nakano T, Kaibuchi K, Ito M.Rho-associated kinase directly induces smooth muscle contraction through myosin light chain phosphorylation. J Biol Chem 1997: 272: 12257-12260.

Kurokawa H, Fujii W, Ohmi K, Sakurai T, Nonomura Y. Simple and rapid purification of brevin. Biochem Biophys Res Commun 1990: 168: 451-457.

Kwiatkowska K, Sobota A. Signaling pathways in phagocytosis. Bioessays 1999: 21: 422-431.

Lad PM, Olson CV, Grewal IS. A step sensitive to pertussis toxin and phorbol ester in human neutrophils regulates chemotaxis and capping but not phagocytosis. FEBS Lett 1986: 200: 91-96.

Langhans-Rajasekaran SA, Wan Y, Huang XY. Activation of Tsk and Btk tyrosine kinases by G protein beta gamma subunits. Proc Natl Acad Sci U S A 1995: 92: 8601-8605.

Laudanna C, Campbell JJ, Butcher EC. Role of Rho in chemoattractant-activated leukocyte adhesion through integrins. Science 1996: 271: 981-983.

Laudanna C, Mochly-Rosen D, Liron T, Constantin G, Butcher EC. Evidence of zeta protein kinase C involvement in polymorphonuclear neutrophil integrin-dependent adhesion and chemotaxis. J Biol Chem 1998: 273: 30306-30315.

Le Good JA, Ziegler WH, Parekh DB, Alessi DR, Cohen P, Parker PJ. Protein kinase C isotypes controlled by phosphoinositide 3-kinase through the protein kinase PDK1. Science 1998: 281: 2042-2045.

Lefkowith JB. Leukocyte migration in immune complex glomerulonephritis: role of adhesion receptors. Kidney Int 1997: 51: 1469-1475.

Lemmon MA. Structural basis for high-affinity phosphoinositide binding by pleckstrin homology domains. Biochem Soc Trans 1999: 27: 617-624.

Leopoldt D, Hanck T, Exner T, Maier U, Wetzker R, Nurnberg B. Gbetagamma stimulates phosphoinositide 3-kinase-gamma by direct interaction with two domains of the catalytic p110 subunit. J Biol Chem 1998: 273: 7024-7029.

Lipnick RN, Iliopoulos A, Salata K, Hershey J, Melnick D, Tsokos GC. Leukocyte adhesion deficiency: report of a case and review of the literature. Clin Exp Rheumatol 1996: 14: 95-98.

Lodi PJ, Garrett DS, Kuscewski J, Tsang MLS, Weatherbee JA, Leonard WJ, Gronenborn AM, Clore GM. High-resolution solution structure of the beta chemokine hMIP-1 beta by multidimensional NMR. Science 1994: 263: 1762-1767.

Loike JD, el Khoury J, Cao L, Richards CP, Rascoff H, Mandeville JT, Maxfield FR, Silverstein SC. Fibrin regulates neutrophil migration in response to interleukin 8, leukotriene B4, tumor necrosis factor, and formyl-methionyl-leucyl-phenylalanine. J Exp Med 1995: 181: 1763-1772.

Lopez-Ilasaca M, Crespo P, Pellici PG, Gutkind JS, Wetzker R. Linkage of G protein-coupled receptors to the MAPK signaling pathway through PI 3-kinase gamma. Science 1997: 275: 394-397.

Lopez-Ilasaca M, Kular GS, Slupsky JR, Weber CK, Bondeva T, Rapp UR, Wetzker R. Phosphoinositide 3-kinase gamma acts as a scaffold for proteins of the MAP kinase cascade. Submitted.

Lukacs NW, Strieter RM, Chensue SW, Widmer M, Kunkel SL. TNF-alpha mediates recruitment of neutrophils and eosinophils during airway inflammation. J Immunol 1995: 154: 5411-5417.

Ma AD, Metjian A, Bagrodia S, Taylor S, Abrams CS. Cytoskeletal reorganization by G protein-coupled receptors is dependent on phosphoinositide 3-kinase gamma, a Rac guanosine exchange factor, and Rac. Mol Cell Biol 1998: 18: 4744-4751.

Ma L, Cantley LC, Janmey PA, Kirschner MW. Corequirement of specific phosphoinositides and small GTP-binding protein Cdc42 in inducing actin assembly in Xenopus egg extracts. J Cell Biol 1998: 140: 1125-1136.

Ma L, Rohatgi R, Kirschner MW. The Arp2/3 complex mediates actin polymerization induced by the small GTP-binding protein Cdc42. Proc Natl Acad Sci U S A 1998: 95: 15362-15367.

Machesky LM, Atkinson SJ, Ampe C, Vandekerckhove J, Pollard TD. Purification of a cortical complex containing two unconventional actins from Acanthamoeba by affinity chromatography on profilin-agarose. J Cell Biol 1994: 127: 107-115.

Machesky LM, Insall RH. Scar1 and the related Wiskott-Aldrich syndrome protein, WASP, regulate the actin cytoskeleton through the Arp2/3 complex. Curr Biol 1998: 8: 1347-1356.

Machesky LM, Mullins RD, Higgs HN, Kaiser DA, Blanchoin L, May RC, Hall ME, Pollard TD. Scar, a WASp-related protein, activates nucleation of actin filaments by the Arp2/3 complex. Proc Natl Acad Sci U S A 1999: 96: 3739-3744.

Machesky LM, Reeves E, Wientjes F, Mattheyse FJ, Grogan A, Totty NF, Burlingame AL, Hsuan JJ, Segal AW. Mammalian actin-related protein 2/3 complex localizes to regions of lamellipodial protrusion and is composed of evolutionarily conserved proteins. Biochem J 1997: 328: 105-112.

Maciver SK, Zot HG, Pollard TD. Characterization of actin filament severing by actophorin from Acanthamoeba castellanii. J Cell Biol 1991: 115: 1611-1620.

MacLean-Fletcher S, Pollard TD. Identification of a factor in conventional muscle actin preparations which inhibits actin filament self-association. Biochem Biophys Res Commun 1980: 96: 18-27.

Maekawa M, Ishizaki T, Boku S, Watanabe N, Fujita A, Iwamatsu A, Obinata T, Ohashi K, Mizuno K, Narumiya S. Signaling from Rho to the actin cytoskeleton through protein kinases ROCK and LIM-kinase. Science 1999: 285: 895-898.

Mahadevan D, Thanki N, Singh J, McPhie P, Zangrilli D, Wang LM, Guerrero C, LeVine H 3rd, Humblet C, Saldanha J, et al. Structural studies on the PH domains of Db1, Sos1, IRS-1, and beta ARK1 and their differential binding to G beta gamma subunits. Biochemistry 1995: 34: 9111-9117.

Malumbres M, Mangues R, Ferrer N, Lu S, Pellicer A. Isolation of high molecular weight DNA for reliable genotyping of transgenic mice. Biotechniques 1997: 22: 1114-1119.

Mangeat P, Roy C, Martin M. ERM proteins in cell adhesion and membrane dynamics. Trends Cell Biol. 1999: 9: 187-192.

Mano H, Ishikawa F, Nishida J, Hirai H, Takaku F. A novel protein-tyrosine kinase, tec, is preferentially expressed in liver. Oncogene 1990: 5: 1781-1786.

Mellor H, Parker PJ. The extended protein kinase C superfamily. Biochem J 1998: 332: 281-292.

Menegazzi R, Cramer R, Patriarca P, Scheurich P, Dri P. Evidence that tumor necrosis factor alpha (TNF)-induced activation of neutrophil respiratory burst on biologic surfaces is mediated by the p55 TNF receptor. Blood 1994: 84: 287-293.

Mery L, Boulay F. The NH2-terminal region of C5aR but not that of FPR is critical for both protein transport and ligand binding. J Biol Chem 1994: 269: 3457-3463.

Michiels F, Stam JC, Hordijk PL, van der Kammen RA, Ruuls-Van Stalle L, FeltkampCA, Collard JG. Regulated membrane localization of Tiam1, mediated by the NH2-terminal pleckstrin homology domain, is required for Rac-dependent membrane ruffling and C-Jun NH2-terminal kinase activation. J Cell Biol 1997: 137: 387-398.

Miki H, Miura K, Takenawa T. N-WASP, a novel actin-depolymerizing protein, regulates the cortical cytoskeletal rearrangement in a PIP2-dependent manner downstream of tyrosine kinases. EMBO J 1996: 15: 5326-5335.

Miki H, Sasaki T, Takai Y, Takenawa T. Induction of filopodium formation by a WASP-related actin-depolymerizing protein N-WASP. Nature 1998: 391: 93-96.

Miki H, Suetsugu S, Takenawa T. WAVE, a novel WASP-family protein involved in actin reorganization induced by Rac. EMBO J 1998b: 17: 6932-6941.

Ming WJ, Bersani L, Mantovani A. Tumor necrosis factor is chemotactic for monocytes and polymorphonuclear leukocytes. J. Immunol 1987: 138:1469-1474.

Monteclaro FS, Charo IF. The amino-terminal extracellular domain of the MCP-1 receptor, but not the RANTES/MIP-1alpha receptor, confers chemokine selectivity. Evidence for a two-step mechanism for MCP-1 receptor activation. J Biol Chem 1996: 271: 19084-19092.

Moreau V, Way M. Cdc42 is required for membrane dependent actin polymerization in vitro. FEBS Lett 1998: 427: 353-356.

Moriyama K, Iida K, Yahara I. Phosphorylation of Ser-3 of cofilin regulates its essential function on actin. Genes Cells 1996: 1: 73-86.

Moser B, Loetscher M, Piali L, Loetscher P. Lymphocyte responses to chemokines. Int Rev Immunol 1998: 16: 323-344.

Mrowietz U, Ternowitz T, Schroder JM, Christophers E. Recombinant human tumour necrosis factor beta (lymphotoxin) lacks chemotactic activity for human peripheral blood neutrophils, monocytes, and T cells. Scand J Immunol 1989: 30: 373-377.

Mullins RD, Heuser JA, Pollard TD. The interaction of Arp2/3 complex with actin: nucleation, high affinity pointed end capping, and formation of branching networks of filaments. Proc Natl Acad Sci U S A 1998b: 95: 6181-6186.

Mullins RD, Kelleher JF, Xu J, Pollard TD. Arp2/3 complex from Acanthamoeba binds profilin and cross-links actin filaments. Mol Biol Cell 1998a: 9: 841-852.

Mullins RD, Pollard TD. Rho-family GTPases require the Arp2/3 complex to stimulate actin polymerizationin Acanthamoeba extracts. Curr Biol 1999: 9: 405-415.

Mullins RD, Stafford WF, Pollard TD. Structure, subunit topology, and actin-binding activity of the Arp2/3 complex from Acanthamoeba. J Cell Biol 1997: 136: 331-343.

Murphy PM. The molecular biology of leukocyte chemoattractant receptors. Annu Rev Immunol 1994: 12: 593-633.

Nagase T, Seki N, Ishikawa K, Ohira M, Kawarabayasi Y, Ohara O, Tanaka A, Kotani H, Miyajima N, Nomura N. Prediction of the coding sequences of unidentified human genes. VI. The coding sequences of 80 new genes (KIAA0201-KIAA0280) deduced by analysis of cDNA clones from cell line KG-1 and brain. DNA Res 1996: 3: 321-329.

Neet K, Hunter T. Vertebrate non-receptor protein-tyrosine kinase families. Genes Cells 1996: 1: 147-169.

Neptune ER, Bourne HR. Receptors induce chemotaxis by releasing the betagamma subunit of Gi, not by activating Gq or Gs. Proc Natl Acad Sci U S A 1997: 94: 14489-14494.

Neptune ER, Iiri T, Bourne HR. Galphai is not required for chemotaxis mediated by Gi-coupled receptors. J Biol Chem 1999: 274: 2824-2828.

Nern A, Arkowitz RA. A GTP-exchange factor required for cell orientation. Nature 1998: 391: 195-198.

Newman I, Wilkinson PC. Chemotactic activity of lymphotoxin and tumour necrosis factor alpha for human neutrophils. Immunology 1989: 66: 318-320.

Niggli V, Keller H. Inhibition of chemotactic peptide-induced development of cell polarity and locomotion by the protein kinase C inhibitor CGP 41 251 in human neutrophils correlates with inhibition of protein phosphorylation. Exp Cell Res 1993: 204: 346-355.

Niggli V, Keller H. On the role of protein kinases in regulating neutrophil actin association with the cytoskeleton. J Biol Chem 1991: 266: 7927-7932.

Niggli V, Keller H. The phosphatidylinositol 3-kinase inhibitor wortmannin markedly reduces chemotactic peptide-induced locomotion and increases in cytoskeletal actin in human neutrophils. Eur J Pharmacol 1997: 335: 43-52.

Niggli V. Rho-kinase in human neutrophils: a role in signalling for myosin light chain phosphorylation and cell migration. FEBS Lett 1999: 445: 69-72.

Nishida K, Kaziro Y, Satoh T. Association of the proto-oncogene product Dbl with G protein betagamma subunits. FEBS Lett 1999: 459: 186-190.

Nobes CD, Hall A. Rho, rac, and cdc42 GTPases regulate the assembly of multimolecular focal complexes associated with actin stress fibers, lamellipodia, and filopodia. Cell 1995: 81: 53-62.

Norman JC, Price LS, Ridley AJ, Hall A, Koffer A. Actin filament organization in activated mast cells is regulated by heterotrimeric and small GTP-binding proteins. J Cell Biol 1994: 126: 1005-1015.

Oldenborg PA, Sehlin J. Insulin-stimulated chemokinesis in normal human neutrophils is dependent on D-glucose concentration and sensitive to inhibitors of tyrosine kinase and phosphatidylinositol 3-kinase. J Leukoc Biol 1998: 63: 203-208.

Olofsson B. Rho guanine dissociation inhibitors: pivotal molecules in cellular signalling. Cell Signal 1999: 11: 545-554.

Olson MF, Sterpetti P, Nagata K, Toksoz D, Hall A. Distinct roles for DH and PH domains in the Lbc oncogene. Oncogene 1997: 15: 2827-2831.

Ottonello L, Tortolina G, Amelotti M, Dallegri F. Soluble Fas ligand is chemotactic for human neutrophilic polymorphonuclear leukocytes. J Immunol 1999: 162: 3601-3606.

Panaro MA, Mitolo V. Cellular responses to FMLP challenging: a mini-review. Immunopharmacol Immunotoxicol 1999: 21: 397-419.

Pardee JD, Spudich JA. Purification of muscle actin. Methods Enzymol 1982: 85: 164-181.

Parent CA, Devreotes PN. A cell's sense of direction. Science 1999: 284: 765-770.

Parent JL, Le Gouill C, Rola-Pleszczynski M, Stankova J. Mutation of an aspartate at position 63 in the human platelet-activating factor receptor augments binding affinity but abolishes G-protein-coupling and inositol phosphate production. Biochem Biophys Res Commun 1996: 219: 968-975.

Park D, Jhon DY, Kriz R, Knopf J, Rhee SG. Cloning, sequencing, expression, and Gq-independent activation of phospholipase C-beta 2. J Biol Chem 1992: 267: 16048-16055.

Peppelenbosch M, Boone E, Jones GE, van Deventer SJ, Haegeman G, Fiers W, Grooten J, Ridley AJ. Multiple signal transduction pathways regulate TNF-induced actin reorganization in macrophages: inhibition of Cdc42-mediated filopodium formation by TNF. J Immunol 1999: 162: 837-845.

Perez HD, Elfman F, Marder S, Lobo E, Ives HE. Formyl peptide-induced chemotaxis of human polymorphonuclear leukocytes does not require either marked changes in cytosolic calcium or specific granule discharge. Role of formyl peptide receptor reexpression (or recycling). J Clin Invest 1989: 83: 1963-1970.

Pollard TD, Cooper JA. Actin and actin-binding proteins. A critical evaluation of mechanisms and functions. Annu Rev Biochem 1986: 55: 987-1035.

Quehenberger O, Pan ZK, Prossnitz ER, Cavanagh SL, Cochrane CG, Ye RD. Identification of an N-formyl peptide receptor ligand binding domain by again-of-function approach. Biochem Biophys Res Commun 1997: 238: 377-381.

Quinn MT, Evans T, Loetterle LR, Jesaitis AJ, Bokoch GM. Translocation of Rac correlates with NADPH oxidase activation. Evidence for equimolar translocation of oxidase components. J Biol Chem 1993: 268: 20983-20987.

Rameh LE, Arvidsson Ak, Carraway KL 3rd, Couvillon AD, Rathbun G, Crompton A, VanRenterghem B, Czech MP, Ravichandran KS, Burakoff SJ, Wang DS, Chen CS, Cantley LC. A comparative analysis of the phosphoinositide binding specificity of pleckstrin homology domains. J Biol Chem 1997: 272: 22059-22066.

Rameh LE, Arvidsson Ak, Carraway KL 3rd, Couvillon AD, Rathbun G, Crompton A, VanRenterghem B, Czech MP, Ravichandran KS, Burakoff SJ, Wang DS, Chen CS, Cantley LC. A comparative analysis of the phosphoinositide binding specificity of pleckstrin homology domains. J Biol Chem 1997: 272: 22059-22066.

Rebecchi MJ, Scarlata S. Pleckstrin homology domains: a common fold with diverse functions. Annu Rev Biophys Biomol Struct 1998: 27: 503-528.

Redmond T, Tardif M, Zigmond SH. Induction of actin polymerization in permeabilized neutrophils. Role of ATP. J Biol Chem 1994: 269: 21657-21663.

Reibman J, Meixler S, Lee TC, Gold LI, Cronstein BN, Haines KA, Kolasinski SL, Weissmann G. Transforming growth factor beta 1, a potent chemoattractant for human neutrophils, bypasses classic signal-transduction pathways.Proc Natl Acad Sci U S A 1991: 88: 6805-6809.

Reif K, Cantrell DA. Networking Rho family GTPases in lymphocytes. Immunity 1998: 8: 395-401.

Ren XD, Bokoch GM, Traynor-Kaplan A, Jenkins GH, Anderson RA, Schwartz MA. Physical association of the small GTPase Rho with a 68-kDa phosphatidylinositol 4-phosphate 5-kinase in Swiss 3T3 cells. Mol Biol Cell 1996: 7: 435-442.

Rengan R, Omann GM. Regulation of oscillations in filamentous actin content in polymorphonuclear leukocytes stimulated with leukotriene B(4) and platelet-activating factor. Biochem Biophys Res Commun 1999: 262: 479-486.

Ridley AJ, Comoglio PM, Hall A. Regulation of scatter factor/hepatocyte growth factor responses by Ras, Rac, and Rho in MDCK cells. Mol Cell Biol 1995: 15: 1110-1122.

Ridley AJ, Hall A. Signal transduction pathways regulating Rho-mediated stress fibre formation: requirement for a tyrosine kinase. EMBO J 1994: 13: 2600-2610.

Ridley AJ, Hall A. The small GTP-binding protein rho regulates the assembly of focal adhesions and actin stress fibers in response to growth factors. Cell 1992: 70: 389-399.

Ridley AJ, Paterson HF, Johnston CL, Diekmann D, Hall A. The small GTP-binding protein rac regulates growth factor-induced membrane ruffling. Cell 1992: 70: 401-410.

Ridley AJ. Rho family proteins and regulation of the actin cytoskeleton. Prog Mol Subcell Biol 1999: 22: 1-22.

Roberts AW, Kim C, Zhen L, Lowe JB, Kapur R, Petryniak B, Spaetti A, Pollock JD, Borneo JB, Bradford GB, Atkinson SJ, Dinauer MC, Williams DA. Deficiency of the hematopoietic cell-specific Rho family GTPase Rac2 is characterized by abnormalities in neutrophil function and host defense. Immunity 1999: 10: 183-196.

Rohatgi R, Ma L, Miki H, Lopez M, Kirchhausen T, Takenawa T, Kirschner MW. The interaction between N-WASP and the Arp2/3 complex links Cdc42-dependent signals to actin assembly. Cell 1999: 97: 221-231.

Rubio I, Rodriguez-Viciana P, Downward J, Wetzker R. Interaction of Ras with phosphoinositide 3-kinase gamma. Biochem J 1997: 326: 891-895.

Sanchez-Madrid F, del Pozo MA. Leukocyte polarization in cell migration and immune interactions. EMBO J 1999: 18: 501-511.

Sanders LC, Matsumura F, Bokoch GM, de Lanerolle P. Inhibition of myosin light chain kinase by p21-activated kinase. Science 1999: 283: 2083-2085.

Sasaki T, Kato M, Takai Y. Consequences of weak interaction of rho GDI with the GTP-bound forms of rho p21 and rac p21. J Biol Chem 1993: 268: 23959-23963.

Satterthwaite AB, Li Z, Witte ON. Btk function in B cell development and response. Semin Immunol 1998: 10: 309-316.

Savage COS, Rees AJ. Role of neutrophils in vasculitis. In: Hellewell PG, Williams TJ, eds. Immunopharmacology of neutrophils. London: Academic Press, 1994: 259-273.

Scheer A, Fanelli F, Costa T, De Benedetti PG, Cotecchia S. Constitutively active mutants of the alpha 1B-adrenergic receptor: role of highly conserved polar amino acids in receptor activation. EMBO J 1996: 15: 3566-3578.

Schreiber RE, Prossnitz ER, Ye RD, Cochrane CG, Bokoch GM. Domains of the human neutrophil N-formyl peptide receptor involved in G protein coupling. Mapping with receptor-derived peptides. J Biol Chem 1994: 269: 326-331.

Scita G, Nordstrom J, Carbone R, Tenca P, Giardina G, Gutkind S, Bjarnegard M, Betsholtz C, Di Fiore PP. EPS8 and E3B1 transduce signals from Ras to Rac. Nature 1999: 401: 290-293.

Segal AW, Shatwell KP. The NADPH oxidase of phagocytic leukocytes. Ann N Y Acad Sci 1997: 832: 215-222.

Seino K, Iwabuchi K, Kayagaki N, Miyata R, Nagaoka I, Matsuzawa A, Fukao K, Yagita H, Okumura K. Chemotactic activity of soluble Fas ligand against phagocytes. J Immunol 1998: 161: 4484-4488.

Self AJ, Hall A. Measurement of intrinsic nucleotide exchange and GTP hydrolysis rates. Methods Enzymol 1995: 256: 67-76.

Shaw G. The pleckstrin homology domain: an intriguing multifunctional protein module. Bioessays 1996: 18: 35-46.

Shibasaki Y, Ishihara H, Kizuki N, Asano T, Oka Y, Yazaki Y. Massive actin polymerization induced by phosphatidylinositol-4-phosphate 5-kinase in vivo. J Biol Chem 1997: 272: 7578-7581.

Sievers EL, Dale DC. Non-malignant neutropenia. Blood Rev 1996: 10: 95-100.

Smith WB, Gamble JR, Vadas MA. The role of granulocyte-macrophage and granulocyte colony-stimulating factors in neutrophil transendothelial migration: comparison with interleukin-8. Exp Hematol 1994: 22: 329-334.

Snapper SB, Rosen FS. The Wiskott-Aldrich syndrome protein (WASP): roles in signaling and cytoskeletal organization. Annu Rev Immunol 1999: 17: 905-929.

Springer TA. Traffic signals on endothelium for lymphocyte recirculation and leukocyte emigration. Annu Rev Physiol 1995: 57:827-872.

Stasia MJ, Jouan A, Bourmeyster N, Boquet P, Vignais PV. ADP-ribosylation of a small size GTP-binding protein in bovine neutrophils by the C3 exoenzyme of Clostridium botulinum and effect on the cell motility. Biochem Biophys Res Commun 1991: 180: 615-622.

Stasia MJ, Strulovici B, Daniel-Issakani S, Pelosin JM, Dianoux AC, Chambaz E, Vignais PV. Immunocharacterization of beta- and zeta-subspecies of protein kinase C in bovine neutrophils. FEBS Lett 1990: 274: 61-64.

Stephens L, Anderson K, Stokoe D, Erdjument-Bromage H, Painter GF, Holmes AB, Gaffney PR, Reese CB, McCormick F, Tempst P, Coadwell J, Hawkins PT. Protein kinase B kinases that mediate phosphatidylinositol 3,4,5-trisphosphate-dependent activation of protein kinase B. Science 1998: 279: 710-714.

Stephens L, Smrcka A, Cooke FT, Jackson TR, Sternweis PC, Hawkins PT. A novel phosphoinositide 3 kinase activity in myeloid-derived cells is activated by G protein beta gamma subunits. Cell 1994: 77: 83-93.

Stephens LR, Eguinoa A, Erdjument-Bromage H, Lui M, Cooke F, Coadwell J, Smrcka AS, Thelen M, Cadwallader K, Tempst P, Hawkins PT. The G beta gamma sensitivity of a PI3K is dependent upon a tightly associated adaptor, p101. Cell 1997: 89: 105-114.

Stoyanov B, Volinia S, Hanck T, Rubio I, Loubtchenkov M, Malek D, Stoyanova S, Vanhaesebroeck B, Dhand R, Nurnberg B, Gierschik P, Seedorf K, Hsuan JJ, Waterfield MD, Wetzker R. Cloning and characterization of a G protein activated human phosphoinositide-3 kinase. Science 1995: 269: 690-693.

Stoyanova S, Bulgarelli-Leva G, Kirsch C, Hanck T, Klinger R, Wetzker R, Wymann MP. Lipid kinase and protein kinase activities of G-protein-coupled phosphoinositide 3-kinase gamma: structure-activity analysis and interactions with wortmannin. Biochem J 1997: 324: 489-495.

Suetsugu S, Miki H, Takenawa T. Identification of two human WAVE/SCAR homologues as general actin regulatory molecules which associate with the Arp2/3 complex. Biochem Biophys Res Commun 1999: 260: 296-302.

Svitkina TM, Borisy GG. Arp2/3 complex and actin depolymerizing factor/cofilin in dendritic organization and treadmilling of actin filament array in lamellipodia. J Cell Biol 1999: 145: 1009-1026.

Symons M, Derry JM, Karlak B, Jiang S, Lemahieu V, Mccormick F, Francke U, Abo A. Wiskott-Aldrich syndrome protein, a novel effector for the GTPase CDC42Hs, is implicated in actin polymerization. Cell 1996: 84: 723-734.

Symons M. Rho family GTPases: the cytoskeleton and beyond. Trends Biochem Sci 1996: 21: 178-181.

Takahashi K, Sasaki T, Mammoto A, Takaishi K, Kameyama T, Tsukita S, Takai Y. Direct interaction of the Rho GDP dissociation inhibitor with ezrin/radixin/moesin initiates the activation of the Rho small G protein. J Biol Chem 1997: 272: 23371-23375.

Takubo T, Tatsumi N. Distribution of myosin and actin in moving human neutrophils detected by double-fluorescence staining. Anal Quant Cytol Histol 1997: 19: 233-238.

Tan JL, Ravid S, Spudich JA. Control of nonmuscle myosins by phosphorylation. Annu Rev Biochem 1992: 61: 721-759.

Tarr PE. Granulocyte-macrophage colony-stimulating factor and the immune system. Med Oncol 1996: 13: 133-140.

Thelen M, Uguccioni M, Bosiger J. PI 3-kinase-dependent and independent chemotaxis of human neutrophil leukocytes. Biochem Biophys Res Commun 1995: 217: 1255-1262.

Therrien S, Naccache PH. Guanine nucleotide-induced polymerization of actin in electropermeabilized human neutrophils. J Cell Biol 1989: 109: 1125-1132.

Thrasher AJ, Keep NH, Wientjes F, Segal AW. Chronic granulomatous disease. Biochim Biophys Acta 1994: 1227: 1-24.

Tolias KF, Cantley LC, Carpenter CL. Rho family GTPases bind to phosphoinositide kinases. J Biol Chem 1995: 270: 17656-17659.

Tolias KF, Couvillon AD, Cantley LC, Carpenter CL. Characterization of a Rac1- and RhoGDI-associated lipid kinase signaling complex. Mol Cell Biol 1998: 18: 762-770.

Tsukada S, Simon MI, Witte ON, Katz A. Binding of beta gamma subunits of heterotrimeric G proteins to the PH domain of Bruton tyrosine kinase. Proc Natl Acad Sci U S A 1994: 91: 11256-11260.

Unger VM, Hargrave PA, Baldwin JM, Schertler GF. Arrangement of rhodopsin transmembrane alpha-helices. Nature 1997: 389: 203-206.

Valerius NH, Stendahl O, Hartwig JH, Stossel TP. Distribution of actin-binding protein and myosin in polymorphonuclear leukocytes during locomotion and phagocytosis. Cell 1981: 24: 195-202.

Van Aelst L, D'Souza-Schorey C. Rho GTPases and signaling networks. Genes Dev 1997: 11: 2295-2322.

Van Aelst L, D'Souza-Schorey C. Rho GTPases and signaling networks. Genes Dev 1997: 11: 2295-2322.

Vicente-Manzanares M, Rey M, Jones DR, Sancho D, Mellado M, Rodriguez-Frade JM, del Pozo MA, Yanez-Mo M, de Ana AM, Martinez-A C, Merida I, Sanchez-Madrid F. Involvement of phosphatidylinositol 3-kinase in stromal cell-derived factor-1 alpha-induced lymphocyte polarization and chemotaxis. J Immunol 1999: 163: 4001-4012.

Virchow S, Ansorge N, Rosskopf D, Rubben H, Siffert W. The G protein beta3 subunit splice variant Gbeta3-s causes enhanced chemotaxis of human neutrophils in response to interleukin-8. Naunyn Schmiedebergs Arch Pharmacol 1999: 360: 27-32.

Wallach D, Varfolomeev EE, Malinin NL, Goltsev YV, Kovalenko AV, Boldin MP. Tumor necrosis factor receptor and Fas signaling mechanisms. Annu Rev Immunol 1999: 17: 331-367.

Wang T, Pentyala S, Rebecchi MJ, Scarlata S. Differential association of the pleckstrin homology domains of phospholipases C-beta 1, C-beta 2, and C-delta 1 with lipid bilayers and the beta gamma subunits of heterotrimeric G proteins. Biochemistry 1999: 38: 1517-1524.

Warrick HM, Spudich JA. Myosin structure and function in cell motility. Annu Rev Cell Biol 1987: 3: 379-421.

Watt SM, Burgess AW, Metcalf D. Isolation and surface labeling of murine polymorphonuclear neutrophils. J Cell Physiol 1979: 100: 1-21.

Weil D, Power MA, Smith SI, Li CL. Predominant expression of murine Bmx tyrosine kinase in the granulo-monocytic lineage. Blood 1997: 90: 4332-4340.

Welch MD, Iwamatsu A, Mitchison TJ. Actin polymerization is induced by Arp2/3 protein complex at the surface of Listeria monocytogenes. Nature 1997: 385: 265-269.

Welch MD, Rosenblatt J, Skoble J, Portnoy DA, Mitchison TJ. Interaction of human Arp2/3 complex and the Listeria monocytogenes ActA protein in actin filament nucleation. Science 1998: 281: 105-108.

Williams FM. Role of neutrophils in reperfusion injury. In: Hellewell PG, Williams TJ, eds. Immunopharmacology of neutrophils. London: Academic Press, 1994: 245-257.

Williamson MP, Madison VS. Three-dimentional structure of porcine C5adesArg from 1H nuclear magnetic resonance data. Biochemistry 1990: 29: 2895-2905.

Winkler J, Lunsdorf H, Jockusch BM. Flexibility and fine structure of smooth-muscle alpha-actinin. Eur J Biochem 1997: 248: 193-199.

Winter D, Podtelejnikov AV, Mann M, Li R. The complex containing actin-related proteins Arp2 and Arp3 is required for the motility and integrity of yeast actin patches. Curr Biol 1997: 7: 519-529.

Worthen GS, Schwab B 3d, Elson EL, Downey GP. Mechanics of stimulated neutrophils: cell stiffening induces retention in capillaries. Science 1989: 245: 183-186.

Wu D, LaRosa GJ, Simon MI. G protein-coupled signal transduction pathways for interleukin-8. Science 1993: 261: 101-103.

Wymann MP, Bulgarelli-Leva G, Zvelebil MJ, Pirola L, Vanhaesebroeck B, Waterfield MD, Panayotou G. Wortmannin inactivates phosphoinositide 3-kinase by covalent modification of Lys-802, a residue involved in the phosphate transfer reaction. Mol Cell Biol 1996: 16: 1722-1733.

Wymann MP, Kernen P, Bengtsson T, Andersson T, Baggiolini M, Deranleau DA. Corresponding oscillations in neutrophil shape and filamentous actin content. J Biol Chem 1990: 265: 619-622.

Wymann MP, Kernen P, Deranleau DA, Dewald B, von Tscharner V, Baggiolini M. Oscillatory motion in human neutrophils responding to chemotactic stimuli. Biochem Biophys Res Commun 1987: 147: 361-368.

Wymann MP, Pirola L, Katanaev VL, Bulragelli-Leva G. Phosphoinositide 3-kinase signalling - no lipids. Biochem Soc Trans 1999: 27: 629.

Wymann MP, Pirola L. Structure and function of phosphoinositide 3-kinases. Biochim Biophys Acta 1998: 1436: 127-150.

Wymann MP, von Tscharner V, Deranleau DA, Baggiolini M. Chemiluminescence detection of H2O2 produced by human neutrophils during the respiratory burst. Anal Biochem 1987: 165: 371-378.

Xiao YQ, Minami K, Mue S, Ohuchi K. Pharmacological analysis of protein kinases responsible for chemotaxis of rat peritoneal neutrophils. Eur J Pharmacol 1998: 360: 195-204.

Xie W, Jiang H, Wu Y, Wu D. Two basic amino acids in the second inner loop of the interleukin-8 receptor are essential for Galpha16 coupling. J Biol Chem 1997: 272: 24948-24951.

Yang N, Higuchi O, Ohashi K, Nagata K, Wada A, Kangawa K, Nishida E, Mizuno K. Cofilin phosphorylation by LIM-kinase 1 and its role in Rac-mediated actin reorganization. Nature 1998: 393: 809-812.

Yarar D, To W, Abo A, Welch MD. The Wiskott-Aldrich syndrome protein directs actin-based motility by stimulating actin nucleation with the Arp2/3 complex. Curr Biol 1999: 9: 555-558.

Yasui K, Yamazaki M, Miyabayashi M, Tsuno T, Komiyama A. Signal transduction pathway in human polymorphonuclear leukocytes for chemotaxis induced by a

chemotactic factor. Distinct from the pathway for superoxide anion production. J Immunol 1994: 152: 5922-5929.

Yong KL. Granulocyte colony-stimulating factor (G-CSF) increases neutrophil migration across vascular endothelium independent of an effect on adhesion: comparison with granulocyte-macrophage colony-stimulating factor (GM-CSF). Br J Haematol 1996: 94: 40-47.

Zheng Y, Zangrilli D, Cerione RA, Eva A. The pleckstrin homology domain mediates transformation by oncogenic dbl through specific intracellular targeting. J Biol Chem 1996: 271: 19017-19020.

Zhong Q, Iniiss D, Elings VB. Surf. Sci. 1993: 290: L688-L692.

Zicha D, Allen WE, Brickell PM, Kinnon C, Dunn GA, Jones GE, Thrasher AJ. Chemotaxis of macrophages is abolished in the Wiskott-Aldrich syndrome. Br J Haematol 1998: 101: 659-665.

Zigmond SH, Hirsch JG. Effects of cytochalasin B on polymorphonuclear leucocyte locomotion, phagocytosis and glycolysis. Exp Cell Res 1972: 73: 383-393.

Zigmond SH, Joyce M, Borleis J, Bokoch GM, Devreotes PN. Regulation of actin polymerization in cell-free systems by GTPgammaS and Cdc42. J Cell Biol 1997: 138: 363-374.

CURRICULUM VITAE

BIOGRAPHICAL DATA

Born 19.07.1973 in Krasnoyarsk, USSR, Russian citizen, married on Katanayeva Natalya, one child- Leonid.

Languages: Fluent in Russian, English, French.

EDUCATION, PROFESSIONAL EXPERIENCE

1980 - 1990	Krasnoyarsk secondary school; first-grade diploma, May 1990.
1990 - 1994	Biological faculty of Krasnoyarsk State University. University council studentship. The whole 5-year course of studies completed in 4 years. First-grade diploma in biochemistry, June 1994.
1992 - 1995	Institute of Protein Research, Russian Academy of Sciences, Pushchino, Moscow Region. Series of lectures and a set of practical courses organized by Pushchino Branch of Moscow State University and the Institute of Protein Research; honored certificate. Scientific research, advisor: Prof. A.S. Spirin. Subject: regulation of phage Qbeta RNA translation and replication in vitro. International Science Foundation studentship.
1995(June-Dec.)	Institute of Biochemical Engineering, Stuttgart University, Germany. Advisor: Dr. M. Siemann. Project (joint with the Institute of Protein Research and Boehringer Mannheim): biochemical engineering of cell-free translation systems.
1995-present	Ph.D. studies, Institute of Biochemistry, University of Fribourg. Advisor: Dr. M.P. Wymann. Project: Regulation of actin rearrangements and PI3-kinase signalling in blood cells.

ADDITIONAL TRAINING

1. Practical course "Rapid purification of proteins", IIIe Cycle Romand en Sciences Biologiques, June 16-20, 1997, Neuchatel, Switzerland.

2. Practical course "Protein separated by 2D-gel electrophoresis: characterisation by chemical sequencing and mass spectrometry", IIIe Cycle Romand en Sciences Biologiques, October 6-10, 1997, Geneve, Switzerland.

3. Practical course "Introduction to sequence analysis: survival skills in the era of genome sequencing", IIIe Cycle Romand en Sciences Biologiques, September 7-11, 1998, Lausanne, Switzerland.

PROFESSIONAL ORGANIZATIONS

Swiss Society for Biochemistry

Union for Swiss Societies for Experimental Biology

TEACHING

| 1996 | Practicals in Biochemistry, 2nd year medical students, 1 afternoon/ week. |
| 1996- present | Advanced Practical Courses in Biochemistry, 3rd year biochemistry students, "Purification of Proteins". |

PRESENT ADDRESS

Institute of Biochemistry

University of Fribourg Rue du Musee 5

CH-1700 Fribourg Switzerland.

Tel.++ 41 26 300 8648

Fax: ++41 26 300 9735

e-mail: Vladimir.Katanaev@unifr.ch

FUTURE ADDRESS

College of Physicians and Surgeons

Columbia University

701 West 168th Street

New York, NY 10032

Fax: 212 305 3562

PUBLICATIONS

1. Katanaev, V.L., Kurnasov, O.V., and Spirin, A.S. (1995). Viral Qbeta RNA as a high expression vector for mRNA translation in a cell-free system. *FEBS Letters* 359, 89-92.

2. Katanaev, V.L., Spirin, A.S., Reuss, M., and Siemann, M. (1996). Formation of bacteriophage MS2 infectious units in a cell-free translation system. *FEBS Letters* 397, 143-148.

3. Katanaev, V.L., and Wymann, M.P. (1998). GTPgammaS-induced actin polymerisation in vitro: ATP- and phosphoinositide- independent signalling via Rho-family proteins and a plasma membrane-associated guanine nucleotide exchange factor. *Journal of Cell Science* 111, 1583-1594.

4. Katanaev, V.L., and Wymann, M.P. (1998) Microquantification of cellular and in vitro actin by rhodamine phalloidin fluorescence enhancement. *Analitical Biochemistry* 264, 185-190.

5. Wymann, M.P., Pirola, L., Katanaev, V.L., and Bulgarelli-Leva, G. (1999) Phosphoinositide 3-kinase signaling - no lipids. *Biochemical Society Transactions* 27, 629-634.

6. Hirsch, E., Katanaev, V.L., Garlanda, C., Azzolino, O., Pirola, L., Silengo, L., Sozzani, S., Mantovani, A., Altruda, F., and Wymann, M.P. (1999) Central role for the G protein- coupled PI3Kγ in inflammation. *Science*, in press.

CONFERENCES

1. Kurnasov, O.V., Katanaev, V.L., Spirin, A.S. Viral Qbeta RNA as a high expression vector for mRNA translation in a cell-free system. Frontiers in Translation. International Conference on the Structure and Function of the Ribosome, Victoria, Canada, May 20-25, 1995; poster. Abstract published in *Biochemistry and Cell Biology* 73.

2. Katanaev, V.L., Wymann, M.P. A new mechanism for G protein- mediated actin polymerisation in neutrophils. Jacques Monod Conference on "Actin, Cell Motility, and Signalling", Aussois, France, June 22-27, 1997; oral presentation.

3. Katanaev, V.L., Wymann, M.P. Membrane-associated guanine nucleotide exchange factor and cytosolic Rho-family protein signal to actin polymerisation in vitro. 30th annual meeting of the Union of Swiss Societies for Experimental Biology, Lausanne, Switzerland, March 5-6, 1998; poster.

4. Katanaev, V.L., Wymann, M.P. Membrane-associated guanine nucleotide exchange factor and cytosolic Rho-family protein signal to actin polymerisation in vitro in an ATP- and phosphoinositide-independent manner. 17th European Workshop on the Cell Biology of Phagocytes, Catania, Italy, May 27-31, 1998; oral presentation. Abstract published in *European Journal of Haematology* 60, 348.

5. Katanaev, V.L., Wymann, M.P. Method for microquantification of cellular and in vitro F-actin by rhodamine phalloidin fluorescence enhancement. 9th CytoMeet, Bern, Switzerland, October 21, 1998; oral presentation.

6. Pirola, L., Katanaev, V.L., and Wymann. PI3K signalling involves its lipid and protein kinase activity. Lipid-Protein Interplay: Mechanisms and Implications for Cell Function, Joint Meeting of GMB Study Group "Biomembranes" and SFB 197 "Biological and Model Membranes, BioMembranForum '99, April 8-10, 1999, Jena, Germany. Oral presentation. Abstract will be published in *Chemistry and Biology.*

7. Katanaev, V.L., Pirola, L., Bulgarelli-Leva, G., Friederich, S., Hirsch, E., and Wymann, M.P. Signalling by G protein- coupled phosphoinositide-3 kinase γ — neutrophil responses in PI3K γ knock-out mice. 2nd "Molecular Life Sciences at Perolles", June 23, 1999, Fribourg, Switzerland. Oral presentation. Best presentation award.

8. Katanaev, V.L., Hirsch, E., Bulgarelli-Leva, G., and Wymann, M.P. Signalling by G protein- coupled phosphoinositide-3 kinase γ — neutrophil responses in PI3K γ knock-out mice. The Batsheva de Rothschild Seminar on Innate Immunity, October 10-15, 1999, Zichron Yaakov, Israel. Oral presentation. Abstract will be published in the seminar proceedings.

ACKNOWLEDGEMENTS

Vladimir L. Katanaev
Route du Centre 12
CH-1723 Marly

Fribourg, decembre 1999

Aux personnes concernées

Sujet: Thèse présentée à l'Université de Fribourg (Suisse) pour l'obtention du grade de *Doctor rerum naturalium*.

Messieurs,

Par la présent, je certifie que j'ai rédigé ma thèse "Neutrophil Chemotaxis: Crucial Role of Phosphatidylinositol 3 Kinase γ and Rho Family GTP-Binding Proteins" moi-même et sur la base d'un travail personnel sans aide illicite.

Vladimir L. Katanaev